THE HOKENSON COMPANY

(1)

FINAL REPORT

EVALUATION OF AN ADD-ON MUZZLE EXHAUST FLOW MANIPULATOR FOR NOISE SUPPRESSION ON LARGE CALIBER GUNS

SBIR Phase I Contract DAAD03-87-C-0035

Prepared for:

Jefferson Proving Ground

Madison, IN 47250

by:

Gustave J. Hokenson, PhD

January 1988

ELIZABETH K. HOKENSON • CHIEF EXECUTIVE • 840 S. TREMAINE AVE., LOS ANGELES, CA. 90005 • TEL. (213) 935-3743

Encl 1 of Encl 2

UNCLASSIFIED
SECURITY CLASSIFICATION OF THIS PAGE

ADA196601

REPORT DOCUMENTATION PAGE

1a. REPORT SECURITY CLASSIFICATION: Unclassified	1b. RESTRICTIVE MARKINGS
2a. SECURITY CLASSIFICATION AUTHORITY	3. DISTRIBUTION / AVAILABILITY OF REPORT: Unlimited
2b. DECLASSIFICATION / DOWNGRADING SCHEDULE	
4. PERFORMING ORGANIZATION REPORT NUMBER(S)	5. MONITORING ORGANIZATION REPORT NUMBER(S)
6a. NAME OF PERFORMING ORGANIZATION: The Hokenson Company; 6b. OFFICE SYMBOL (If applicable)	7a. NAME OF MONITORING ORGANIZATION
6c. ADDRESS (City, State, and ZIP Code): 840 S. Tremaine Ave. Los Angeles, CA 90005	7b. ADDRESS (City, State, and ZIP Code)
8a. NAME OF FUNDING / SPONSORING ORGANIZATION: Jefferson Proving Ground; 8b. OFFICE SYMBOL (If applicable)	9. PROCUREMENT INSTRUMENT IDENTIFICATION NUMBER: SBIR DAAD03-87-C-0035
8c. ADDRESS (City, State, and ZIP Code): Madison, Indiana 47250	10. SOURCE OF FUNDING NUMBERS: PROGRAM ELEMENT NO. / PROJECT NO / TASK NO. / WORK UNIT ACCESSION NO.

11. TITLE (Include Security Classification)

Evaluation of an Add-on Muzzle Exhaust Flow Manipulator for Noise Suppression on Large Caliber Guns

12. PERSONAL AUTHOR(S)

Dr. Gustave J. Hokenson

13a. TYPE OF REPORT	13b. TIME COVERED	14. DATE OF REPORT (Year, Month, Day)	15. PAGE COUNT
Final	FROM 7/9/87 TO 1/9/88	88JAN09	103

16. SUPPLEMENTARY NOTATION

17. COSATI CODES			18. SUBJECT TERMS (Continue on reverse if necessary and identify by block number)
FIELD	GROUP	SUB-GROUP	Guns Silencers and mufflers, (edc) Environment

19. ABSTRACT (Continue on reverse if necessary and identify by block number)

Direct numerical simulations of gun muzzle blast flowfields, with and without a simole silencer attached to the muzzle, were carried out utilizing the full equations of motion. These computations indicated that the silencer had a significant effect upon the amplitude and temporal structure of the induced sound pressure field. As a result, the feasibility of optimizing such silencer configurations and using them on various caliber guns has been demonstrated. In addition to mitigating the gun noise, this device is attractive based on its size, weight, cost, complexity and reliability. An extensive series of field tests and supportive numerical simulations is required to provide the Army with the required optimal designs. Keywords:

20. DISTRIBUTION / AVAILABILITY OF ABSTRACT: ☐ UNCLASSIFIED/UNLIMITED ☒ SAME AS RPT ☐ DTIC USERS	21. ABSTRACT SECURITY CLASSIFICATION: Unclassified
22a. NAME OF RESPONSIBLE INDIVIDUAL: Kaushik N. Joshi	22b. TELEPHONE (Include Area Code): 1-812-273-7211; 22c. OFFICE SYMBOL: Engr. & Housing

DD FORM 1473, 84 MAR — 83 APR edition may be used until exhausted. All other editions are obsolete.

SECURITY CLASSIFICATION OF THIS PAGE
UNCLASSIFIED

NOTICE

The views, opinions and/or findings contained in this report are those of the author(s) and should not be construed as an official Department of the Army position, policy, or decision, unless so designated by other documentation.

When Government drawings, specifications, or other data are used for any purpose other than in connection with a definitely related Government procurement operation, the United States Government thereby incurs no responsibility nor any obligation whatsoever; and the fact that the Government may have formulated, furnished, or in any way supplied the said drawings, specifications, or other data, is not to be regarded by implication or otherwise as in any manner licensing the holder or any other person or corporation, or conveying any rights or permission to manufacture, use, or sell any patented invention that may in any way be related thereto.

This report has been reviewed and is approved for publication.

FOR THE COMMANDER

Even though this report may contain special release rights held by the controlling office, please do not request copies from Jefferson Proving Ground. If you qualify as a recipient, release approval will be obtained from the originating activity by DTIC. Address your request for additional copies to:

Defense Technical Information Center
Cameron Station
Alexandria, Virginia 22304-6145

If your address has changed, if you wish to be removed from our mailing list, or if the addressee is no longer employed by your organization, please notify Jefferson Proving Ground.

Copies of this report should not be returned unless return is required by security considerations, contractual obligations, or notice on a specific document.

PREFACE

This report describes the efforts of The Hokenson Company, 840 S. Tremaine Ave. Los Angeles, CA as part of the Jefferson Proving Ground Small Business Innovation Research (SBIR) program. The work addresses addresses the possibility for reducing the sound pressure level from large caliber guns through the introduction of a simple add-on silencer. The Jefferson Proving Ground Technical Monitor was Mr. Kaushik N. Joshi.

The work reported herein was performed during the period 9 July 1987 through 9 January 1988 under direction of the author and Principal Investigator, Dr. Gustave J. Hokenson, Chief Scientist of The Hokenson Company. The report was released by the author in January 1988.

This report addresses results from Phase I of a planned multi-phase SBIR and non-SBIR effort to minimize the sound pressure level of large caliber guns. Future work shall be reported in connection with subsequent contracts.

TABLE OF CONTENTS

LIST OF FIGURES

LIST OF FIGURES (CONT'D)

LIST OF FIGURES (CONT'D)

LIST OF FIGURES (CONT'D)

LIST OF FIGURES (CONT'D)

SECTION I

EXECUTIVE SUMMARY

In order to establish the feasibility of reducing the sound pressure level generated by the firing of large guns, numerical simulations of the muzzle blast flowfield have been carried out. The simulations involve finite difference solutions of the full equations of motion, with and without the presence of a simple silencer affixed to the end of the barrel. As a result of these numerical simulations, the effectiveness of this particular class of silencer has been demonstrated, even though its configuration has yet to be optimized. In addition to its favorable impact on the noise field, the design of this type muffler is attractive due to its size, weight, simplicity, reliability and cost advantages relative to more complex geometries. Based on these preliminary results, an extensive series field tests of the silencer relative to its effect on the perceived sound level of 105, 120 and 155 mm guns is indicated, subsequent to a computational optimization of the design for each caliber gun.

SECTION II

INTRODUCTION

With the renewed emphasis on the importance of tactical weaponry, a significant increase in training and testing activities associated with guns of various sizes is anticipated over the coming years. At installations like Jefferson Proving Ground, such gun firing takes place within a few miles of the civilian population and 'noise pollution' of the environment may become a serious problem at the anticipated future levels of firing. In an attempt to reduce this problem, the present work was proposed and executed in order to assess the virtures of a particularly simple class of gun muffler/silencer shown in Figure 1.

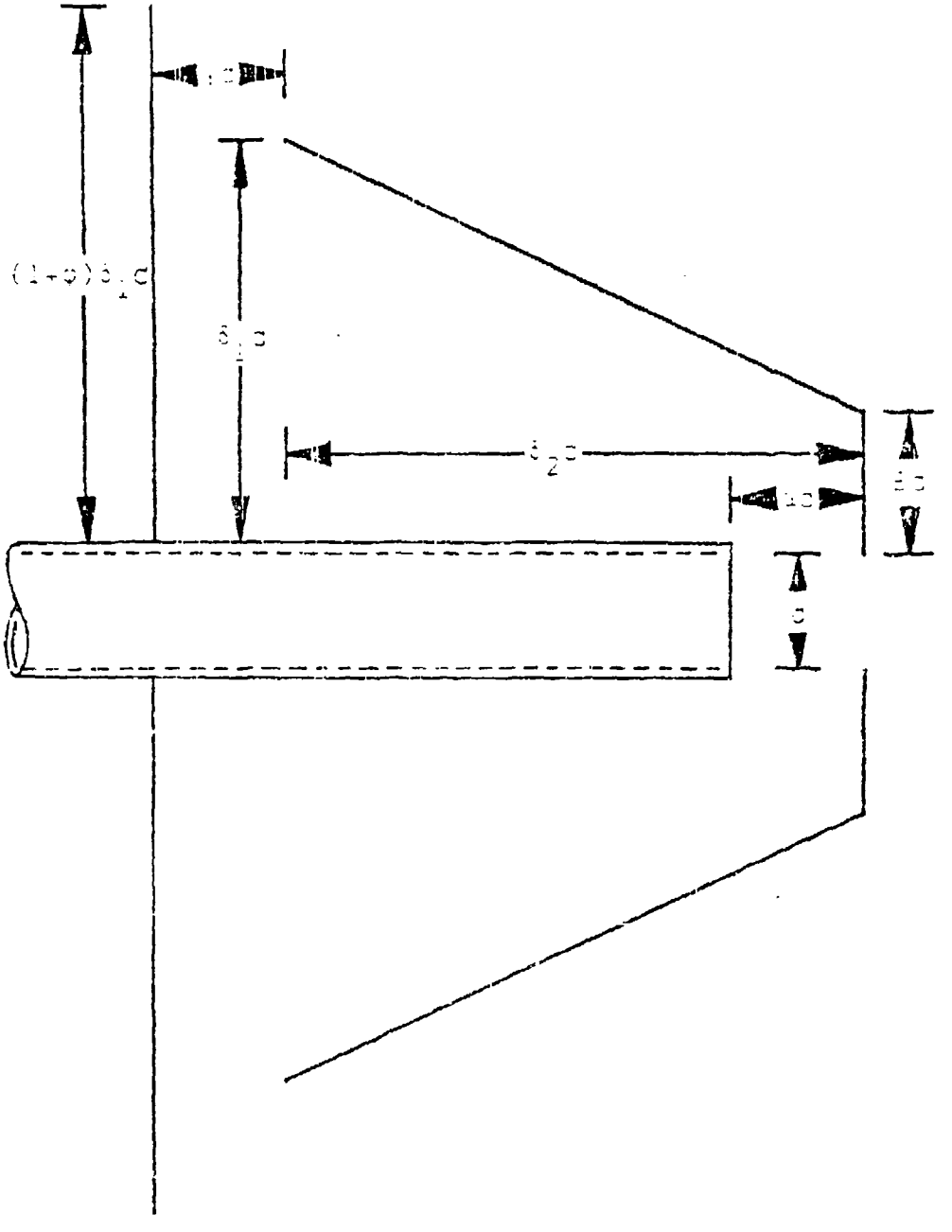

Figure 1. Generic Slender Configuration.

SECTION III

DISCUSSION

The generic silencer geometry which was selected was motivated by observing numerical simulations of muzzle blast flowfield, such as that shown in Figure 2, and noting that, at the instant the projectile base passes the muzzle plane, a radial 'piston' of gas induces the ambient pressure field of primary consequence. Note, however, that the silencer also affects the pressure field associated with flow ahead of the projectile as it proceeds down the barrel. By collecting the radial muzzle blast, re-directing it and allowing it to exhaust over a larger area at a larger radius, it was hypothesized that the noise field would be favorably affected. In addition, the extent to which proximity to the ground plane reinforces the far field noise may be controlled by such a silencer. In this case, the utility of non-axisymmetric versions of the device, in which the final exhaust in the direction towards or away from the ground is controlled, may prove to be beneficial. During Phase I of this work the axisymmetric configuration has been focused upon in order to provide a definitive assessment of the concept feasibility.

Finally, the silencer geometry which has been proposed shall have a favorable effect upon the reaction forces applied to the gun, including both axial loads and torque. This effect remains to be quantified during future tests and numerical simulations.

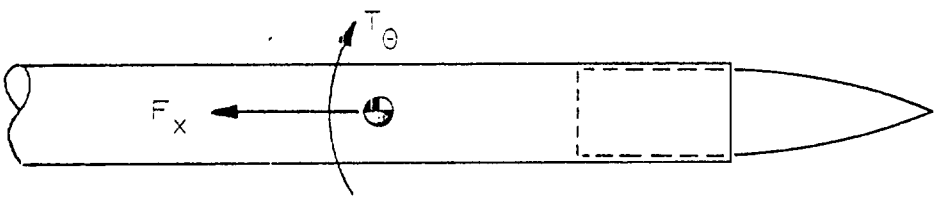

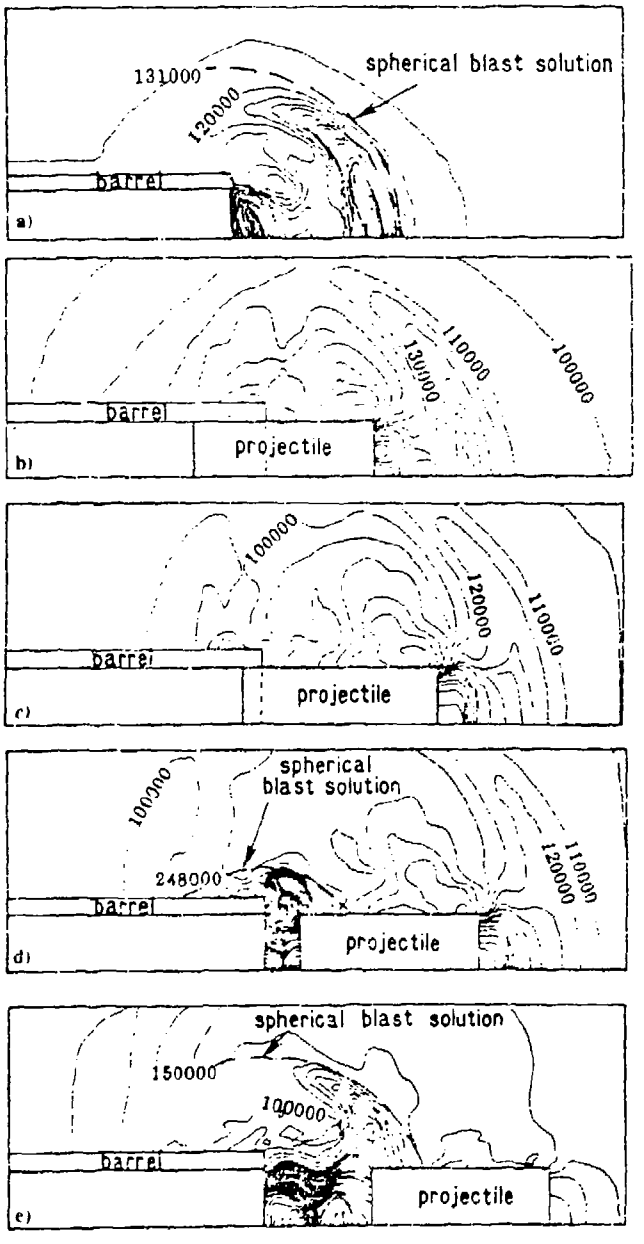

Figure 2. Representative Muzzle Blast Flowfields.

In order to evaluate the effect of such a silencer configuration on the sound pressure level field, numerical simulations utilizing the full time-dependent, multi-dimensional, compressible, viscous and heat conducting equations of motion presented in Figure 3 were executed. During Phase I the flowfield was assumed to be axisymmetric, including swirl. Phase II shall address various three-dimensionalities induced by the ground and, possibly, an optimum non-axisymmetric silencer.

The nomenclature used in Figure 3 is that which is conventional in the fluid mechanics community. In order to solve these equations of motion, MacCormack's hybrid numerical scheme was applied to a non-uniform finite-difference grid overlaying the flowfield. The initial/boundary value problem proceeded by solving for the dependent variables throughout the interior and exterior of the barrel (ahead of and behind the projectile) and silencer. On solid boundary surfaces, all velocities were set to zero relative to the surface, temperature was specified and pressure extrapolated so that wall density may be computed from the gas law. At outflow boundaries, subsonic or supersonic radiation conditions were imposed. At the breech end of the barrel interior, a simple combustion model of the gas and heat release was specified. In addition to this, the projectile dynamics was fully coupled to the gas dynamic flowfield ahead of and behind it, whose pressure difference establishes the projectile acceleration.

Figure 3. Governing Equations.

Compressible Axisymmetric N-S Equations With Swirl

$$Q_{,t} + F_{,x} + (rG)_{,r}/r = H/r$$

$\underline{Q}$	$\underline{F}$	$\underline{G}$	$\underline{H}$
ρ	ρu	ρv	0
ρu	$\rho u^2 + p - \tau_{xx}$	$\rho uv - \tau_{rx}$	0
ρv	$\rho uv - \tau_{xr}$	$\rho v^2 + p - \tau_{rr}$	$\rho w^2 + p - \tau_{\theta\theta}$
ρw	$\rho uw - \tau_{x\theta}$	$\rho wv - \tau_{r\theta}$	$-\rho vw + \tau_{\theta r}$
ρE	$\rho uE + q_x - u\sigma_{xx} - v\tau_{xr} - w\tau_{x\theta}$	$\rho vE + q_r - u\tau_{rx} - v\sigma_{rr} - w\tau_{r\theta}$	0

$$\tau_{xx} = \lambda'\nabla\cdot\vec{V} + 2\mu' u_{,x}$$

$$\tau_{xr} = \mu'(u_{,r} + v_{,x})$$

$$\tau_{x\theta} = \mu' w_{,x}$$

$$\sigma_{xx} = -p + \tau_{xx}$$

$$q_x = -\gamma(\mu/Pr + \mu_t/Pr_t)e_{,x}$$

$$\tau_{rx} = \tau_{xr}$$

$$\tau_{rr} = \lambda'\nabla\cdot\vec{V} + 2\mu' v/r$$

$$\tau_{r\theta} = \mu' r(w/r)_{,r}$$

$$\sigma_{rr} = -p + \tau_{rr}$$

$$q_r = -\gamma(\mu/Pr + \mu_t/Pr_t)e_{,r}$$

$$\tau_{\theta\theta} = \lambda'\nabla\cdot\vec{V} + 2\mu' v/r$$

$$\tau_{\theta r} = \tau_{r\theta}$$

$$E = e + (u^2 + v^2 + w^2)/2$$

$$\nabla\cdot\vec{V} = u_{,x} + (rv)_{,r}/r$$

$$p = (\gamma - 1)\rho e, \text{ or real gas.}$$

$$\mu' = \mu + \mu_t, \quad \lambda' = \lambda + \lambda_t$$

$$\lambda' = -2\mu'/3, \text{ or other.}$$

SECTION IV

RESULTS

Within the context of the aforementioned numerical model, the flowfield incuced by the muzzle blast of a generic 100-mm gun was computed, both with and without a typical silencer in place. Relative to the nomenclature of Figure 1, for these feasibility studies $\alpha=\beta=\gamma=1$, $\delta_2=\delta_1-1$, $\varphi>>1$ and $\delta_1=3.0$, based on preliminary screening computations. With regard to the induced sound pressure, the transient response at an arbitrarily selected point in the field is depicted in Figures 4a & 4b.

It is to be noted that the silencer has a beneficial effect on both the amplitude of the pressure field and its time-dependent structure. Since sound is related to the deviation of the pressure field, and the subjective perception of it, such an effect is significant. For pure tones, equivalent loudnesses at various frequencies may be judged using the traditional concepts. With quasi-steady noise sources, a complex spectral assemblage of pure tones may be used to simulate, for example, traffic noise and its overall band by band improvement in both the perceived sound and sound pressure levels. With regard to the impulsive, low frequency and high amplitude pressure deviations associated with field artillery, the time-constant of a given pressure level change has a significant impact on the perceived loudness. This occurs not only because of the perception aspect but also because, as with the silencer studied here, changes in the temporal structure of the muzzle blast change the physical structure of the radiated shock/pressure field. Therefore, the fact that the silencer alters the peak magnitude and temporal nature of the pressure field is significant. At this point the silencer geometry has not yet been optimized so as to further reduce the amplitude and lengthen the time constant, thereby putting more energy into lower frequencies.

Figure 4a. Transient Pressure Solution at a Point in the Field without the Silencer.

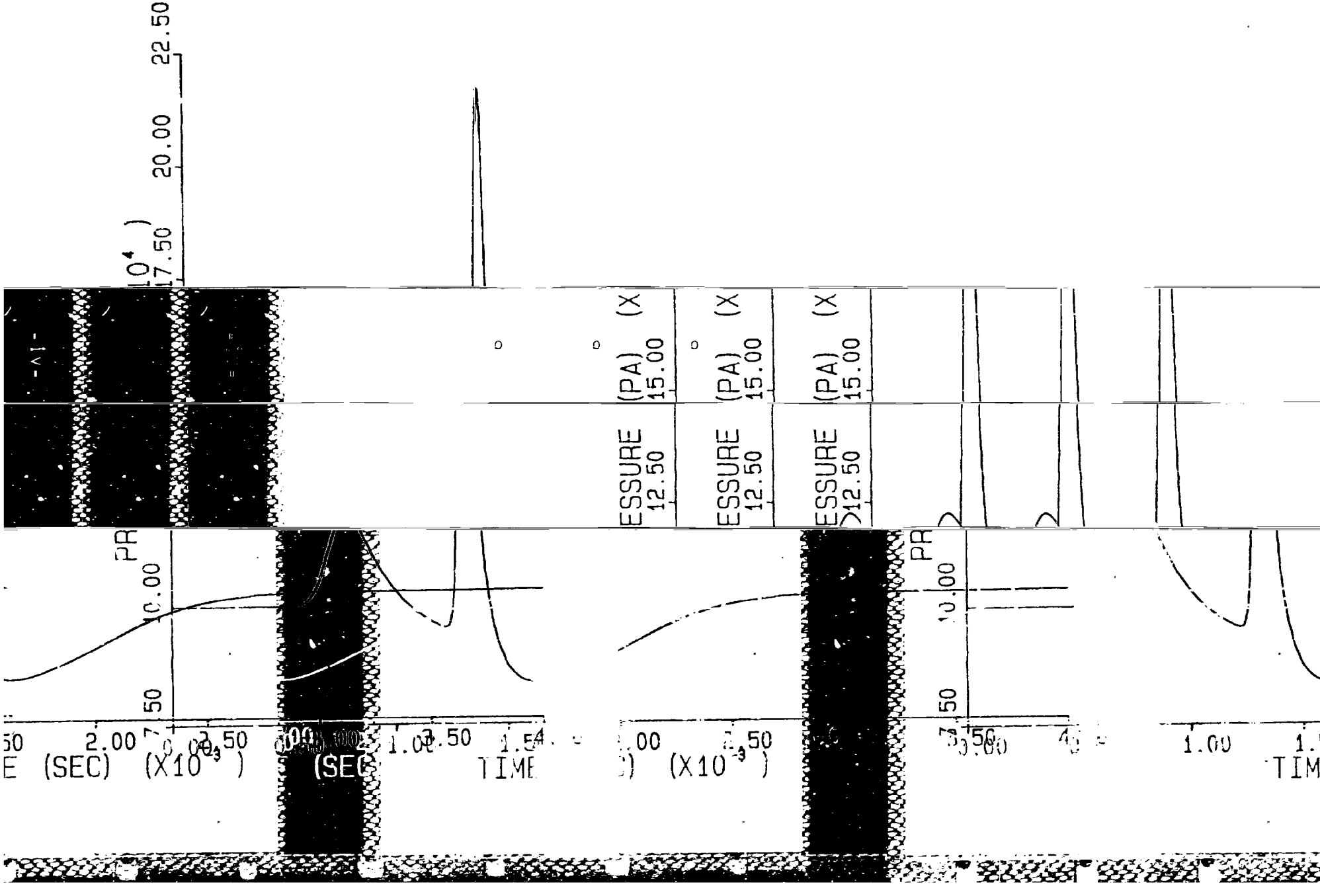

Figure 4b. Transient Pressure Solution at a Point in the Field with the Silencer.

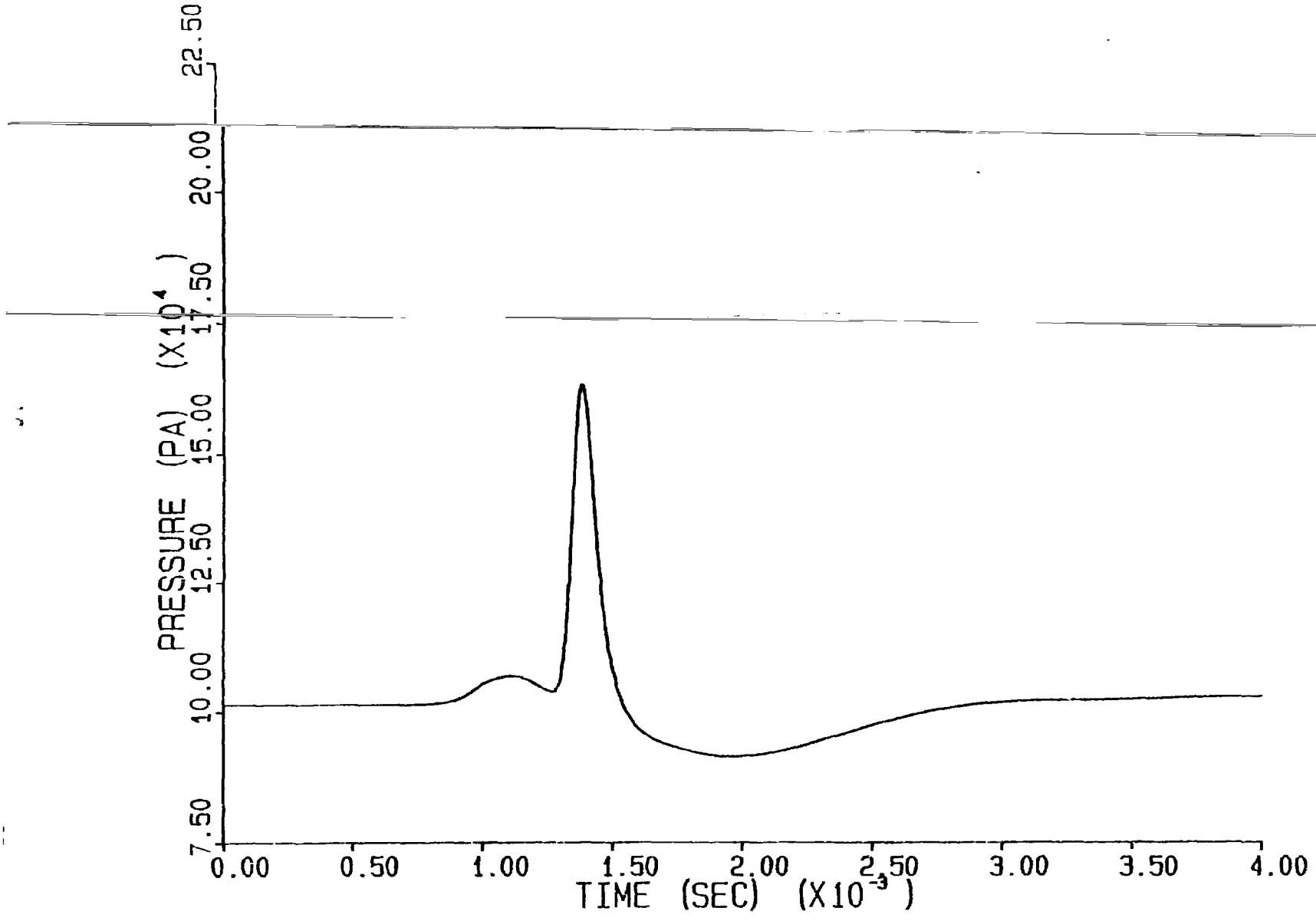

The detailed flowfield solutions at various times after projectile 'pop-out' are presented in Figures 5 - 13 with the silencer in place and Figures 14 - 22 without the silencer.

SECTION V

CONCLUSIONS AND RECOMMENDATIONS

Numerical simulations of the flowfield induced by the muzzle blast from field artillery have indicated that a particular simple silencer geometry can have a significant effect on the amplitude and spectral content of the radiated pressure field, and thereby on the perceived sound level. These simulations suggest that this class of silencer may be optimized to provide noise reduction such that the benefits are maximized while the 'burden', including size, weight, cost and complexity are minimized. The computations have exposed details of the flowfield which previously had not been resolved by numerical simulation.

Field tests on various size guns are required to validate the optimized silencer designs following an extensive series of numerical simulations in order to ascertain the appropriate configurations. Enhancement of the numerical simulations to represent the complex gun flow details more precisely may be required to achieve quantitative alignment between theory and experiment. In addition, the effect of flowfield three-dimensionality, as a result of proximity to the ground or a non-axisymmetric silencer, should also be assessed prior to any extensive field testing.

SECTION VI

BIBLIOGRAPHY

Cooke, C.H. and Fansler, K.S. "Numerical Simulation of Silencers," Proceedings of the 10th International Symposium on Ballistics, San Diego, CA, 27-28 October 1987.

Davis, D., et al, "Theoretical and Experimental Investigations of Mufflers, with Comments of Engine Exhaust Muffler Design," NACA Report No. 1192, 1954.

Fansler, K.S. and Lyon, D.H., "Attenuation of Muzzle Blast Using Configurable Mufflers," Proceedings of the 10th International Symposium on Ballistics, San Diego, CA, 27-28 October 1987.

Fansler, K.S., and Schmidt, E.M., "The Relationship Between Interior Ballistics, Gun Exhaust Parameters and the Muzzle Blast Overpressure," Proceedings of the AIAA/ASME 3rd Joint Thermophysics, Fluids, Plasma and Heat Transfer Conference, St. Louis, Missouri, 7-11 June 1982.

Fansler, K.S., "A Simple Method for Predicting Muzzle Brake Effectiveness and Baffle-Surface Pressure," U.S. Army Ballistic Technical Report ARBRL-TR-02335, June 1981. (AD-A102349)

Fansler, K.S., "Dependence of Free Field Impulse on the Decay Time of Energy Effiux for a Jet Flow," presented at the 56th Shock and Vibration Symposium, U.S. Naval Postgraduate School, Monterey, California, 22-24 October 1985.

Heaps, C.W., Fansler, K.S., and Schmidt, E.M., "Computer Implementation of a Muzzle Blast Prediction Technique," U.S. Army Ballistic Research Laboratory Technical Report ARBRL-MR-3443, Aberdeen Proving Ground, Maryland, May 1985.

Mason, W.P., "Silencer," U.S. Patent No. 2448382 assigned to Bell Laboratories, August 31, 1948.

Morl, Y., Hijikata, K., and Shimizu, T., "Attenuation of Shock by Multi-Orifice," Proceedings of the 10th International Shock Tube Symposium, Japan 1975.

Smith, F., "A Theoretical Model of the Blast from Stationary and Moving Guns," First International Symposium on Ballistics, Orlando, FL, 13-15 November 1074.

Widhopf, G.F., Buell, J.E., and Schmidt, E.M., "Time-Dependent Near Field Muzzle Brake Flow Simulations," Proceedings of the AIAA/ASME 3rd Joint Thermo-Physics, Fluids, Plasma, and Heat Transfer Conference, AIAA Paper-82-0973, 7-11 June 1982, St Louis, Missouri.

Figure 5a. Velocity Vector Field with the Silencer at T = .2 ms.

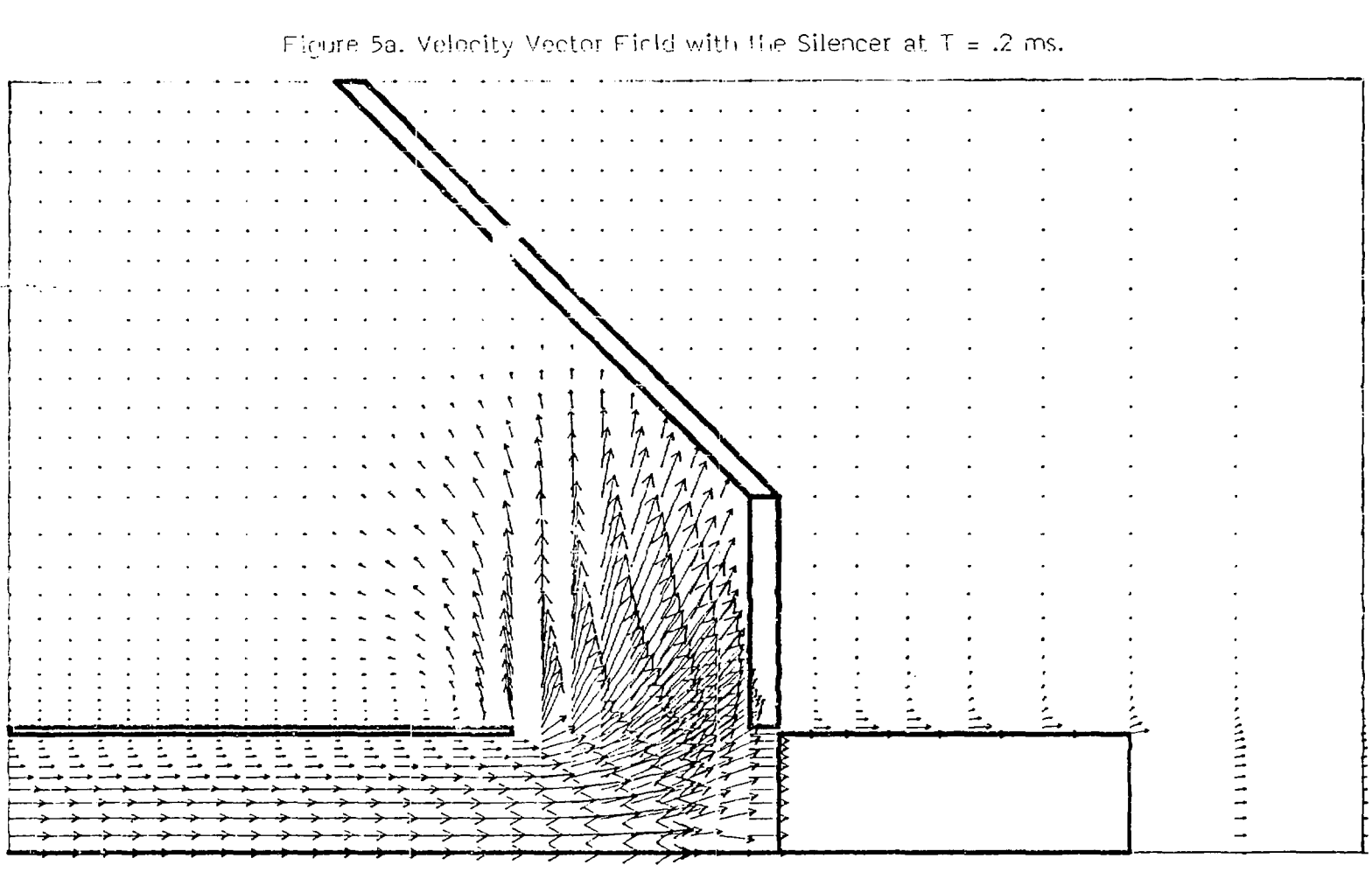

Figure 5b. Pressure Field with the Silencer at T = .2 ms.

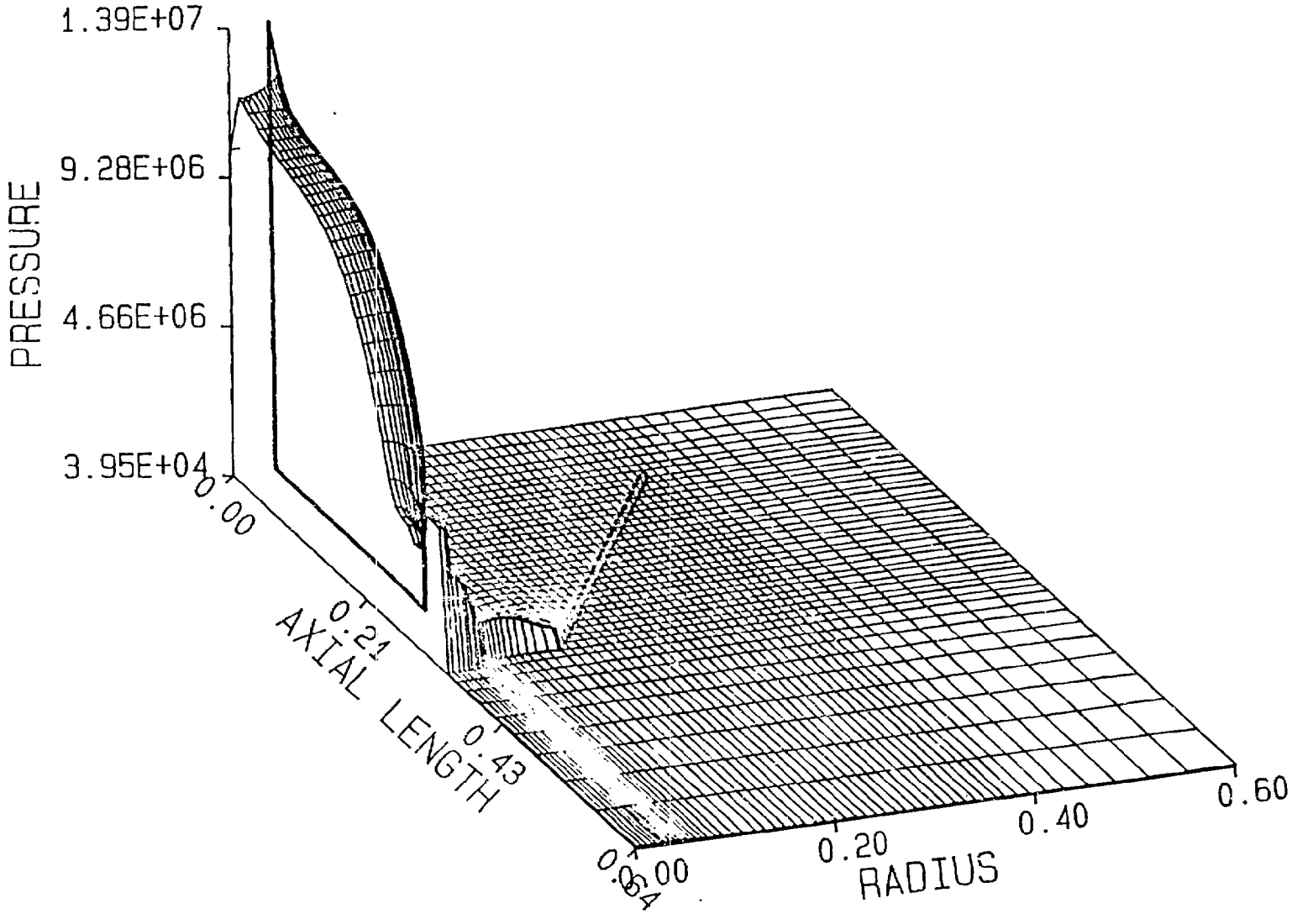

Figure 5c. Axial Velocity Field with the Silencer at T = .2 ms.

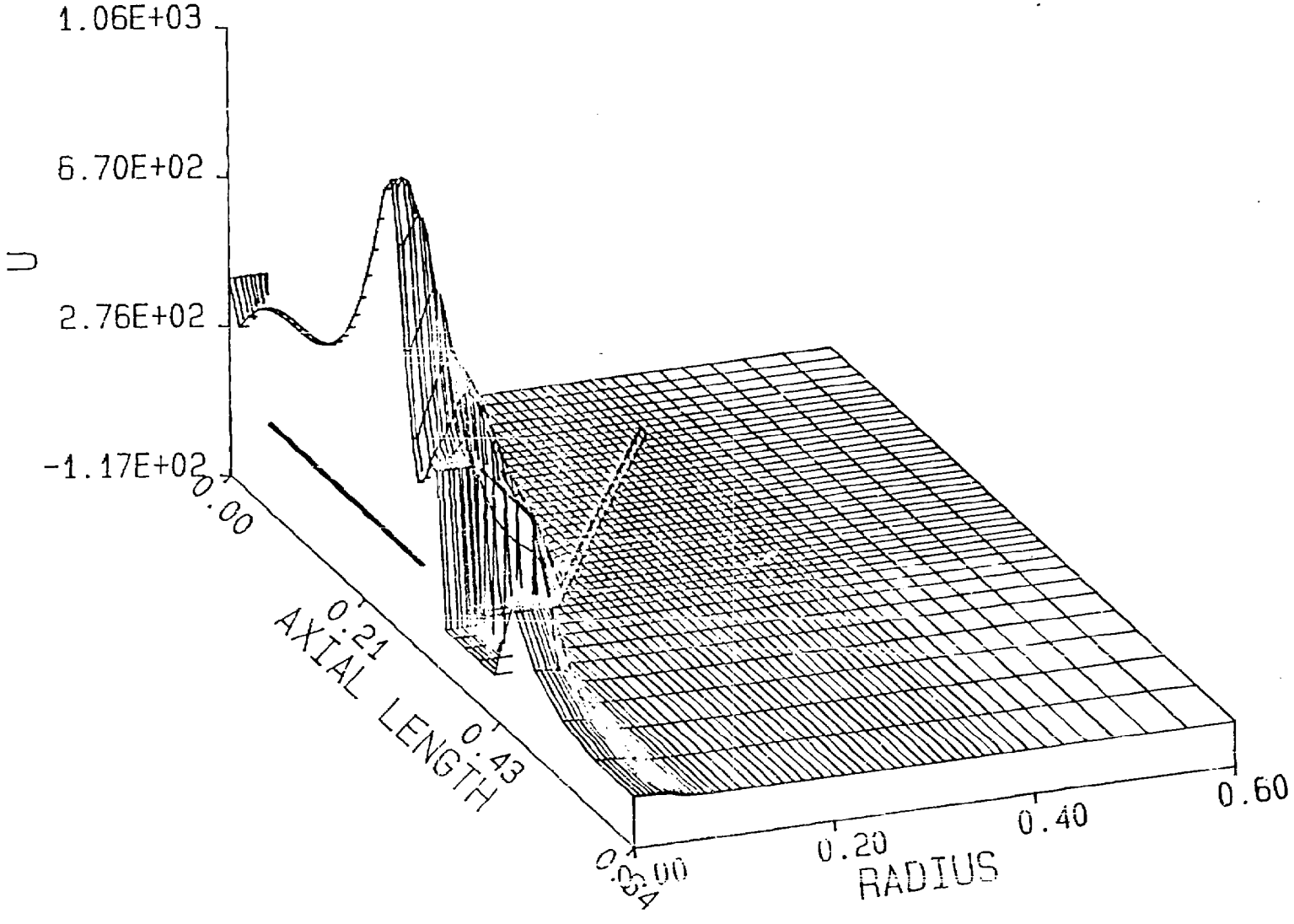

Figure 5d. Radial Velocity Field with the Silencer at T = .2 ms.

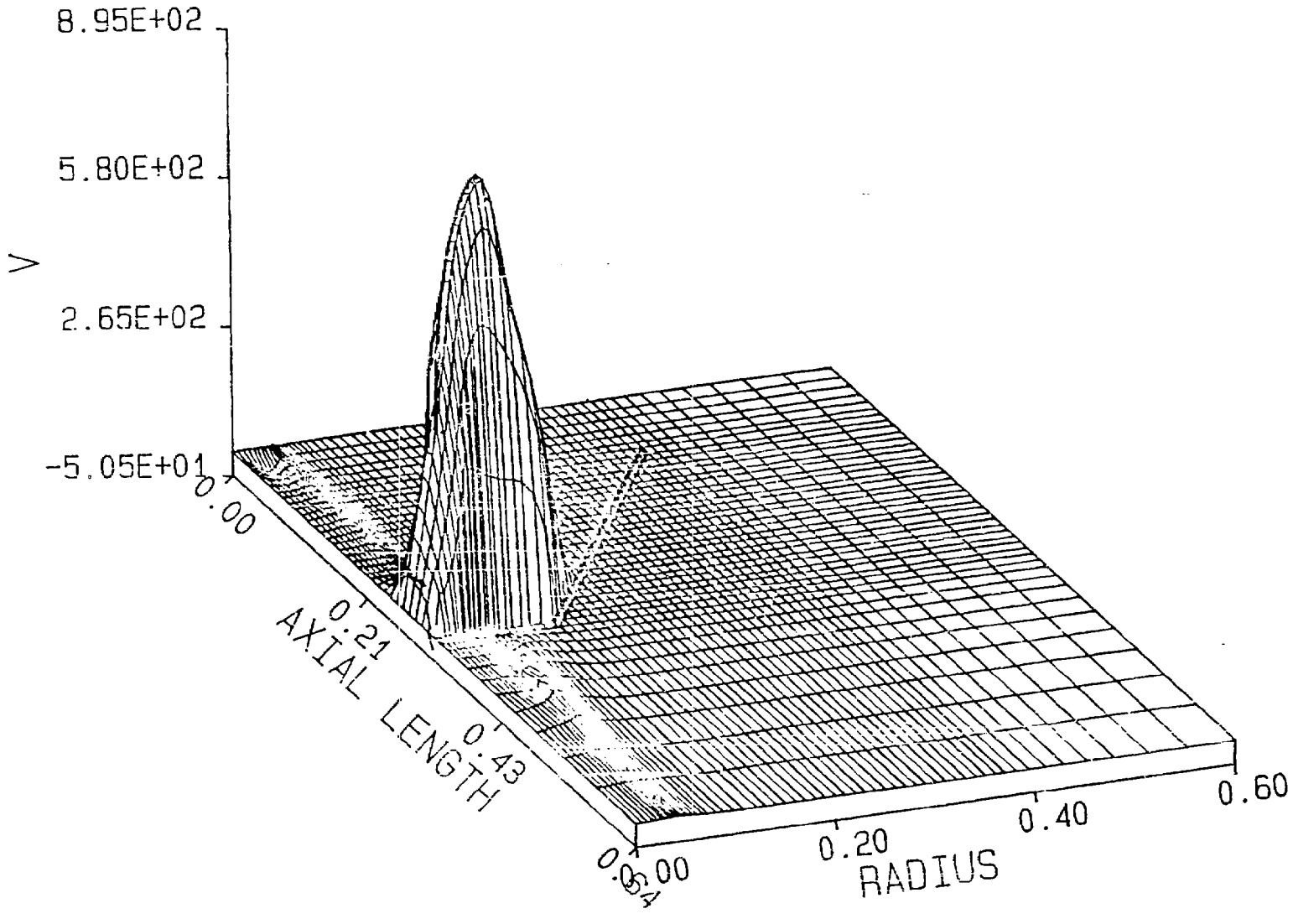

Figure 5e. Mach Number Field with the Silencer at T = .2 ms.

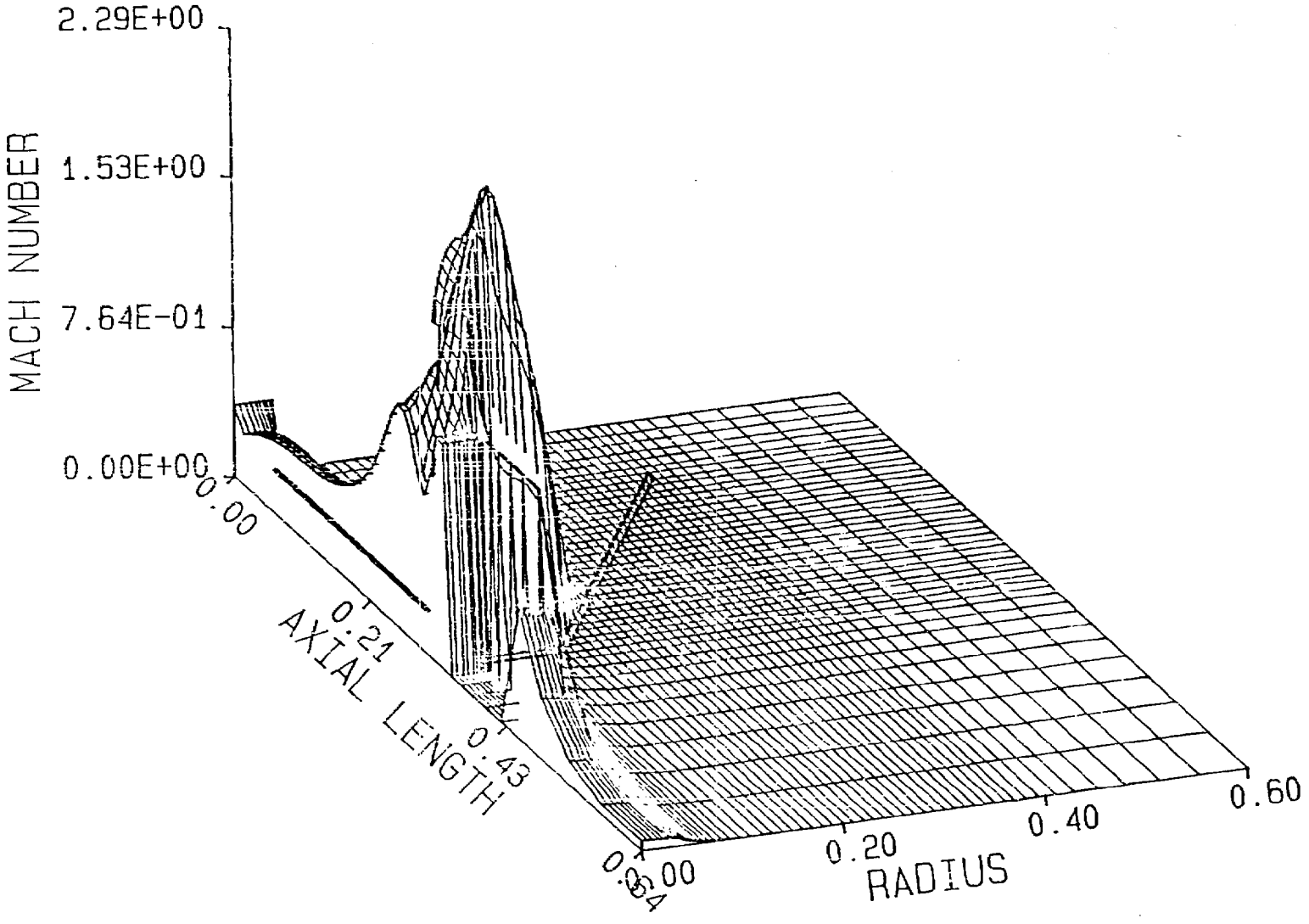

Figure 6a. Velocity Vector Field with the Silencer at T = .4 ms.

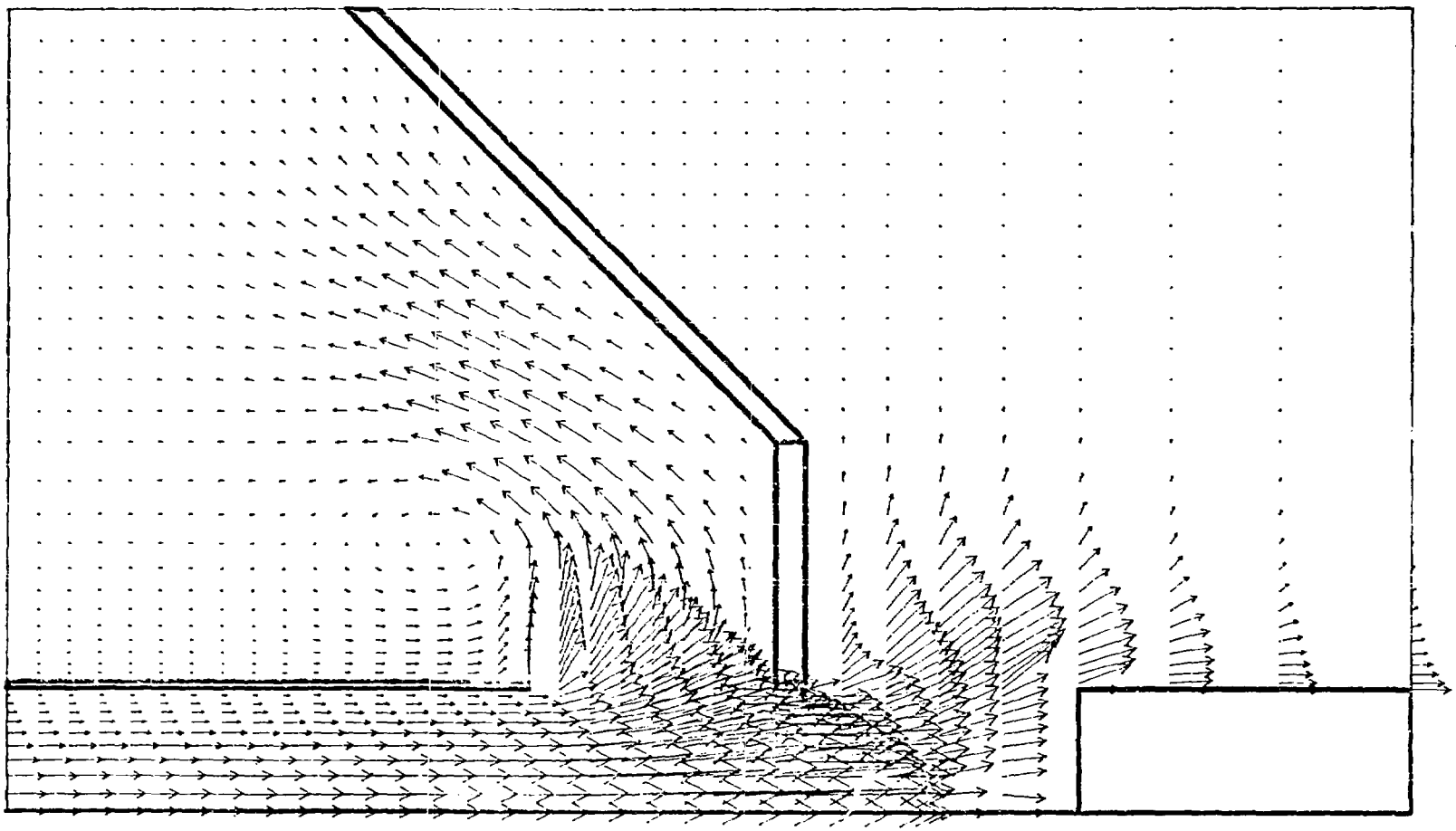

Figure 6b. Pressure Field with the Silencer at T = .4 ms.

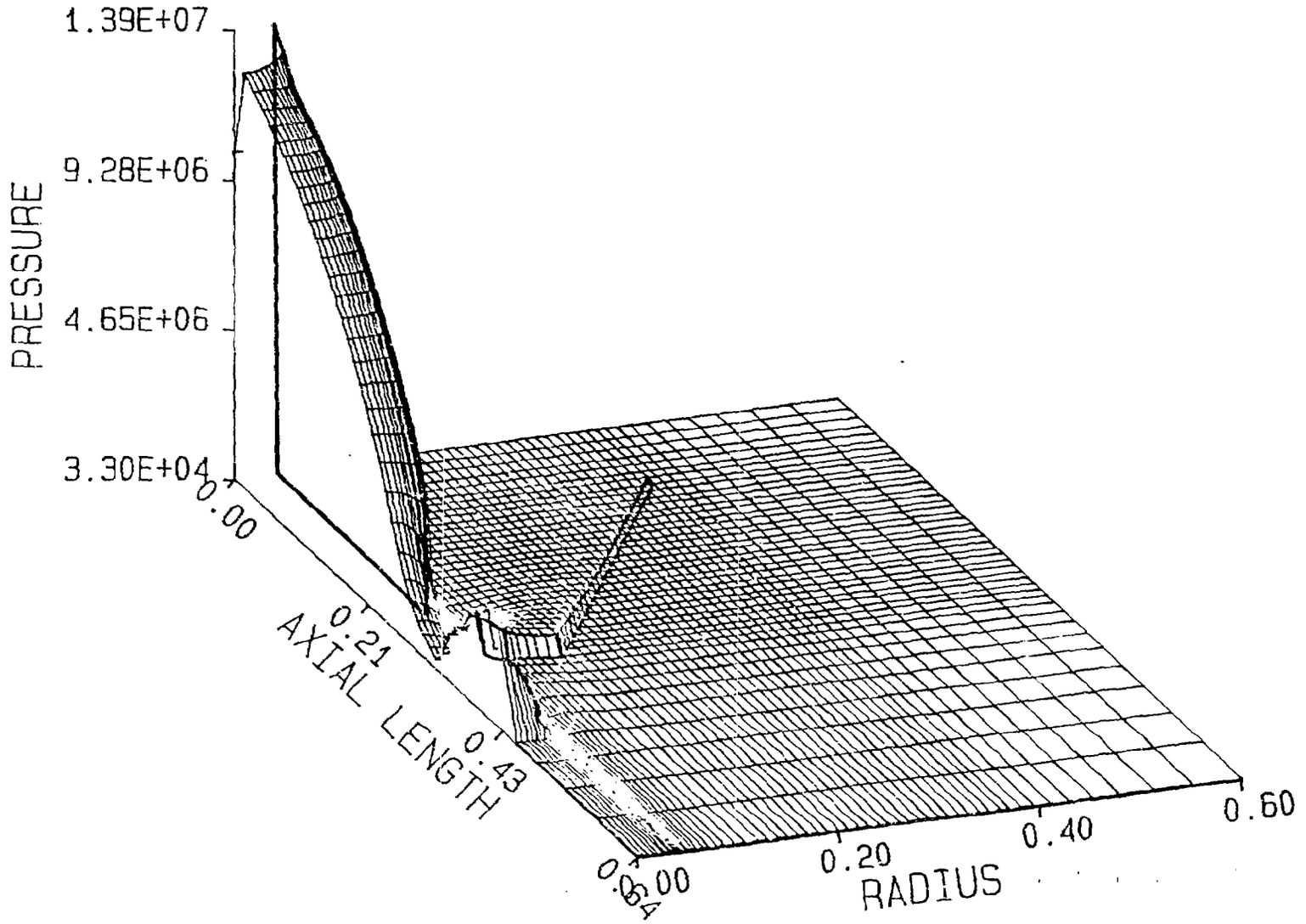

Figure 6c. Axial Velocity Field with the Silencer at T = .4 ms.

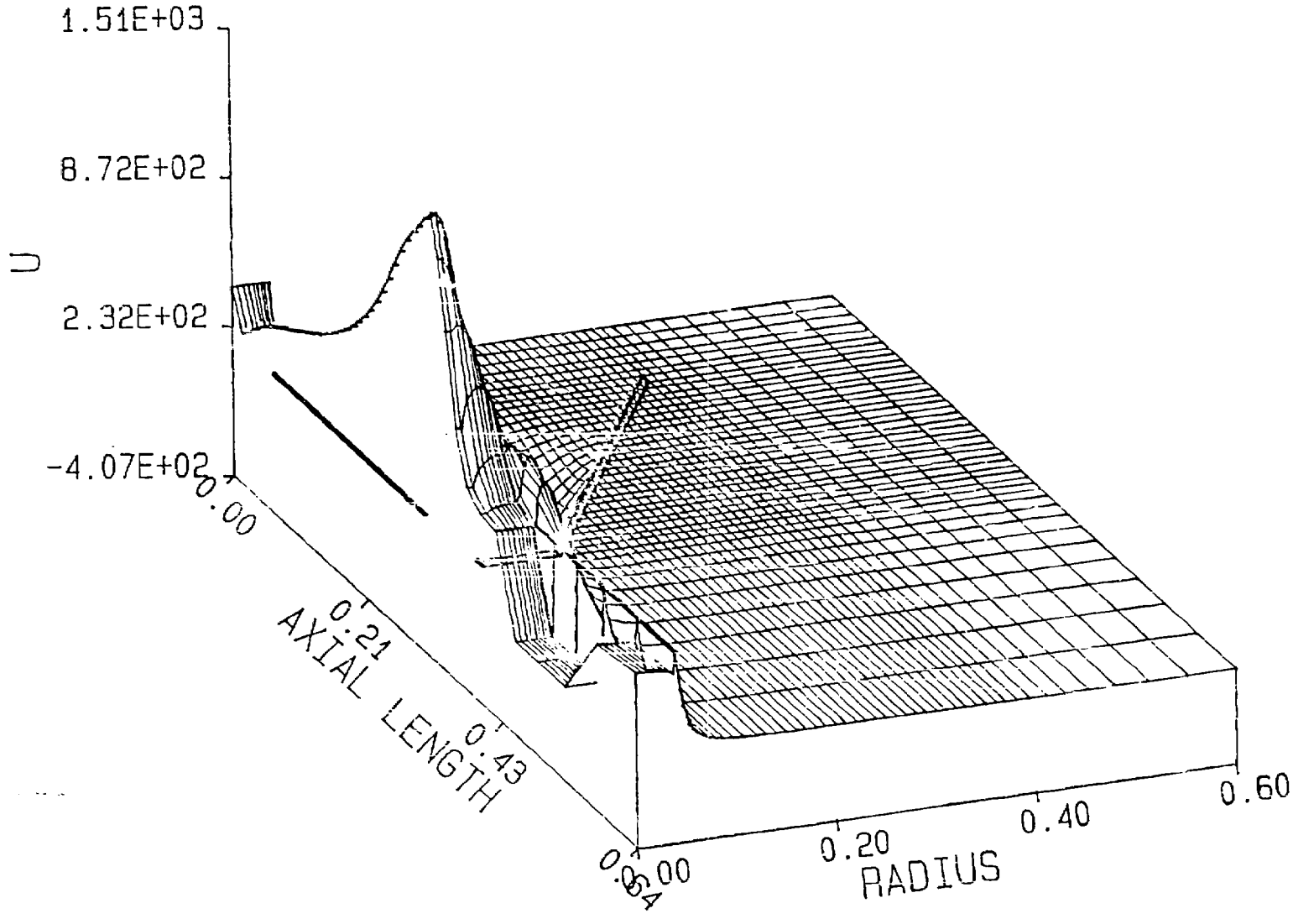

Figure 61. Radial Velocity Field with the Silencer at T = .4 ms.

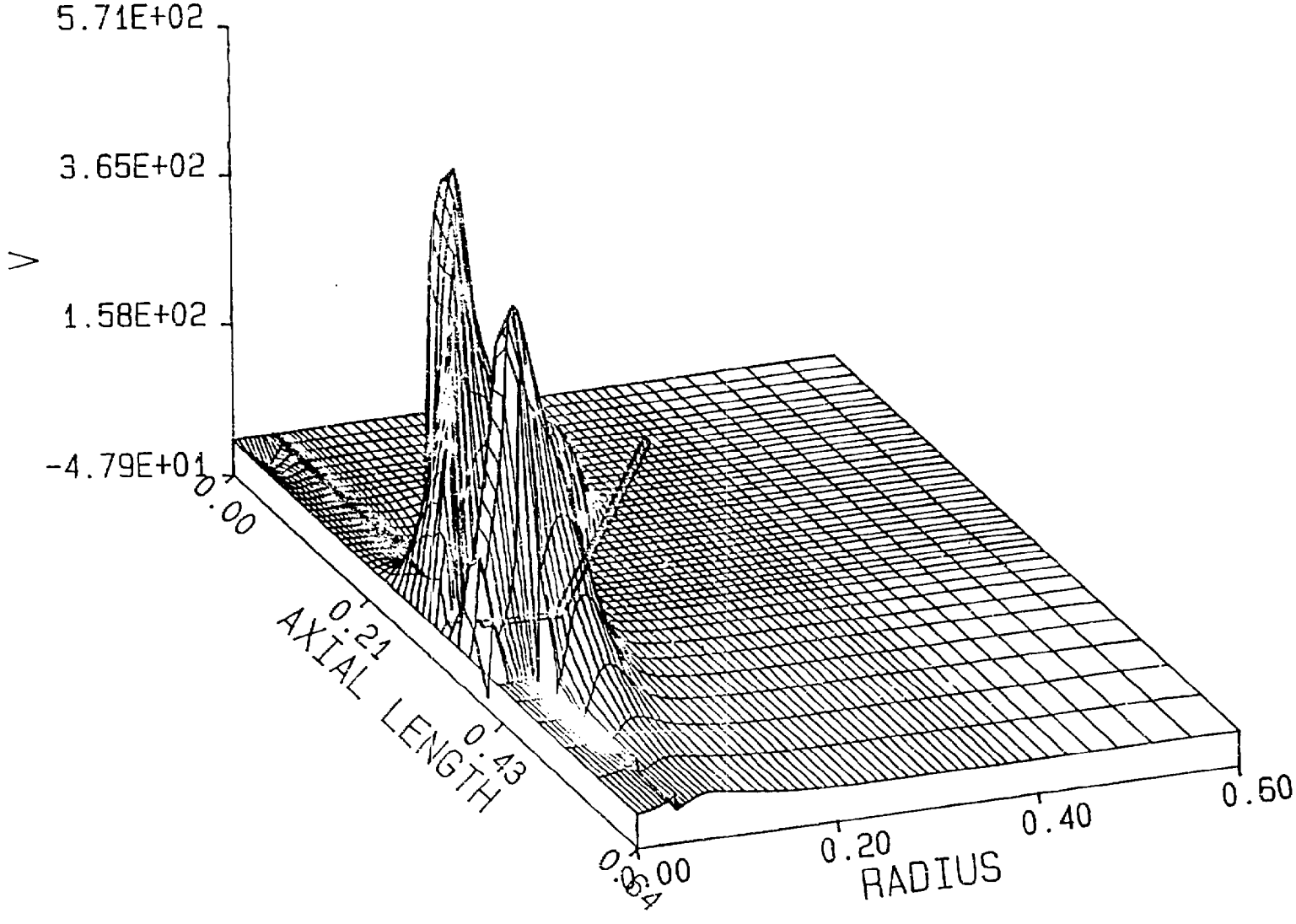

Figure 6e. Mach Number Field with the Silencer at T = .4 ms.

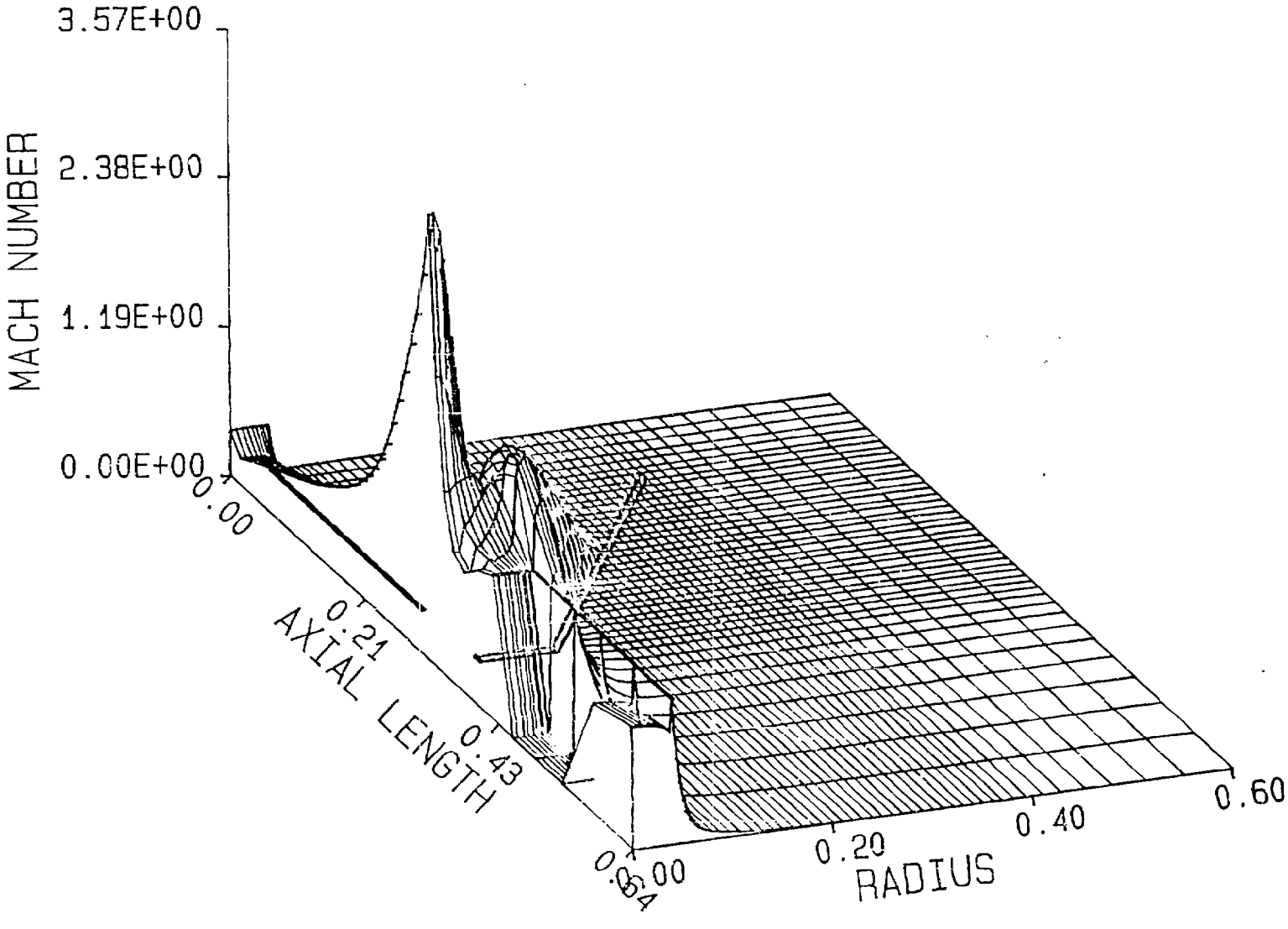

Figure 7a. Velocity Vecotr Field with the Silencer at T = .6 ms.

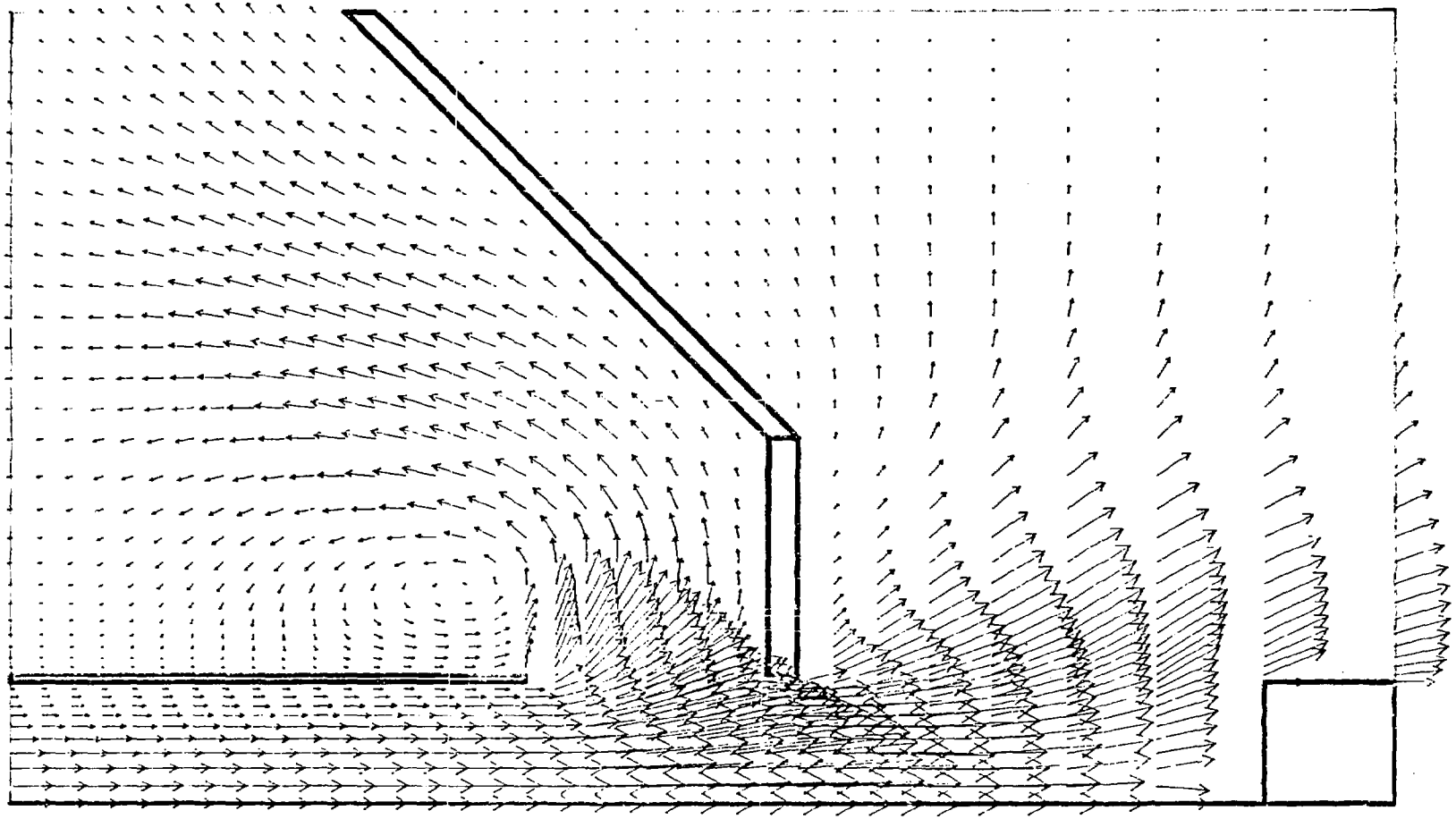

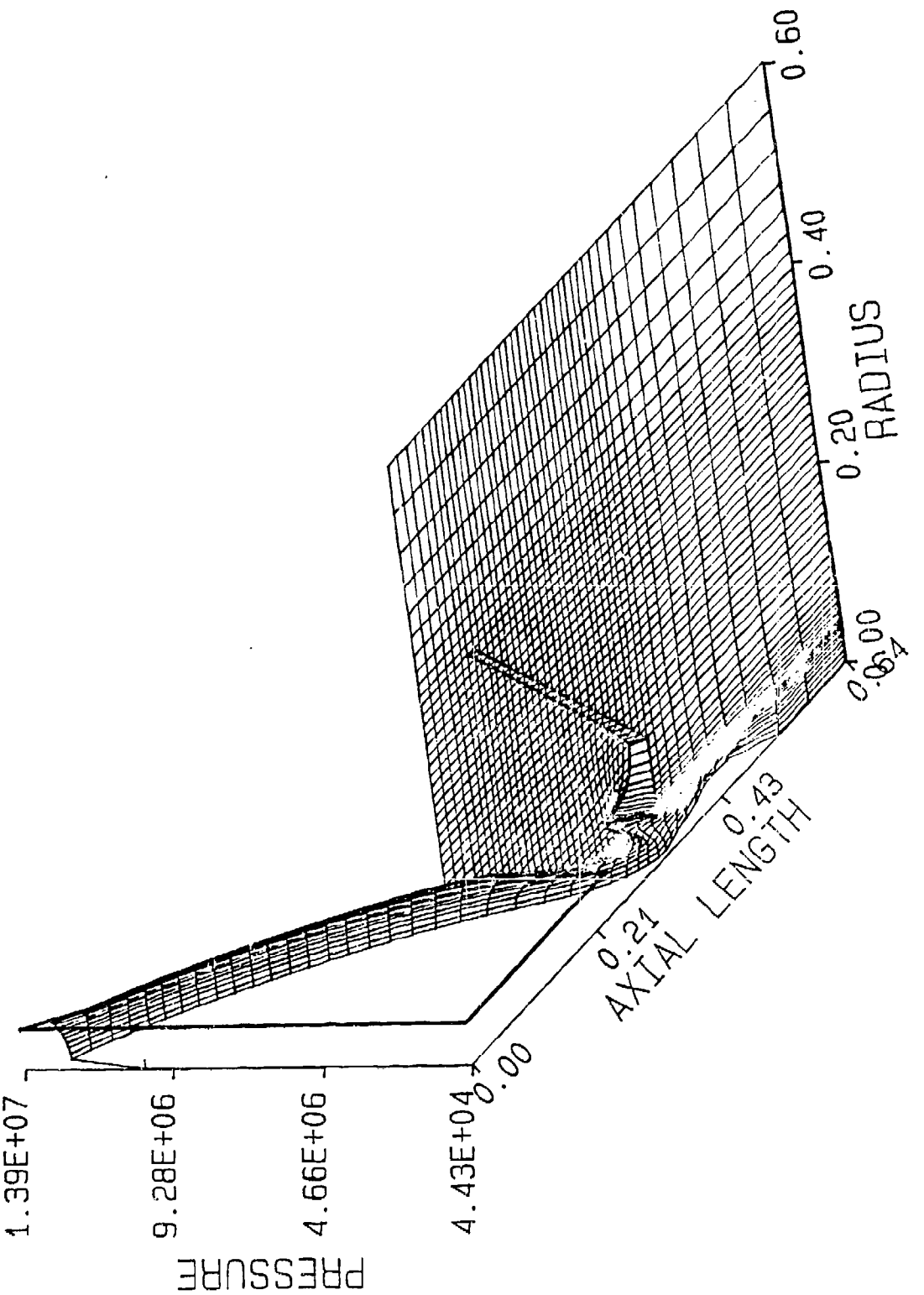

Figure 7b. Pressure Field with the Silencer at T = .6 ms.

Figure 7c. Axial Velocity Field with the Silencer at T = .6 ms.

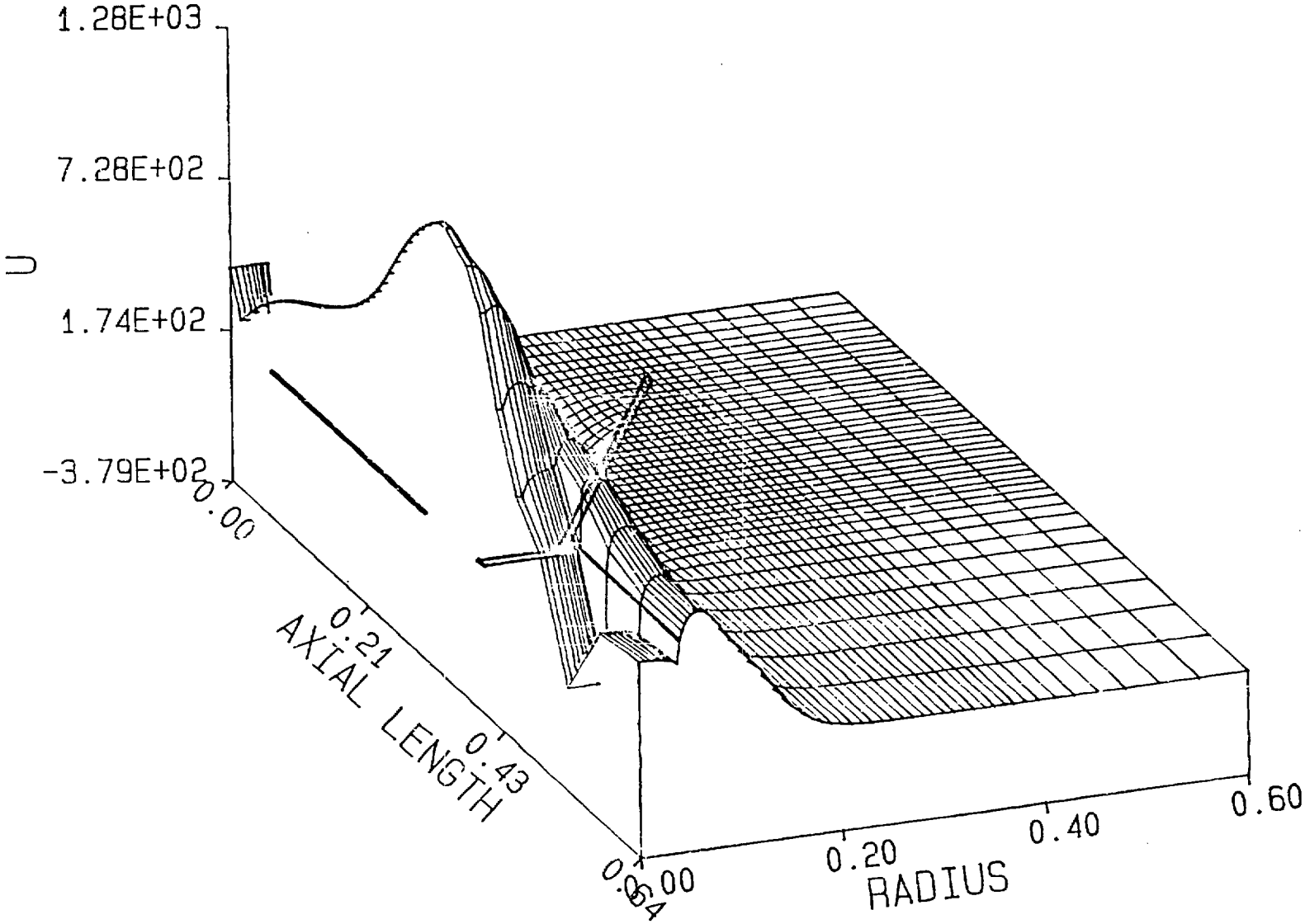

Figure 7d. Radial Velocity Field with the Silencer at T = .6 ms.

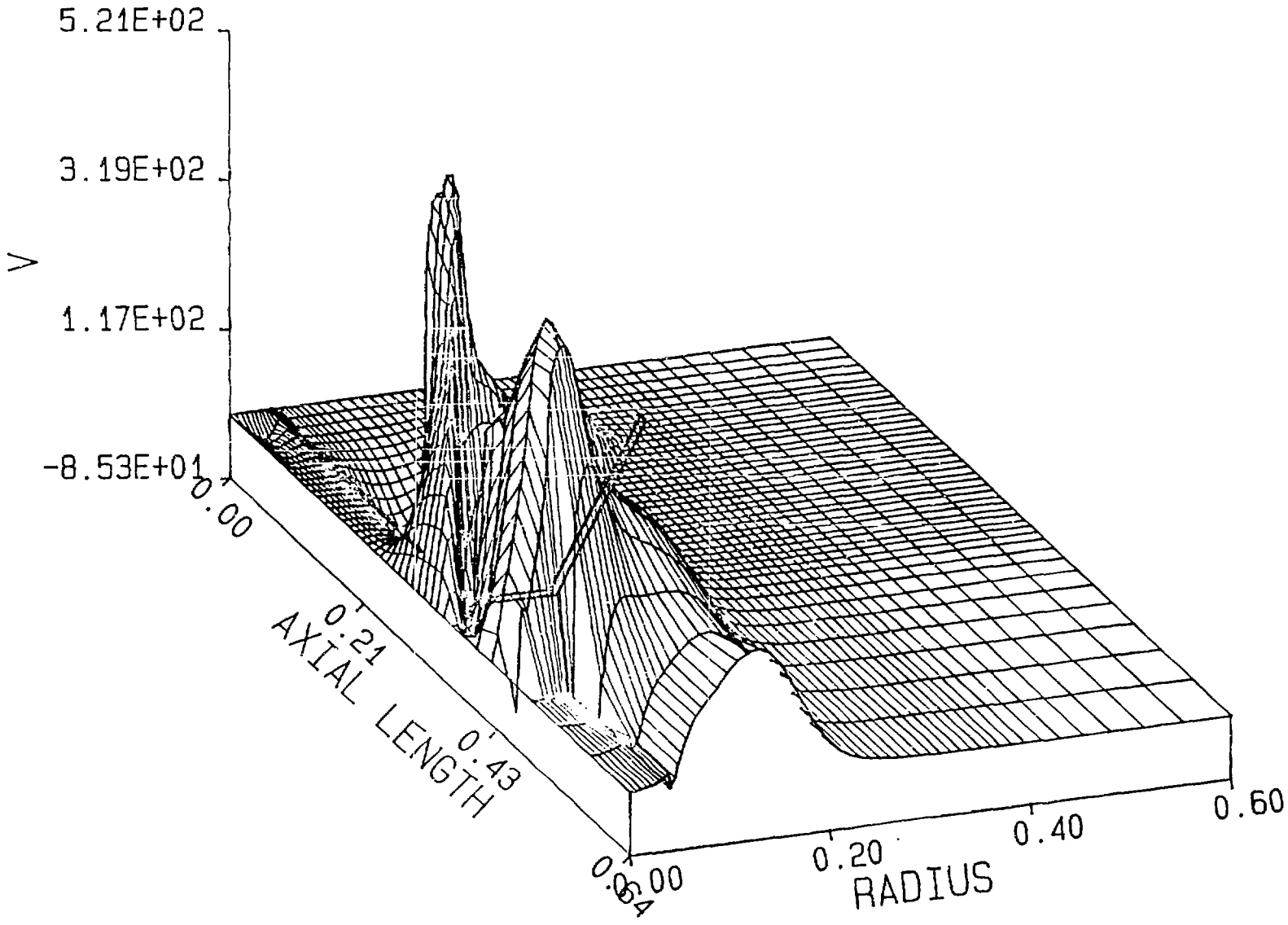

Figure 7e. Mach Number Field with the Silencer at T = .6 ms.

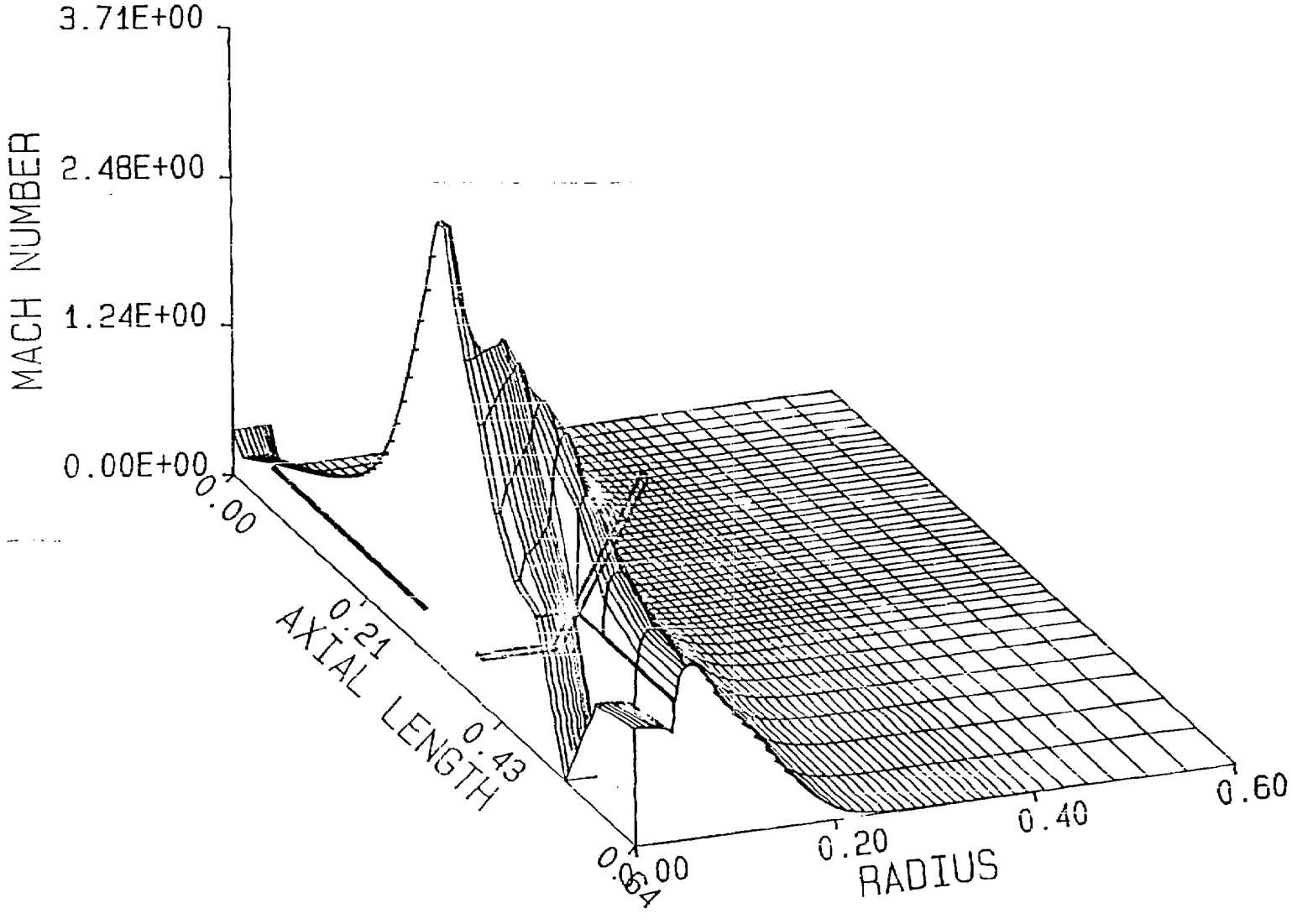

Figure 8a. Velocity Vector Field with the Silencer at T = .8 ms.

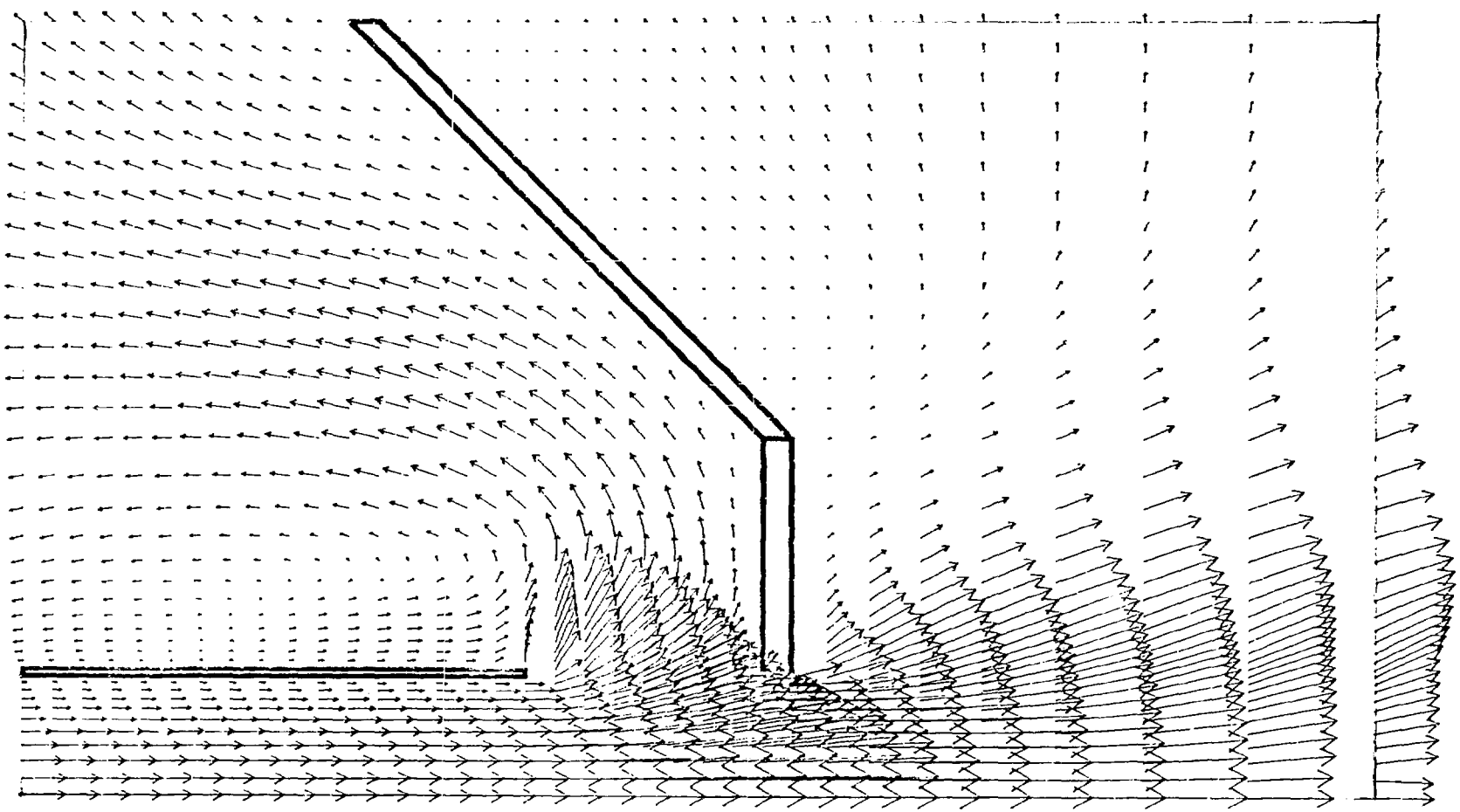

Figure 8b. Pressure Field with the Silencer at T = .8 ms.

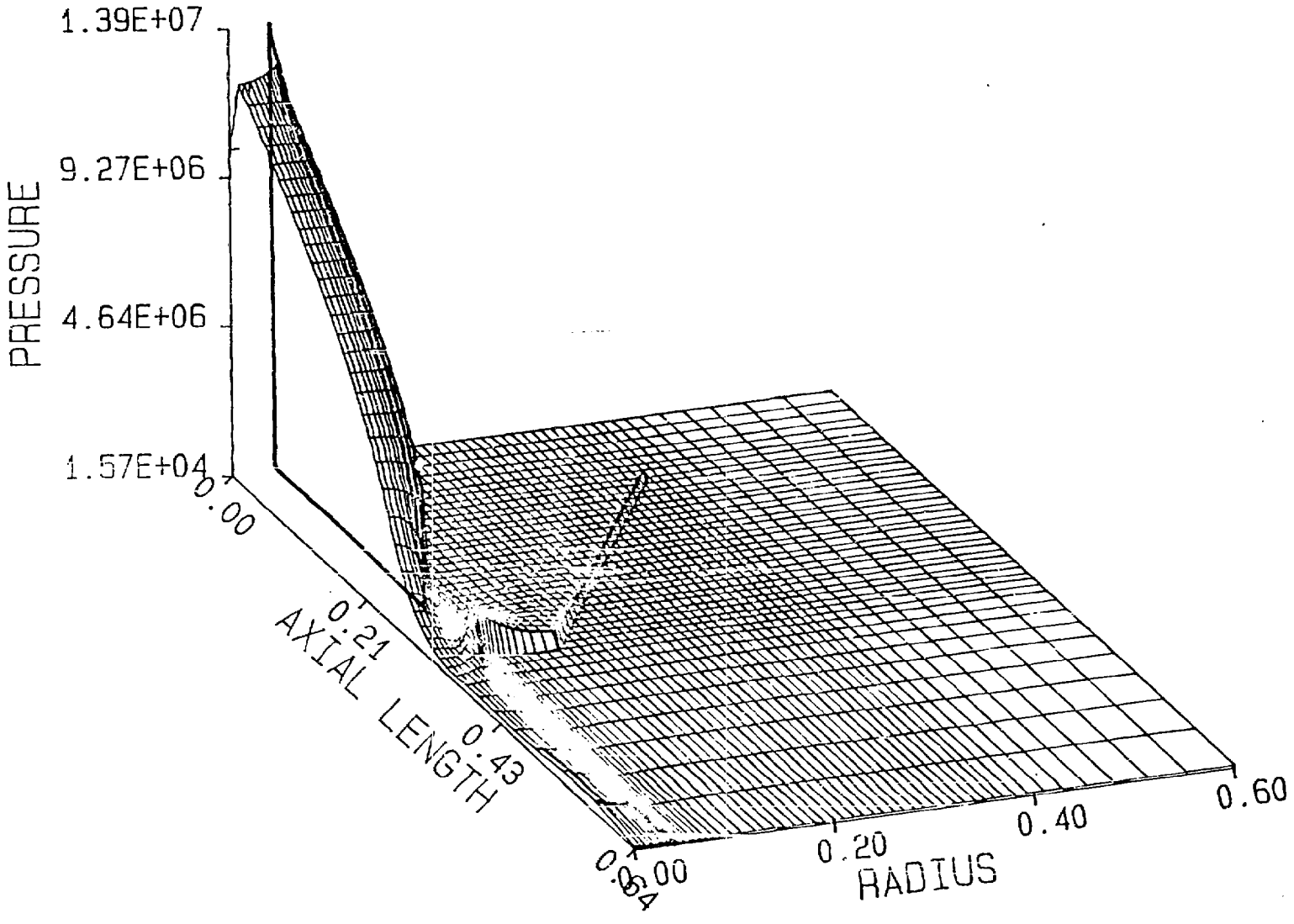

Figure 8c. Axial Velocity Field with the Silencer at T = .8 ms.

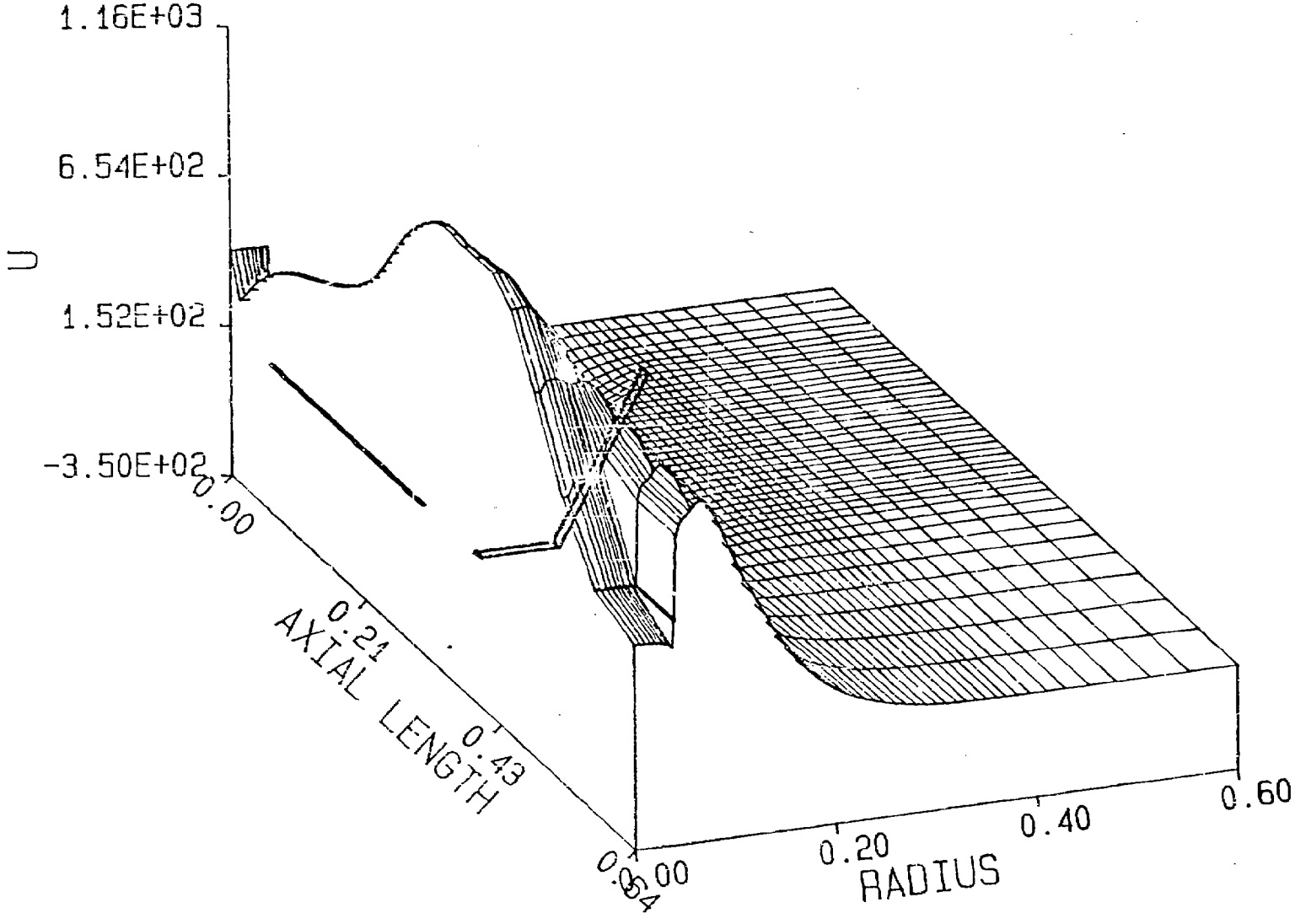

Figure 8d. Radial Velocity Field with the Silencer at T = .8 ms.

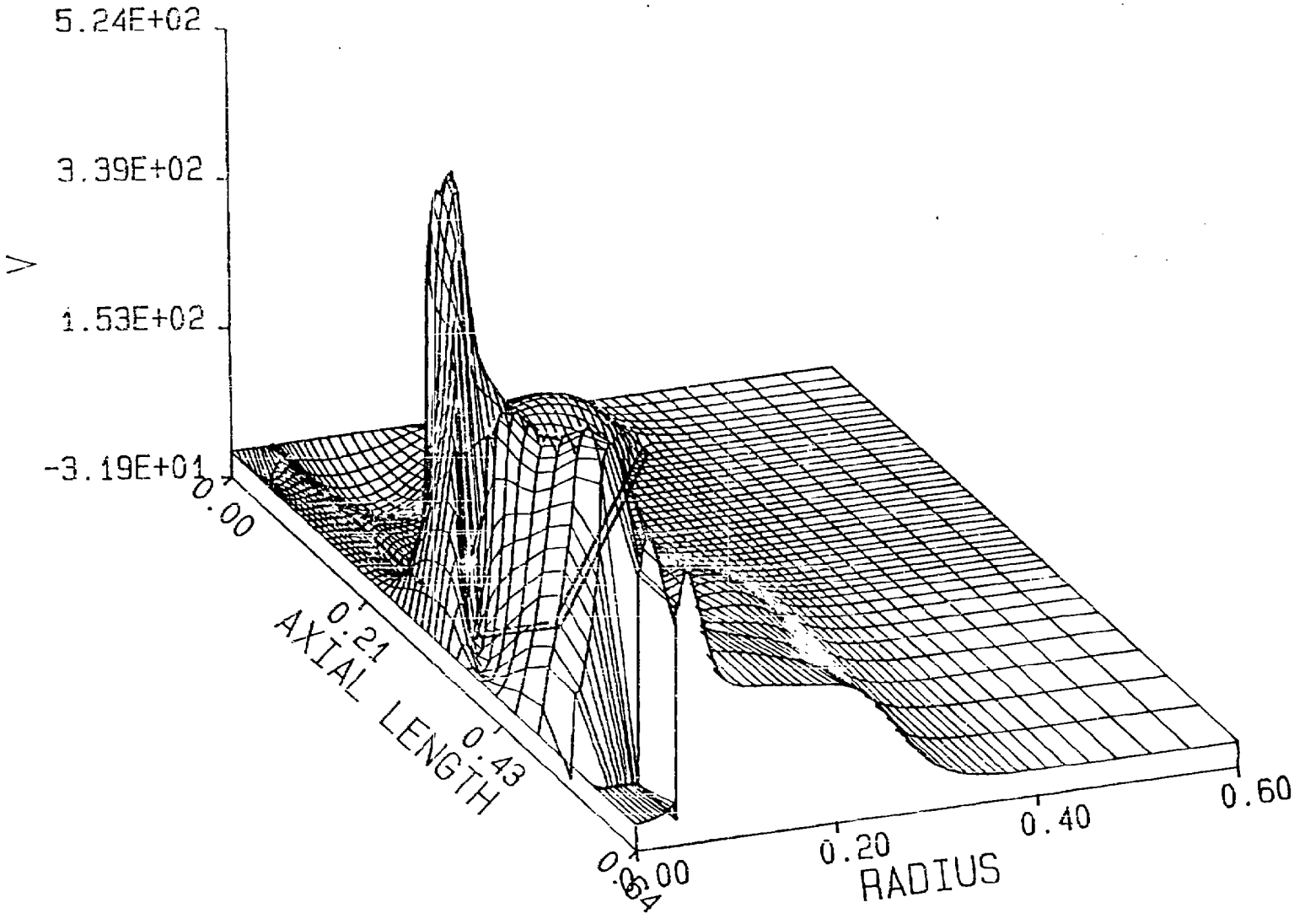

Figure 8e. Mach Number Field with the Silencer at T = .8 ms.

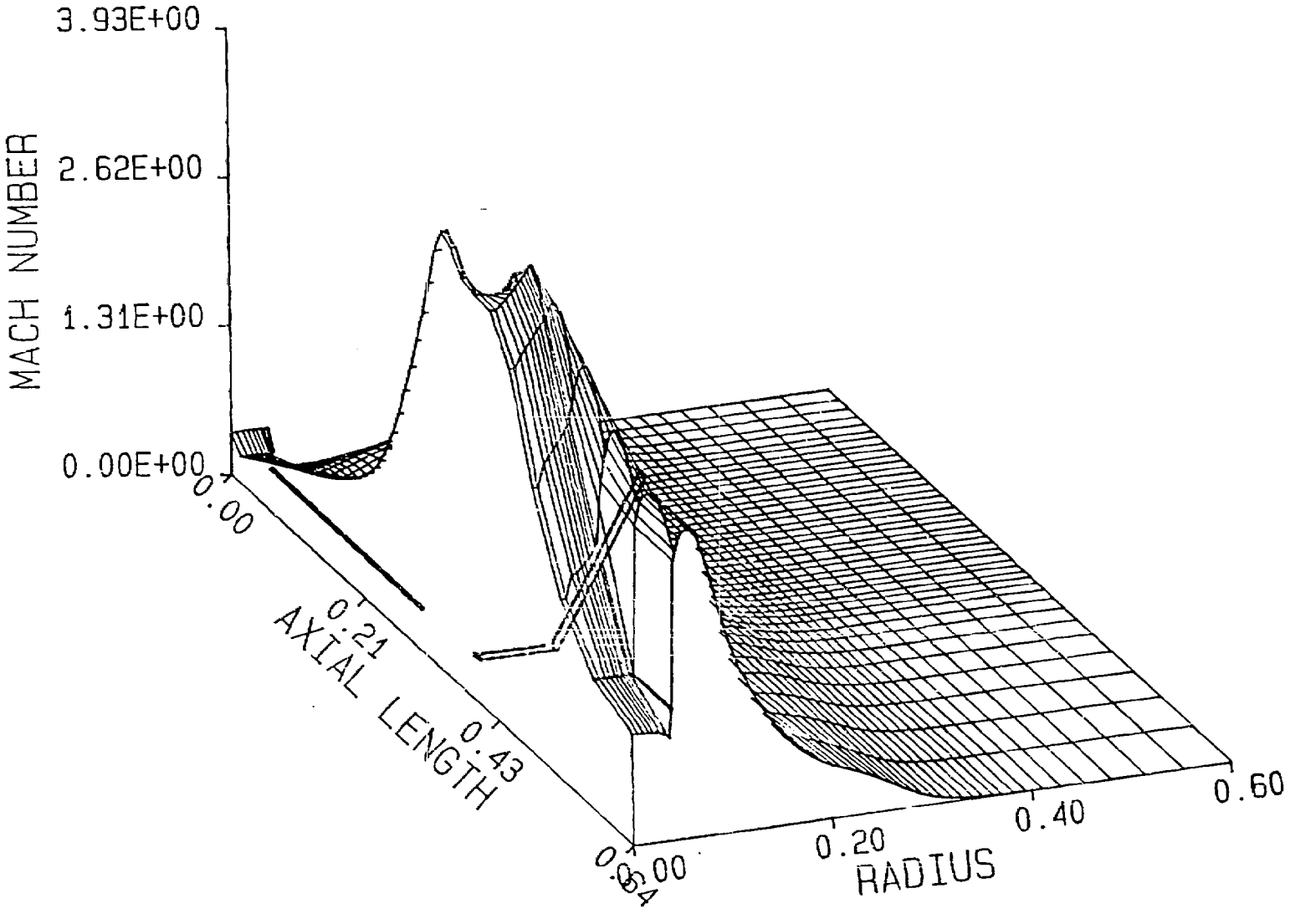

Figure 9a. Velocity Vector Field with the Silencer at T = 1.0 ms.

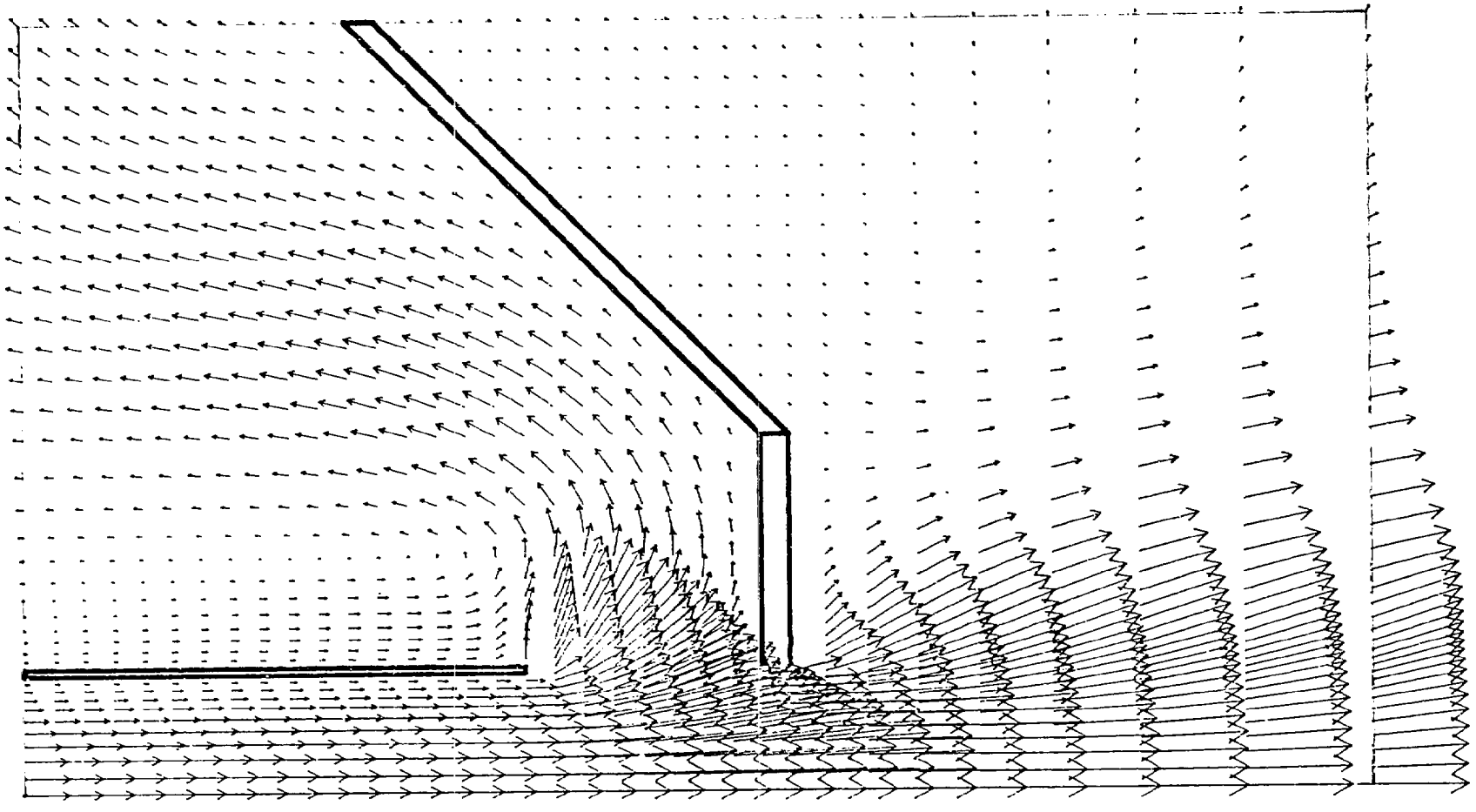

Figure 9b. Pressure Field with the Silencer at T = 1.0 ms.

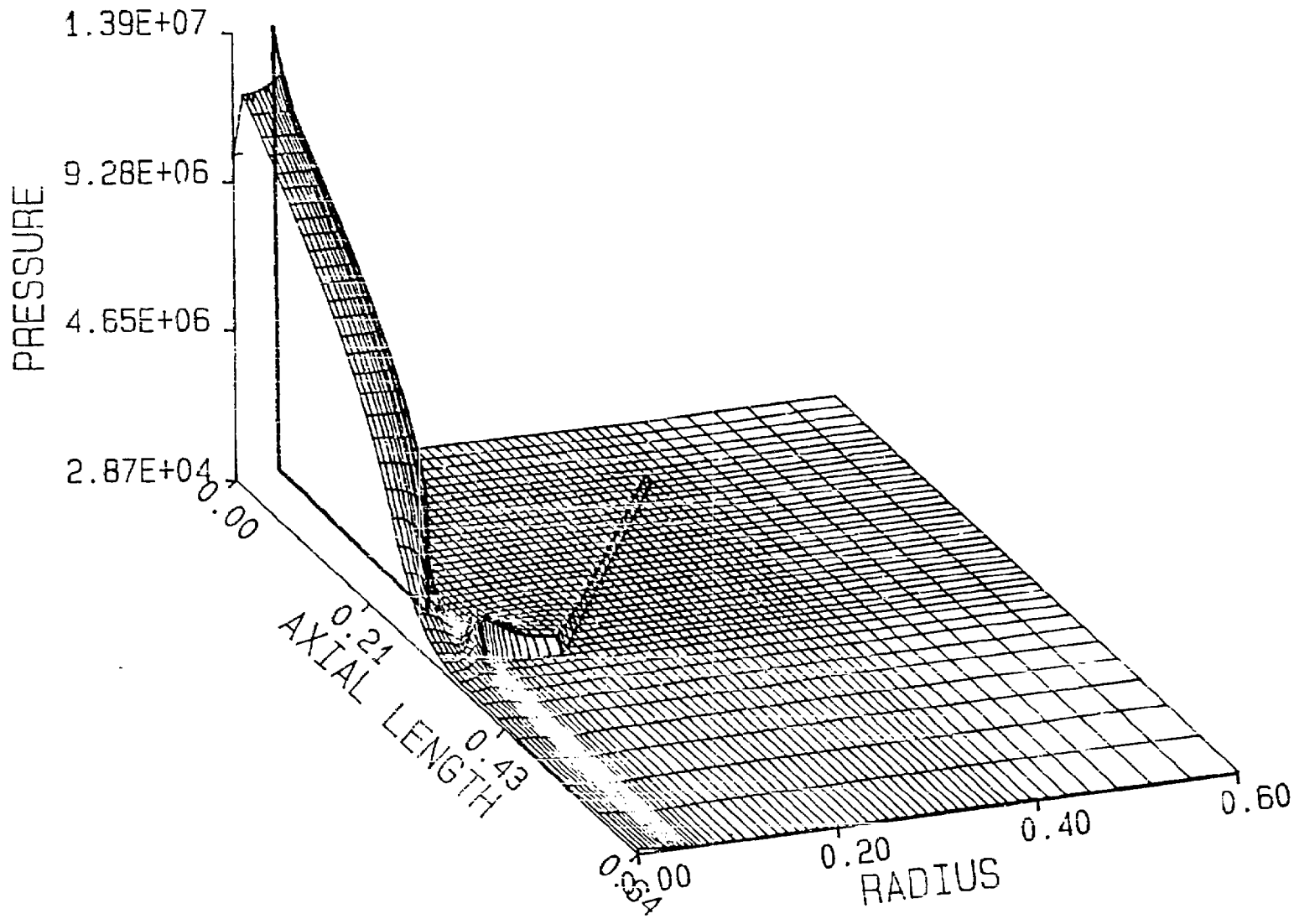

Figure 9c. Axial Velocity Field with the Silencer at T = 1.0 ms.

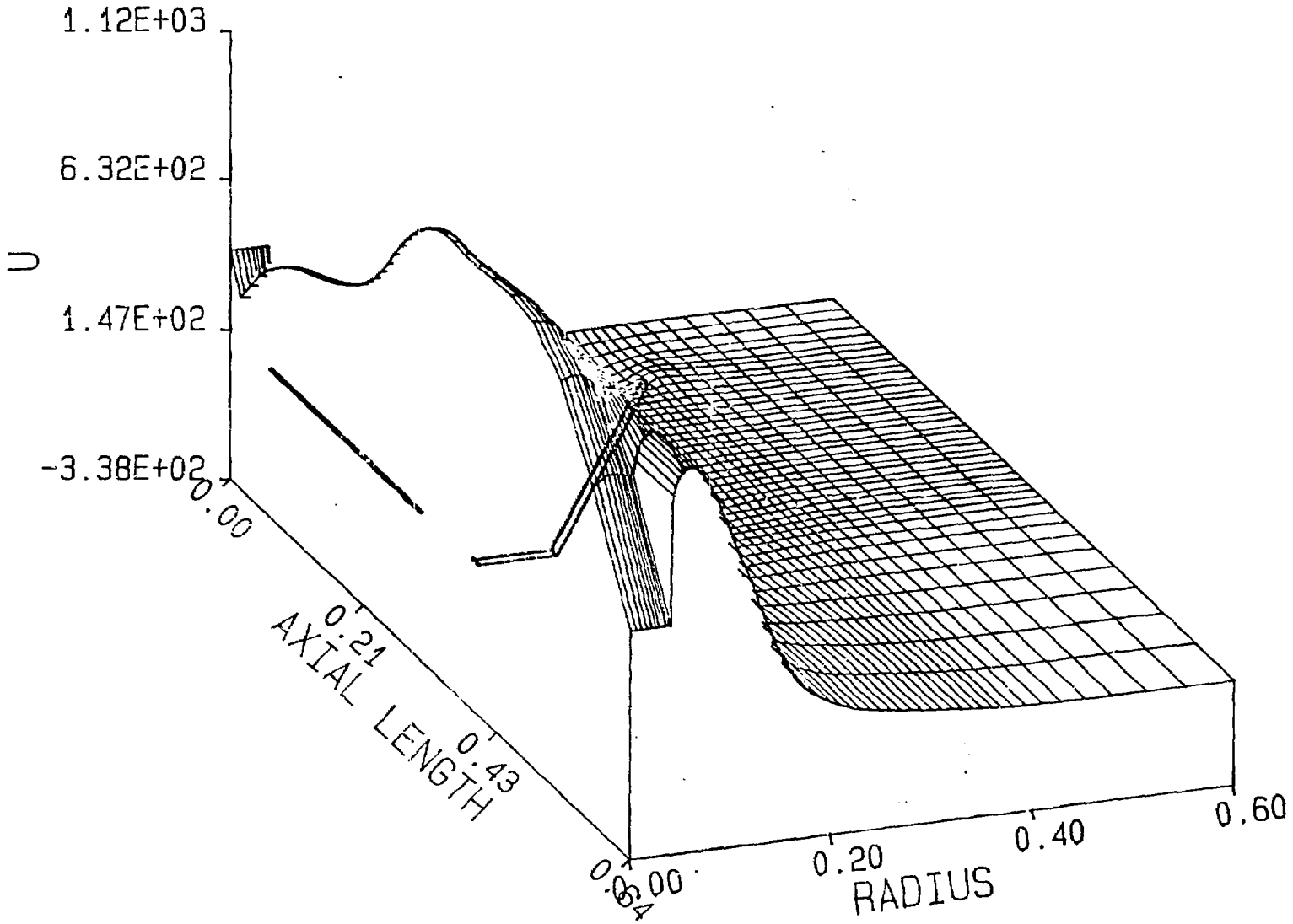

Figure 9d. Radial Velocity Field with the Silencer at T = 1.0 ms.

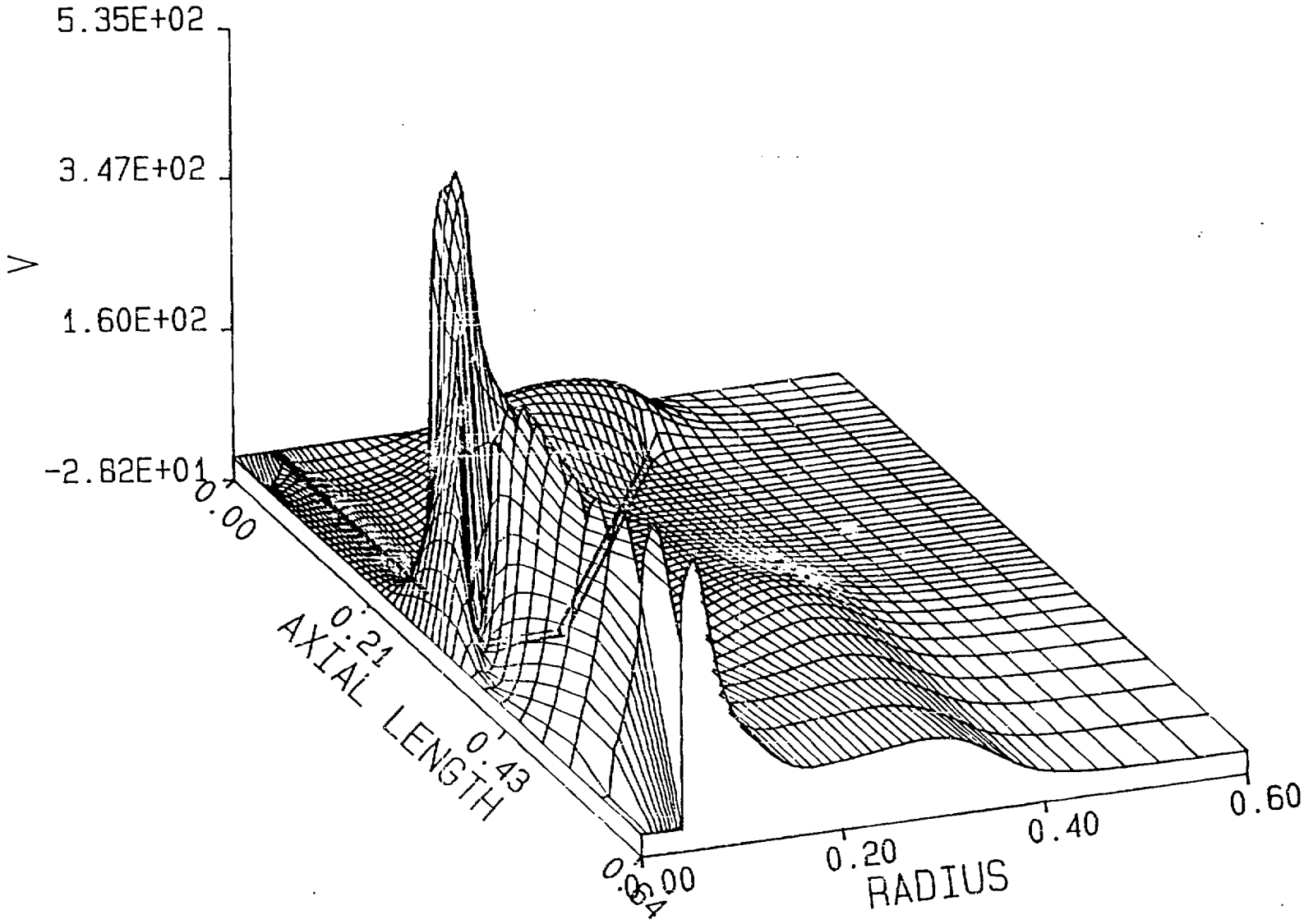

Figure 9e. Mach Number Field with the Silencer at T = 1.0 ms.

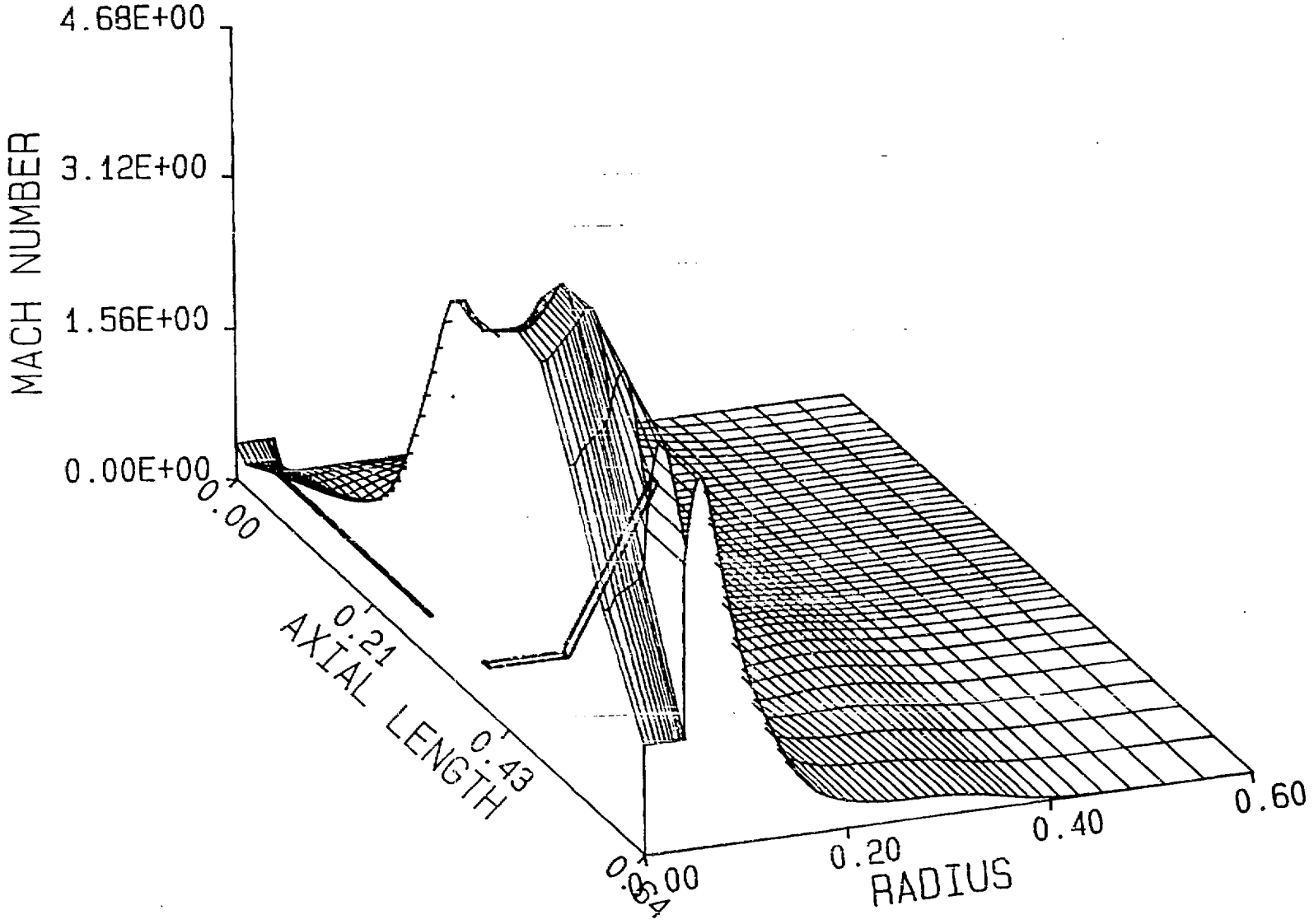

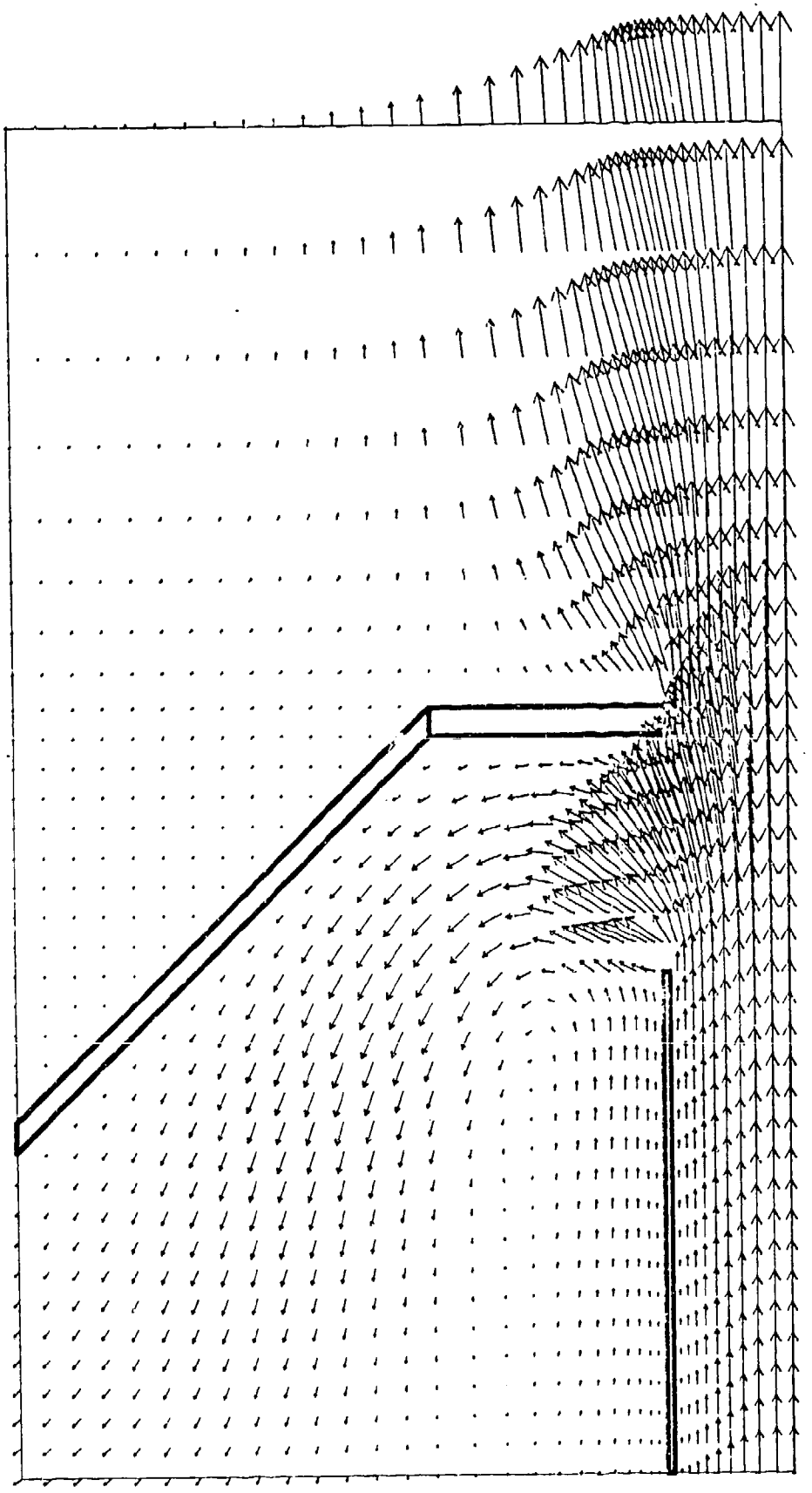

Figure 10a. Velocity Vector Field with the Silencer at T = 1.5 ms.

Figure 10b. Pressure Field with the Silencer at T = 1.5 ms.

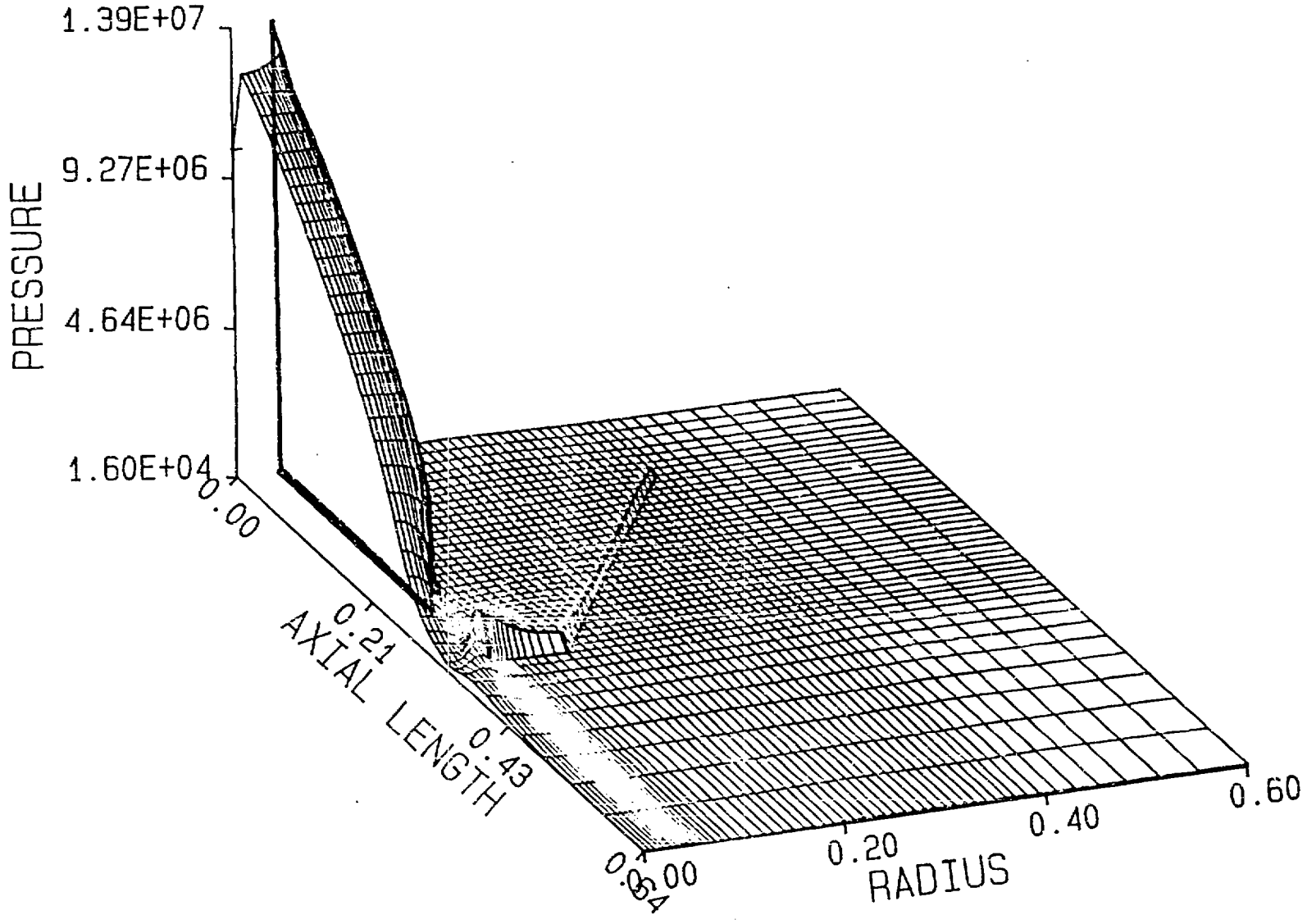

Figure 10c. Axial Velocity Field with the Silencer at T = 1.5 ms.

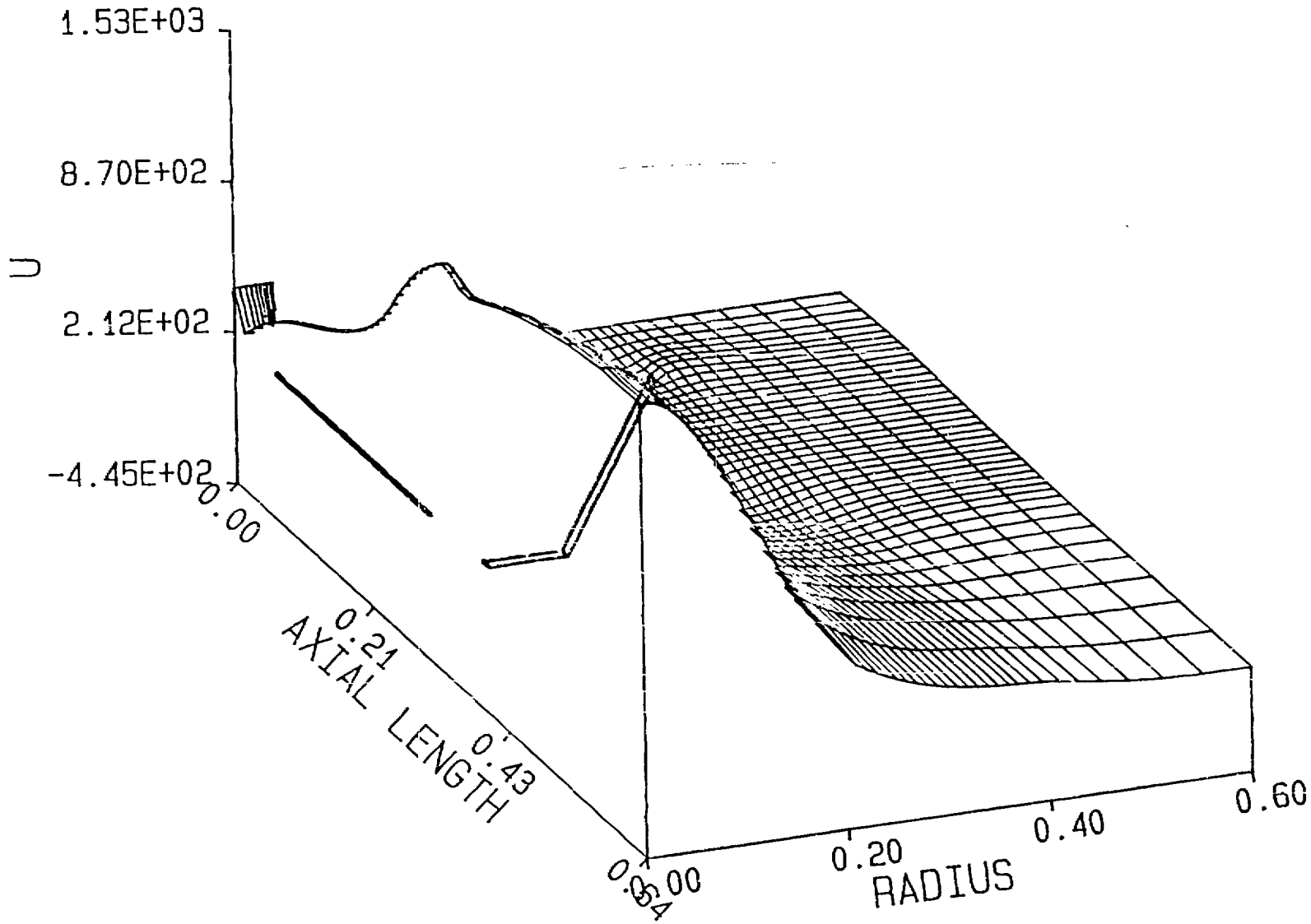

Figure 10d. Radial Velocity Field with the Silencer at T = 1.5 ms.

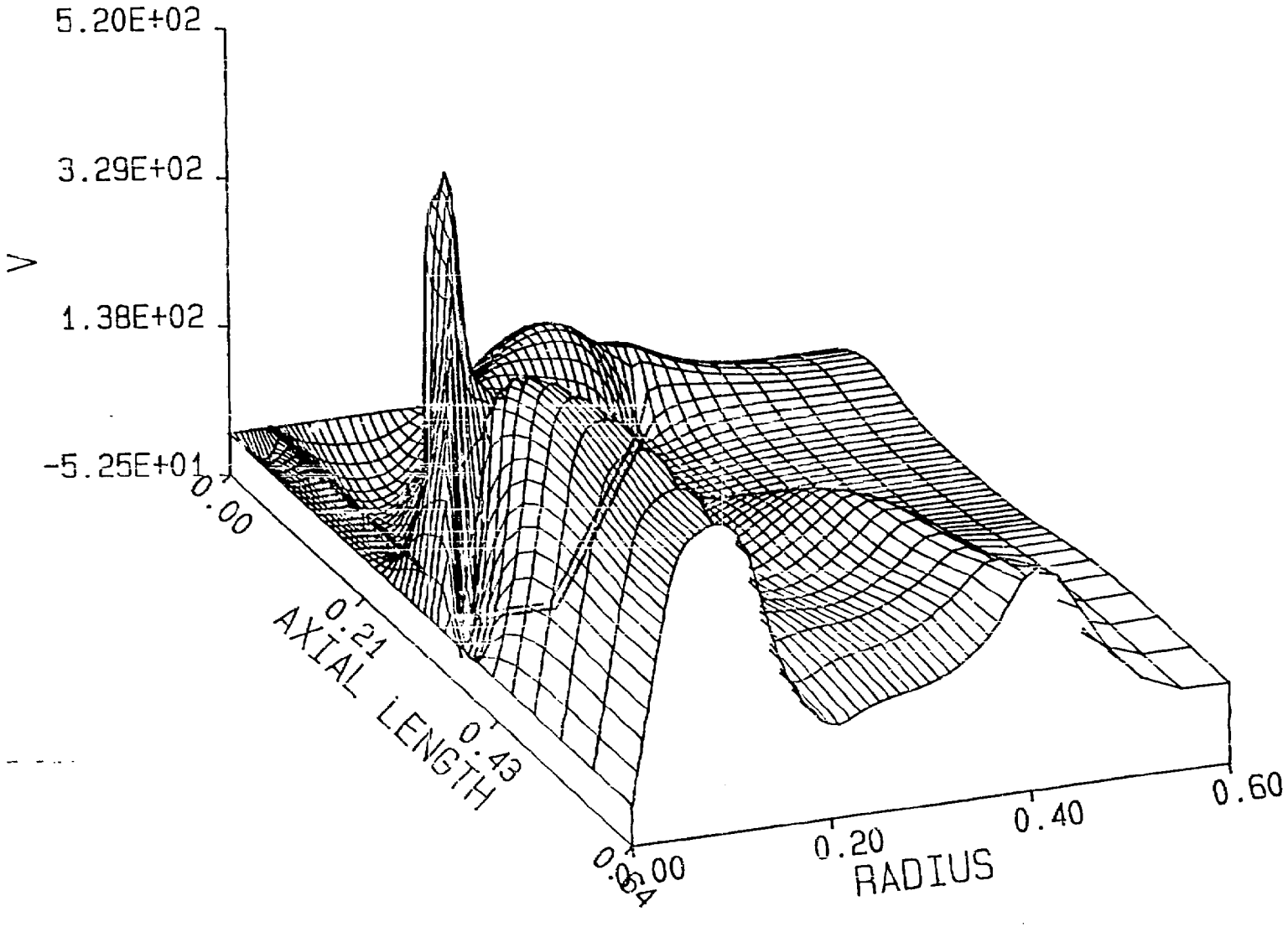

Figure 10e. Mach Number Field with the Silencer at T = 1.5 ms.

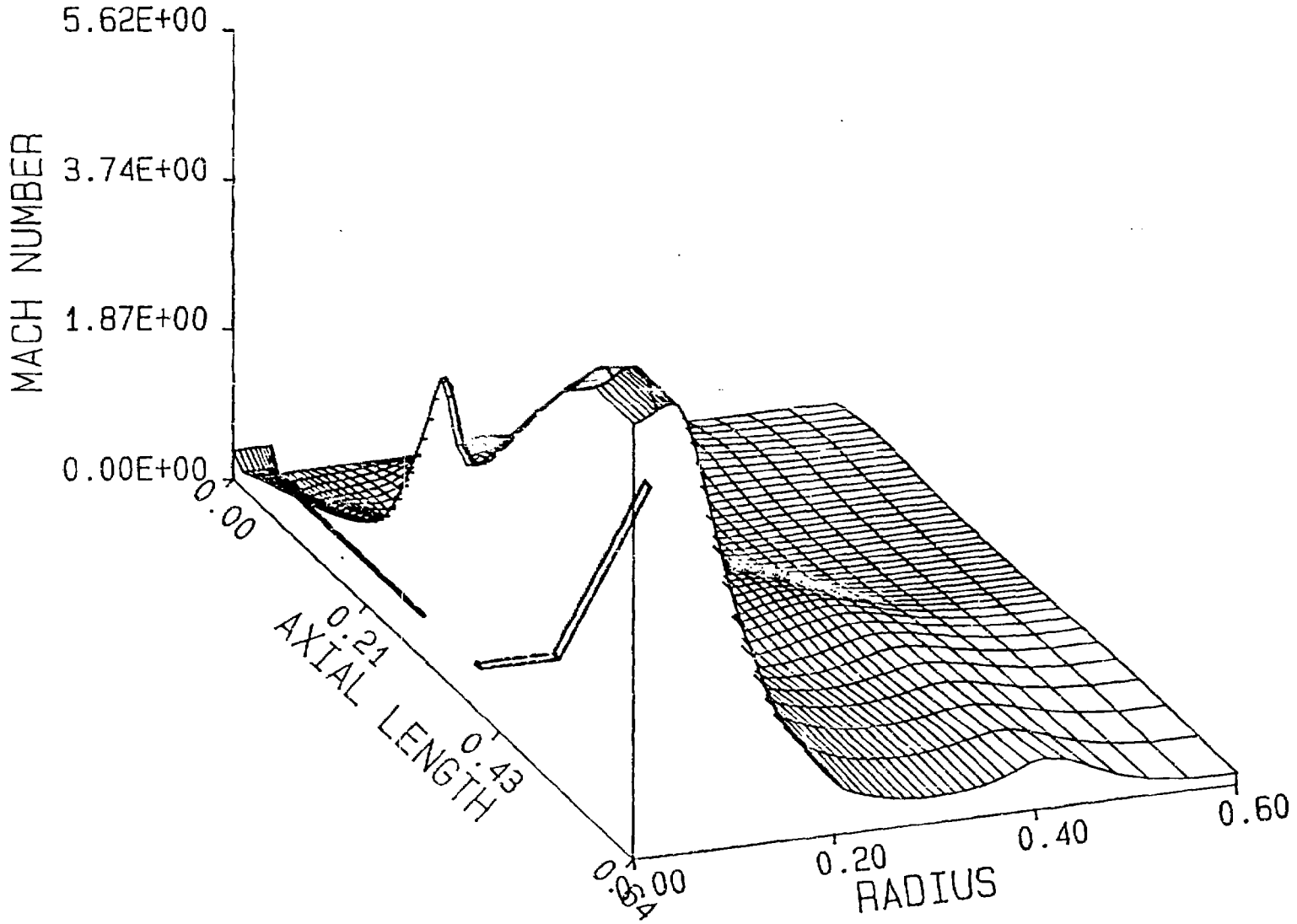

Figure 11a. Velocity Vector Field with the Silencer at T = 2.0 ms.

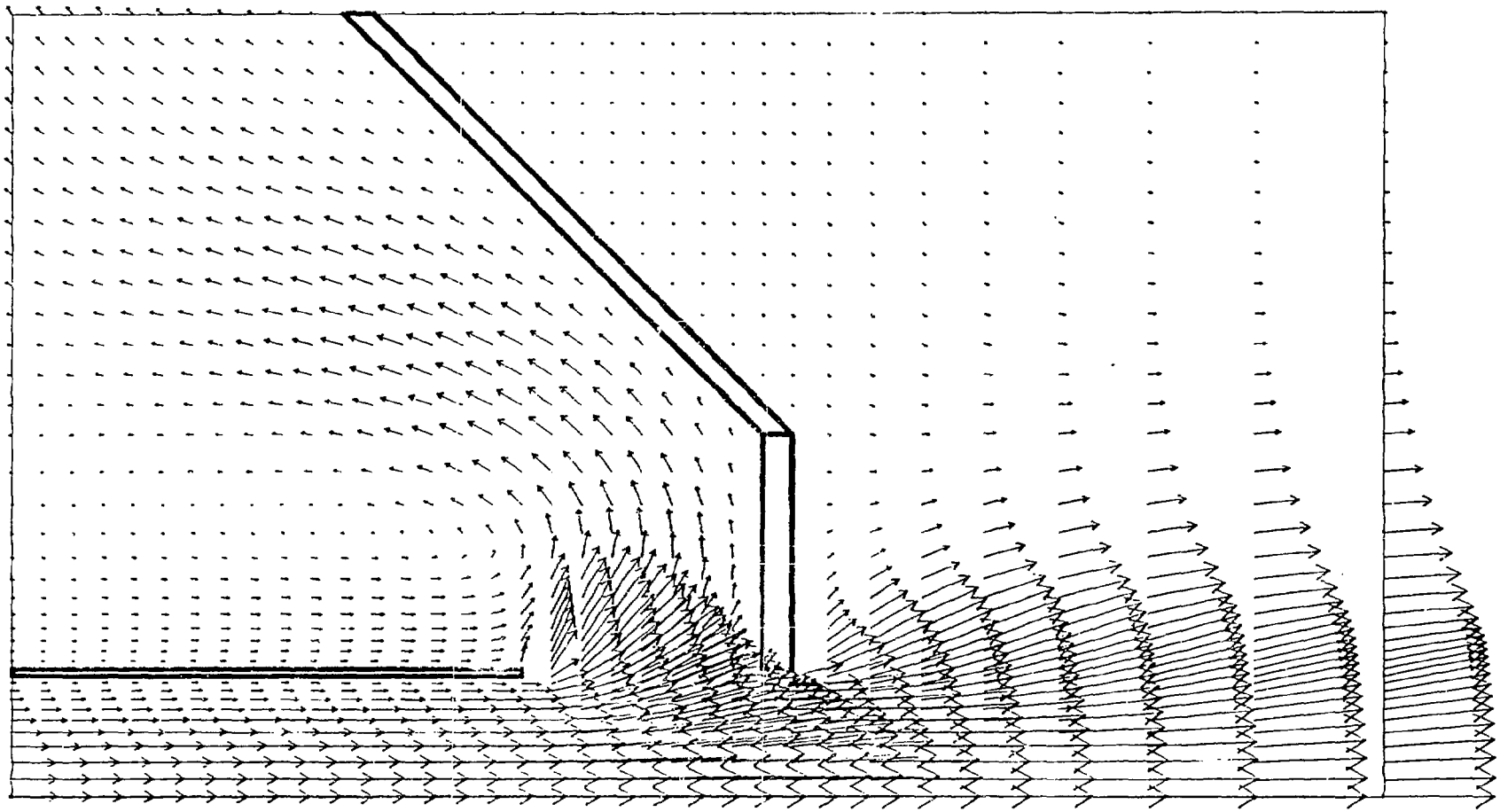

Figure 11h. Pressure Field with the Silencer at T = 2.0 ms.

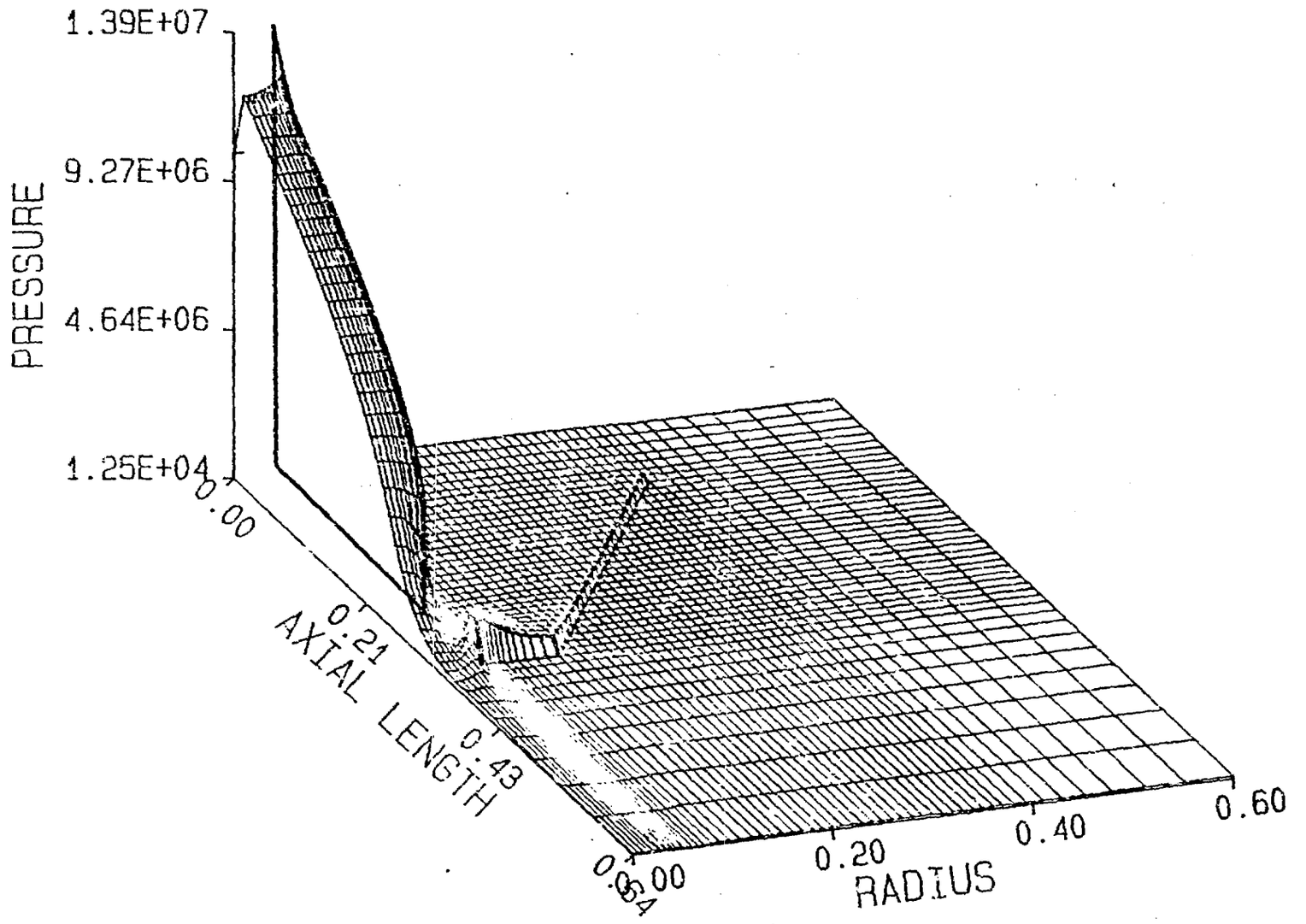

Figure 11c. Axial Velocity Field with the Silencer at T = 2.0 ms.

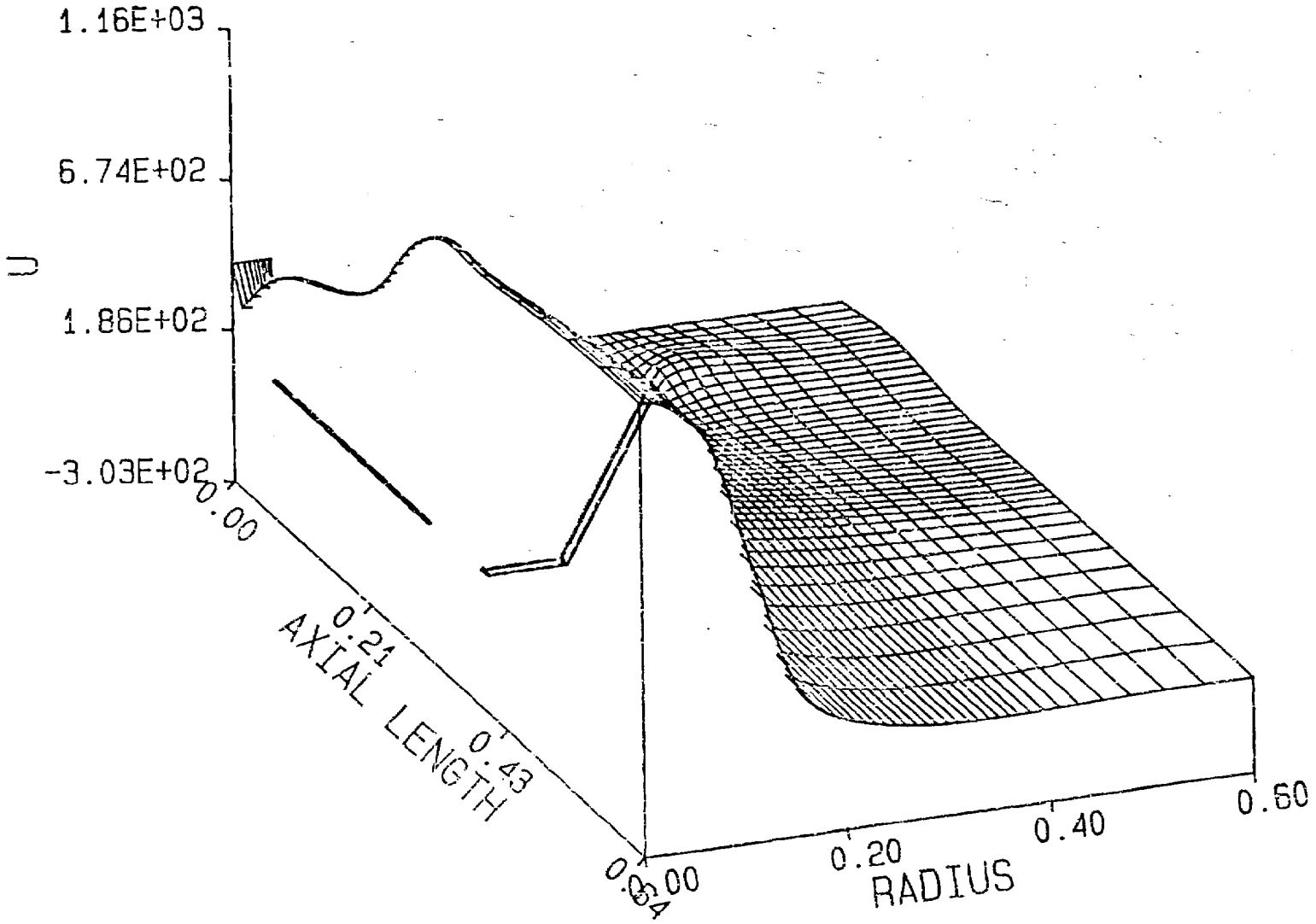

Figure 11d. Radial Velocity Field with the Silencer at T = 2.0 ms.

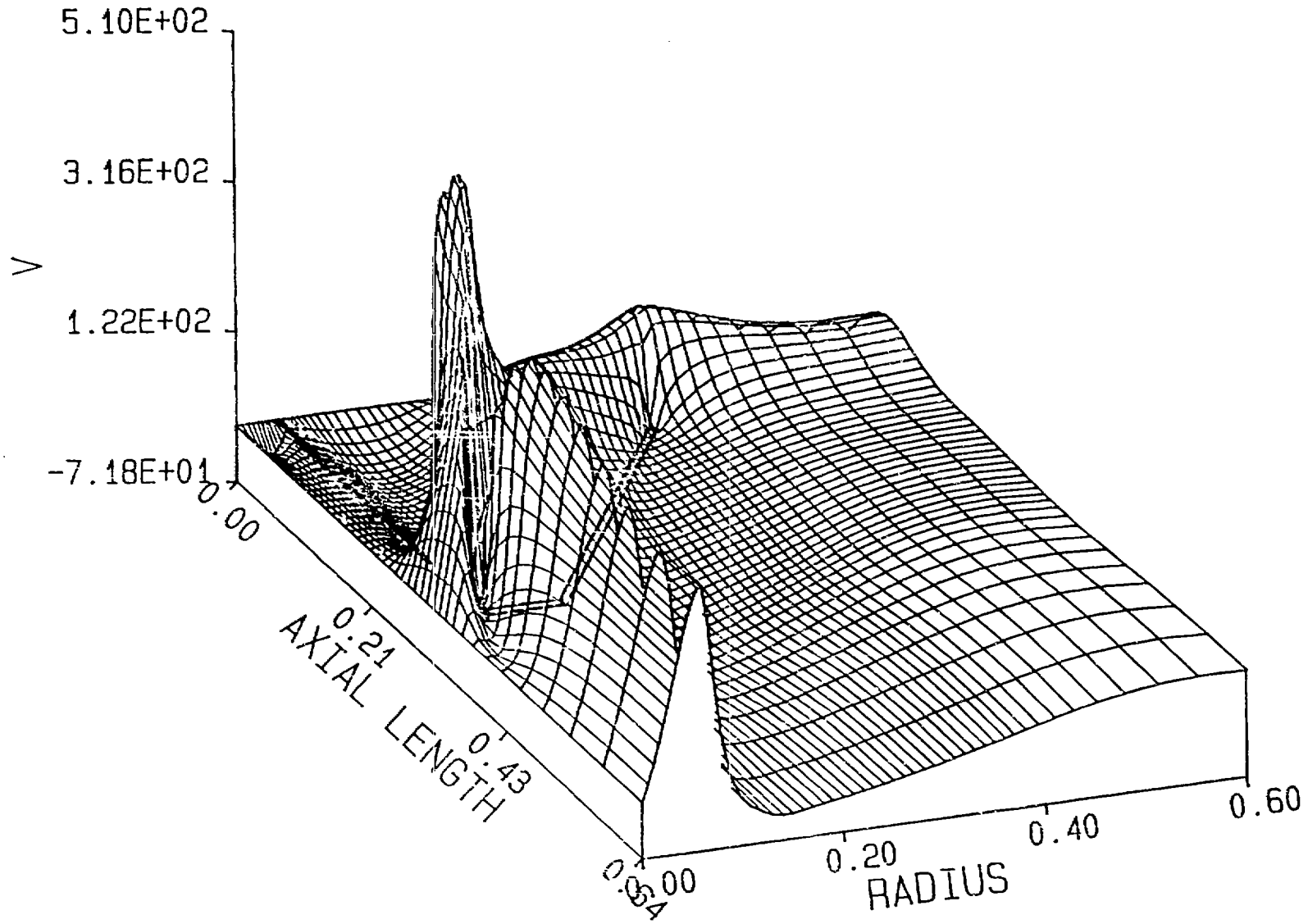

Figure 11e. Mach Number Field with the Silencer at T = 2.0 ms.

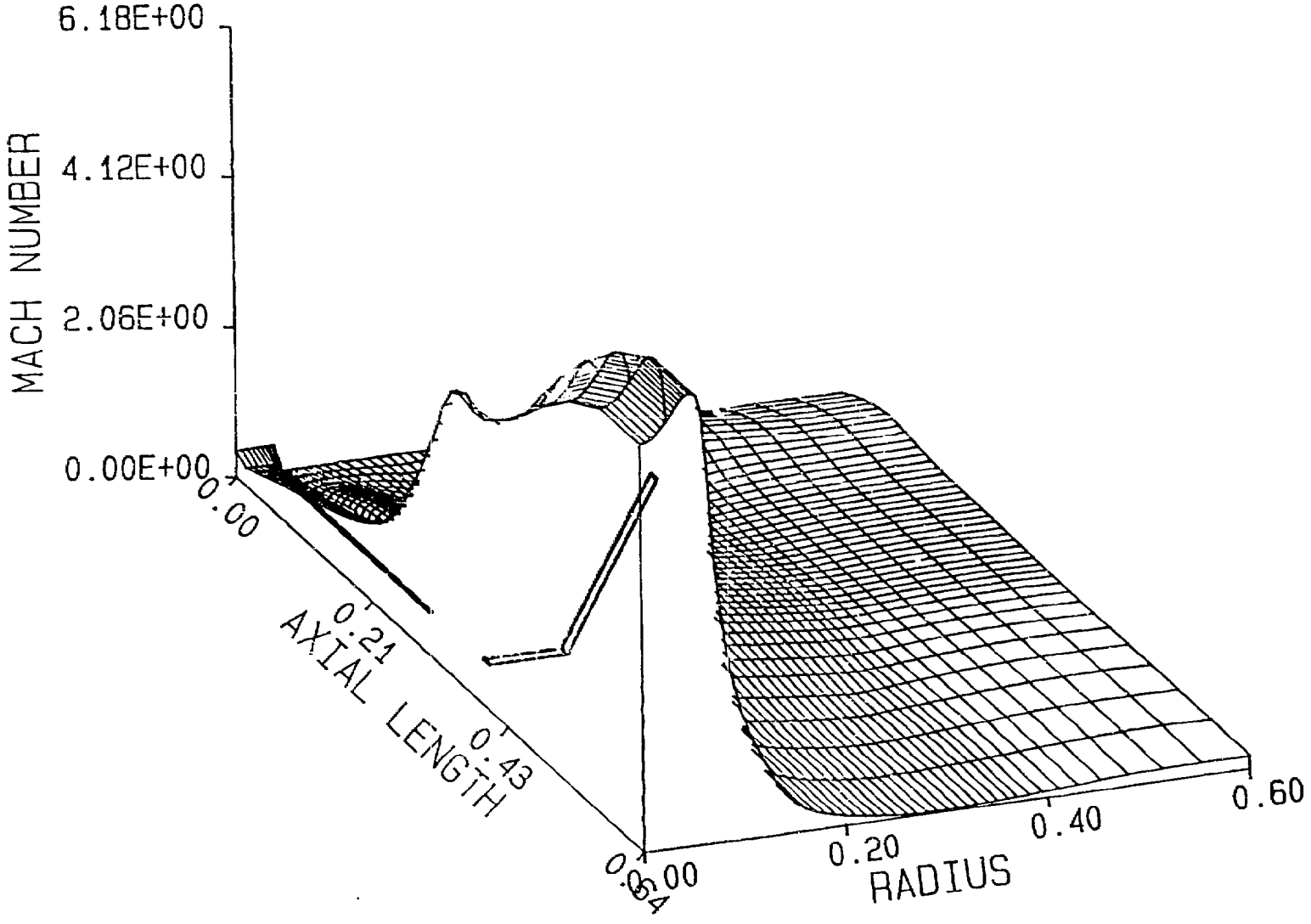

Figure 12a. Velocity Vector Field with the Silencer at T = 3.0 ms.

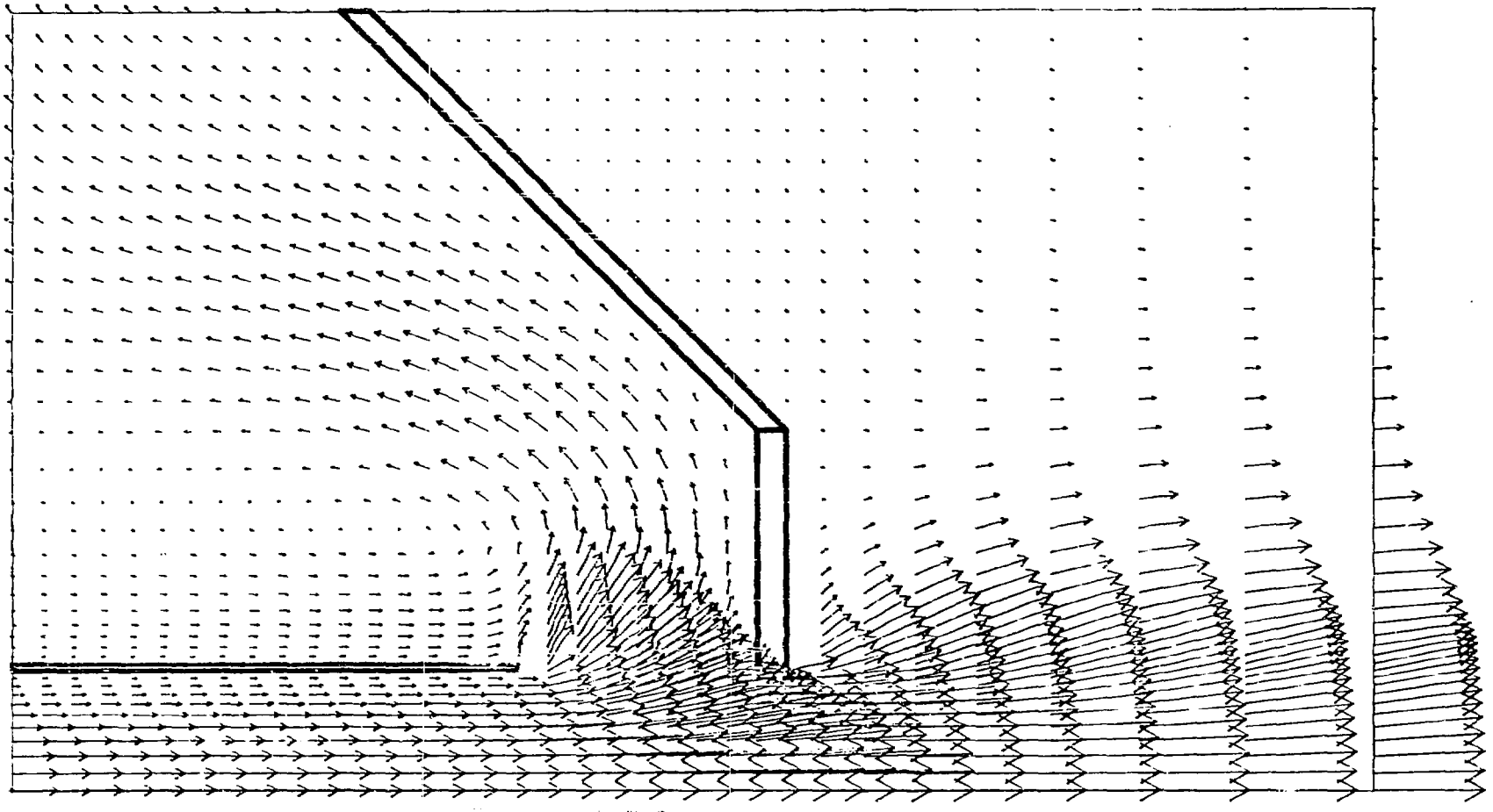

Figure 12b. Pressure Field with the Silencer at T = 3.0 ms.

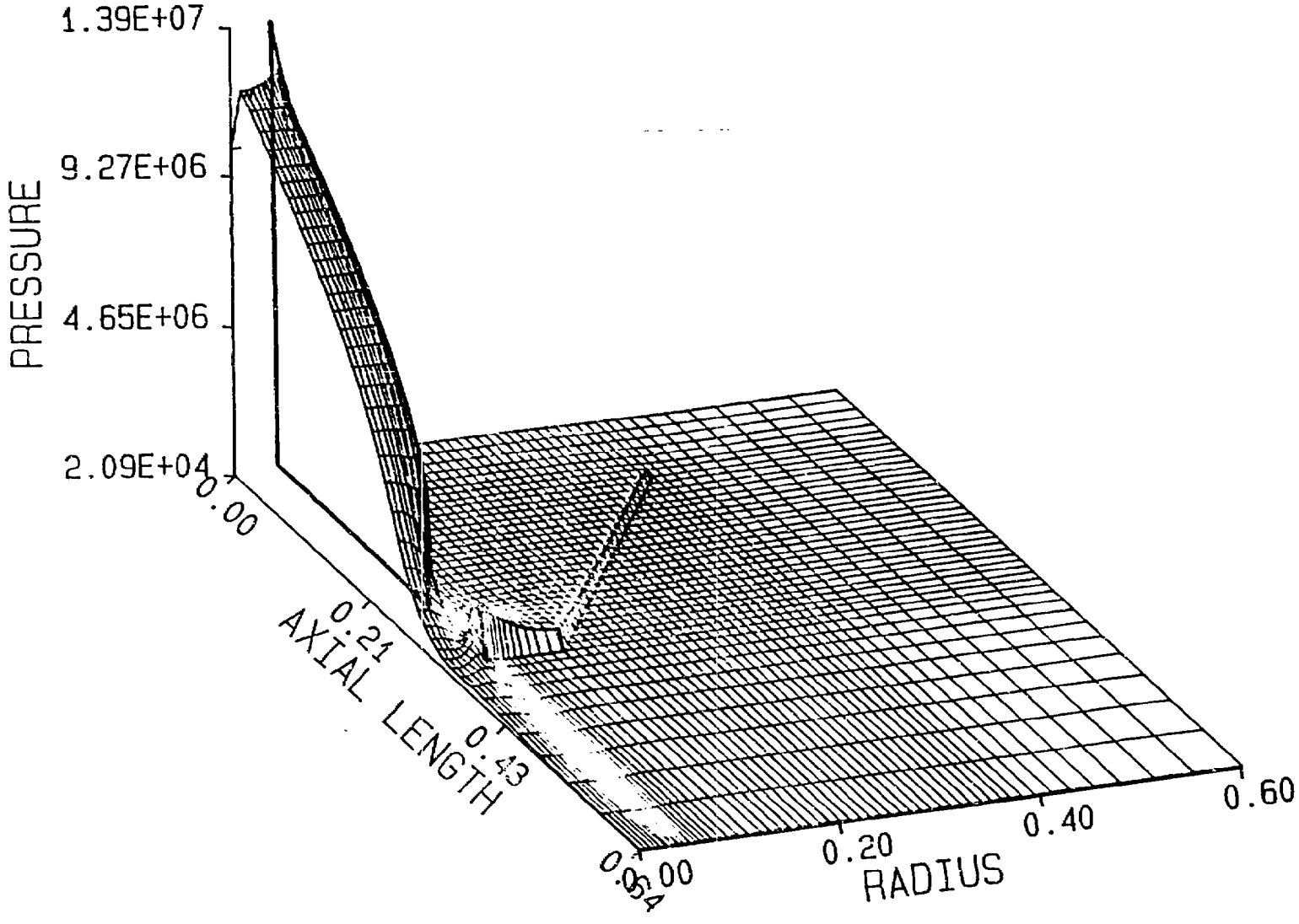

Figure 12c. Axial Velocity Field with the Silencer at T = 3.0 ms.

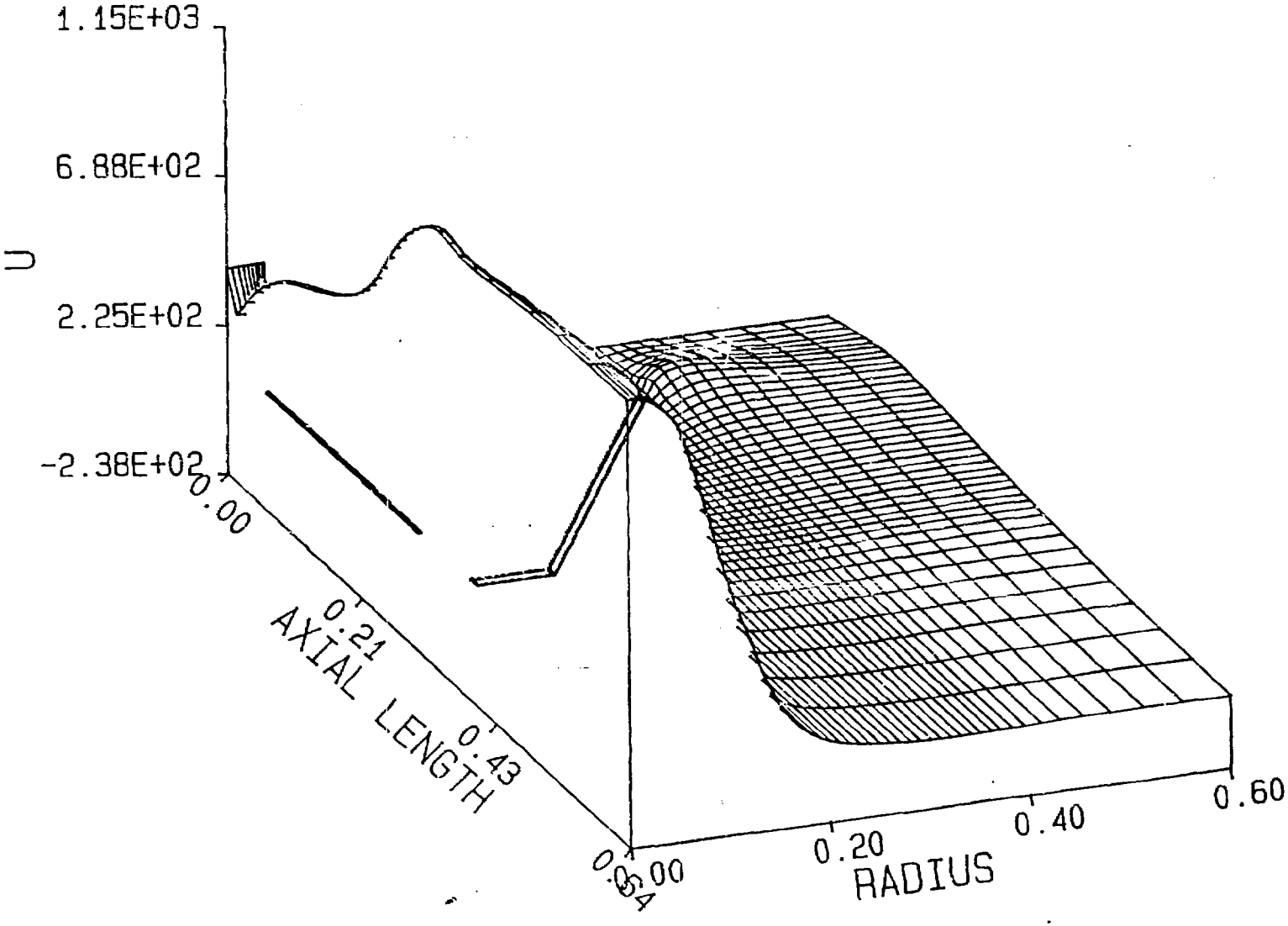

Figure 12d. Radial Velocity Field with the Silencer at T = 3.0 ms.

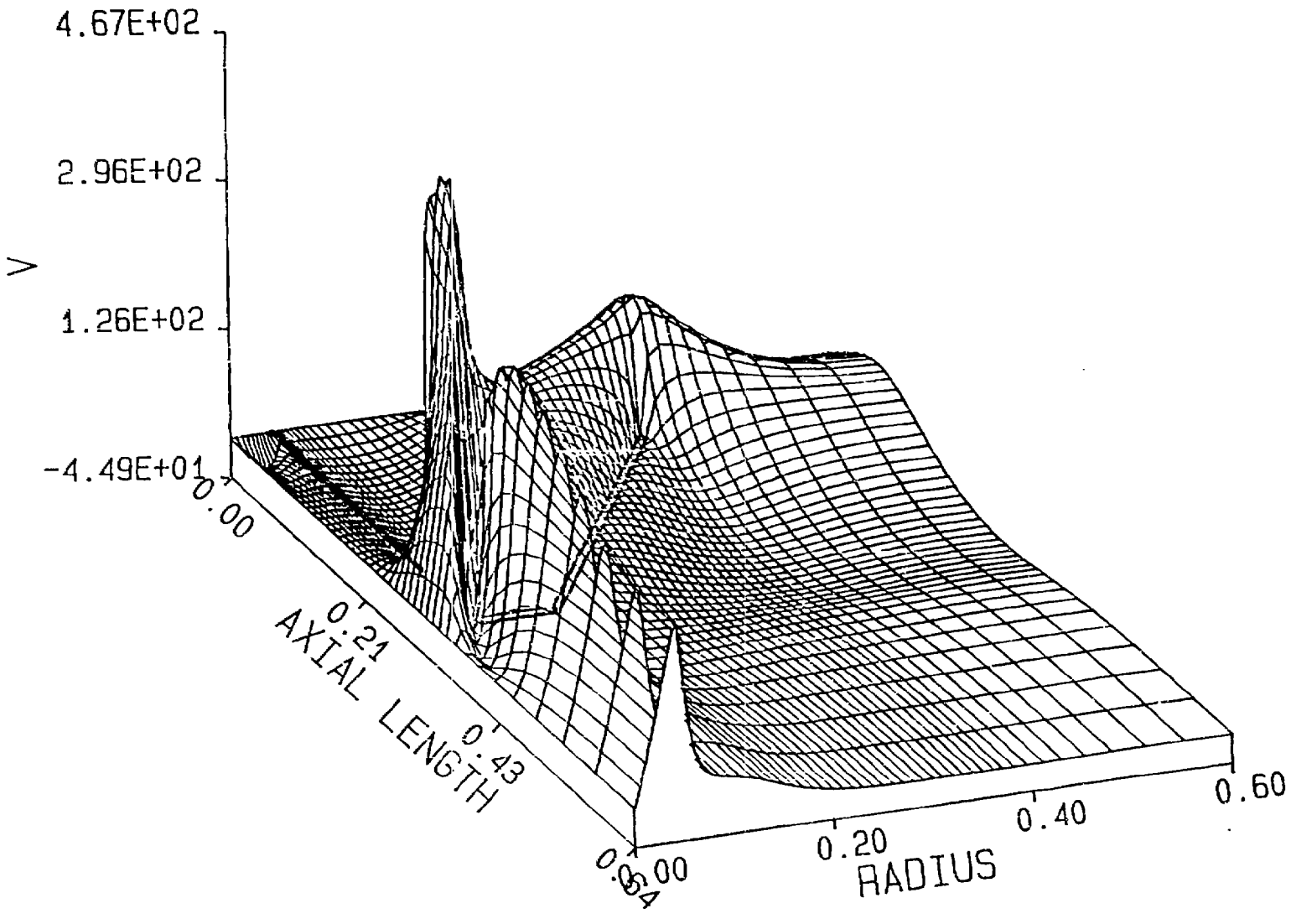

Figure 12e. Mach Number Field with the Silencer at T = 3.0 ms.

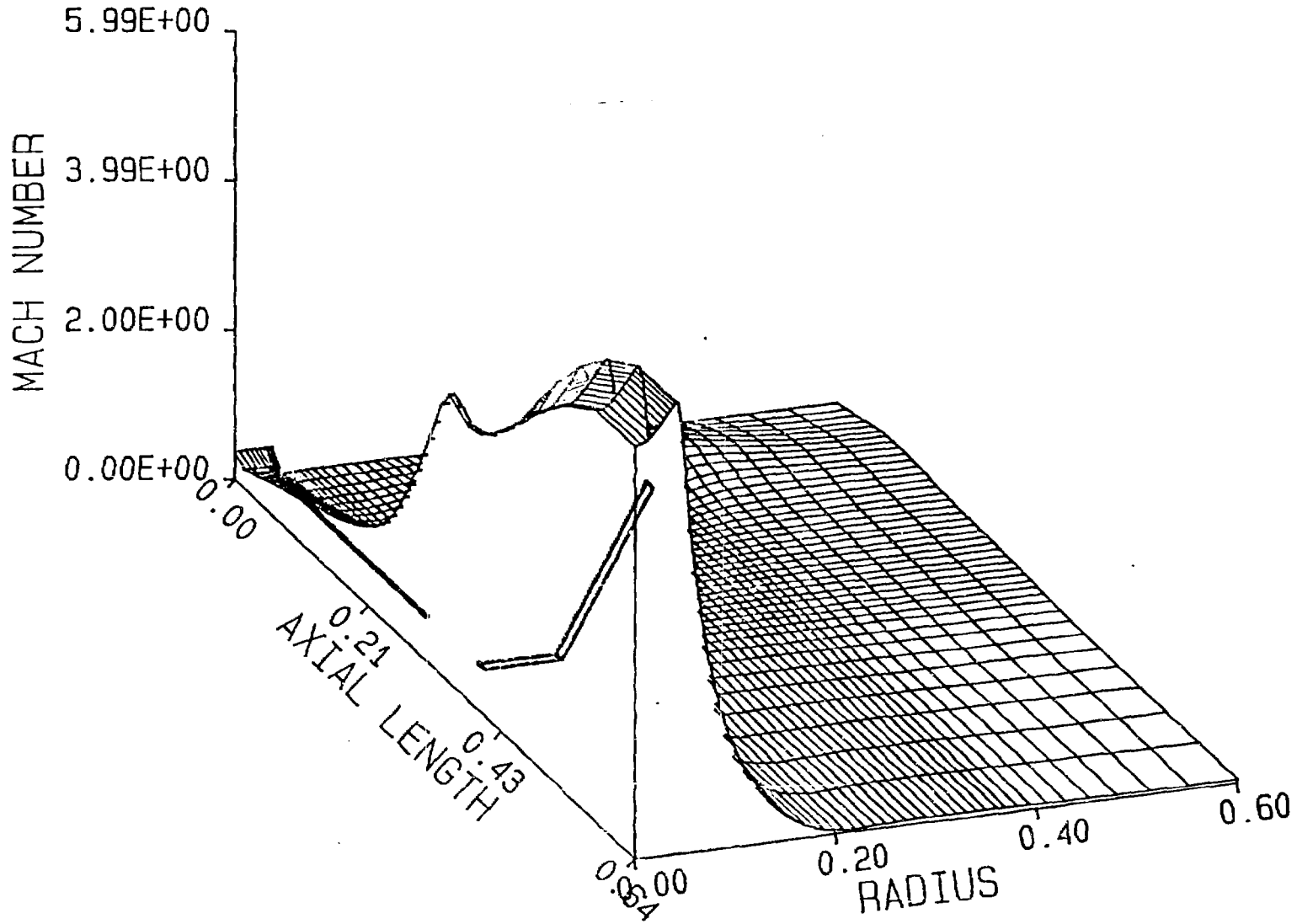

Figure 13a. Velocity Vector Field with the Silencer at T = 4.0 ms.

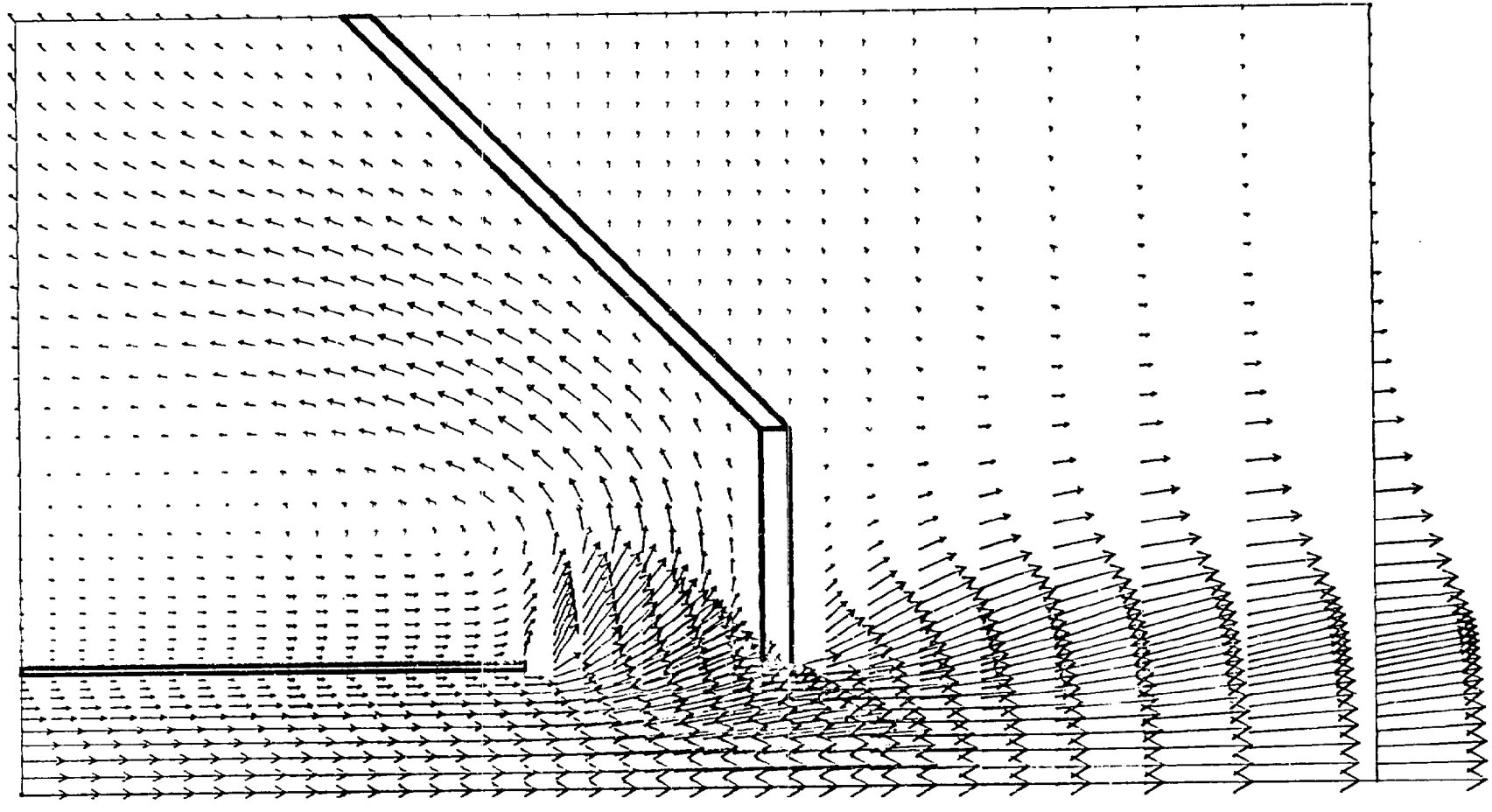

Figure 13b. Pressure Field with the Silencer at T = 4.0 ms.

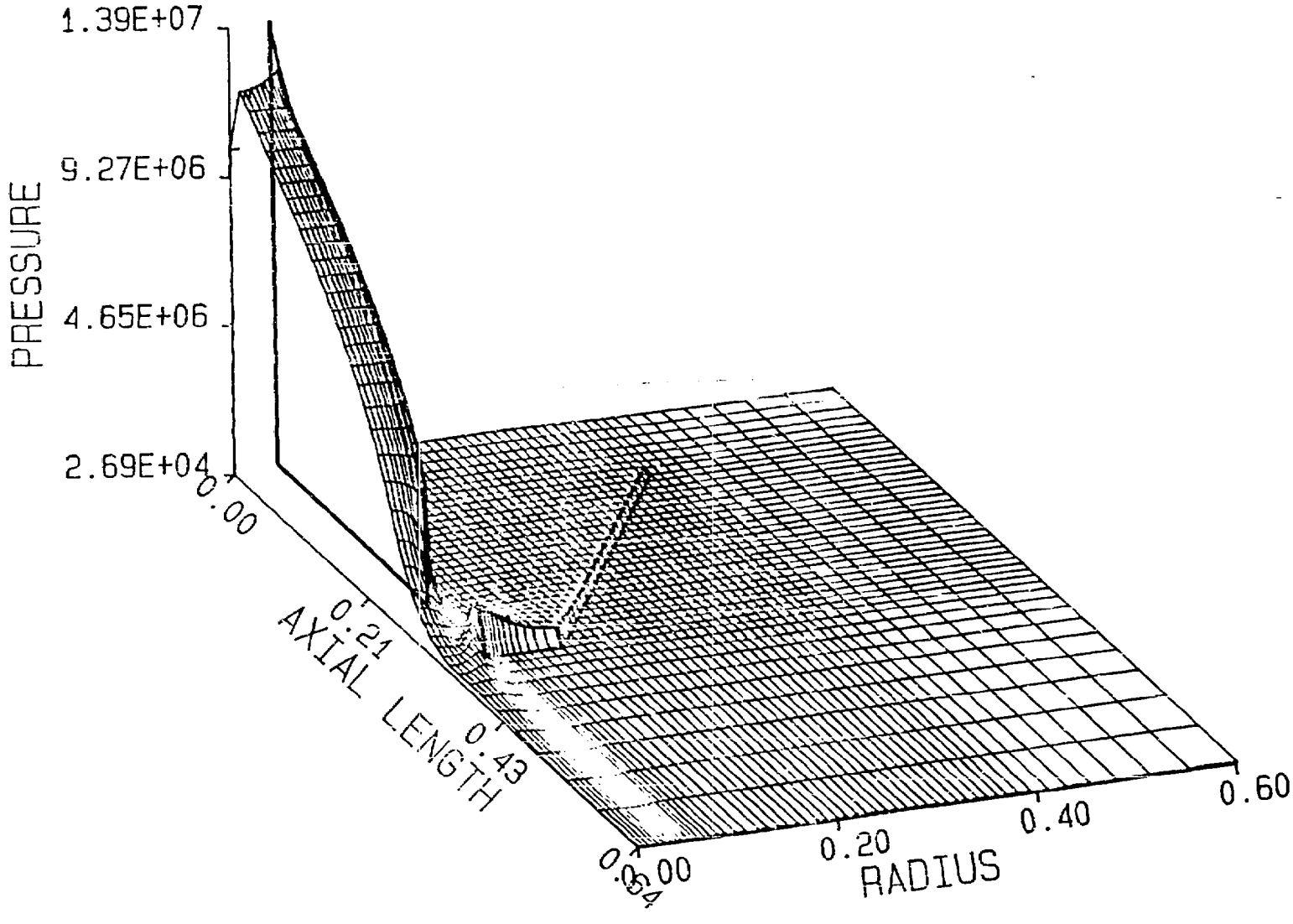

Figure 13c. Axial Velocity Field with the Silencer at T = 4.0 ms.

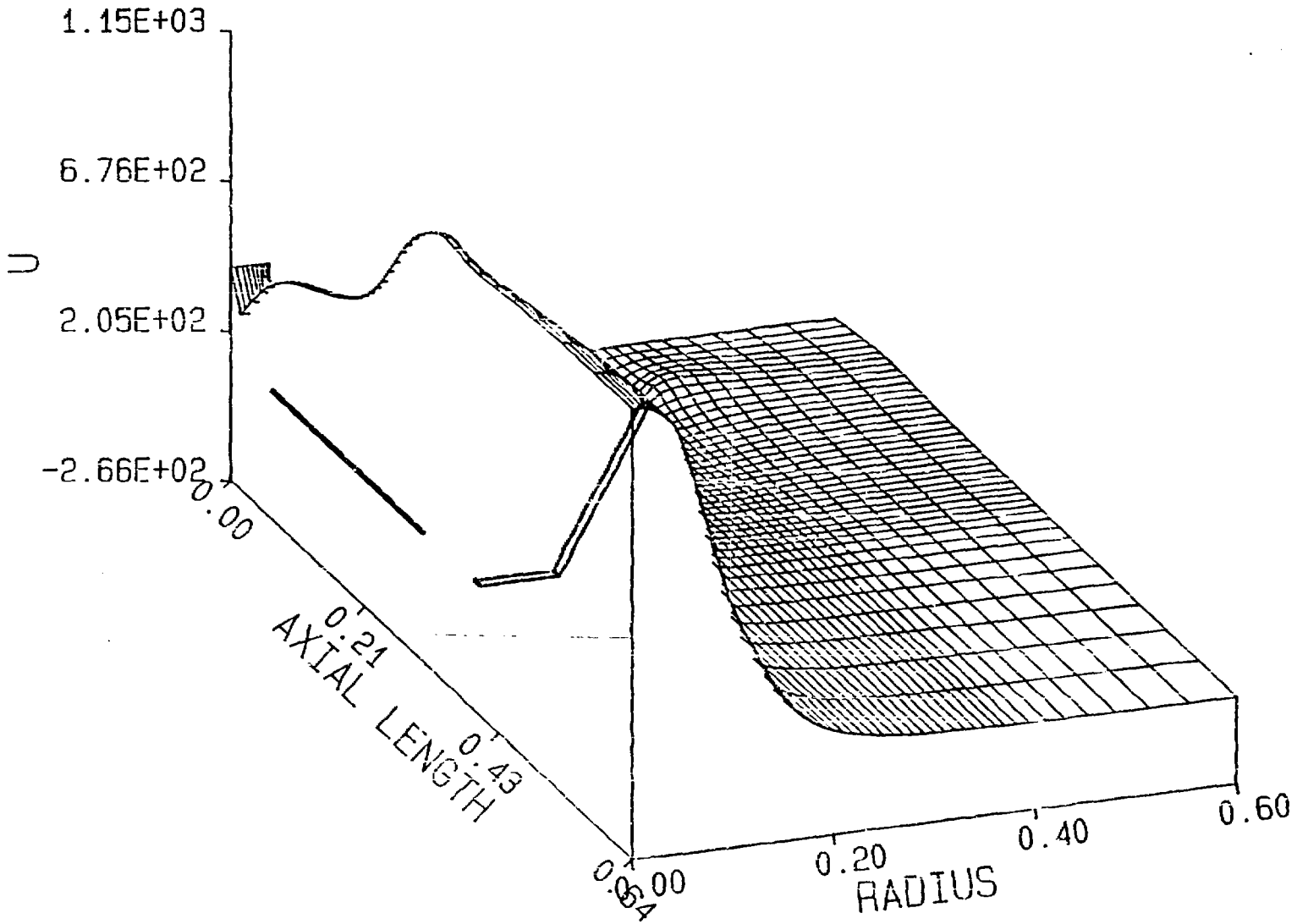

Figure 13d. Radial Velocity Field with the Silencer at T = 4.0 ms.

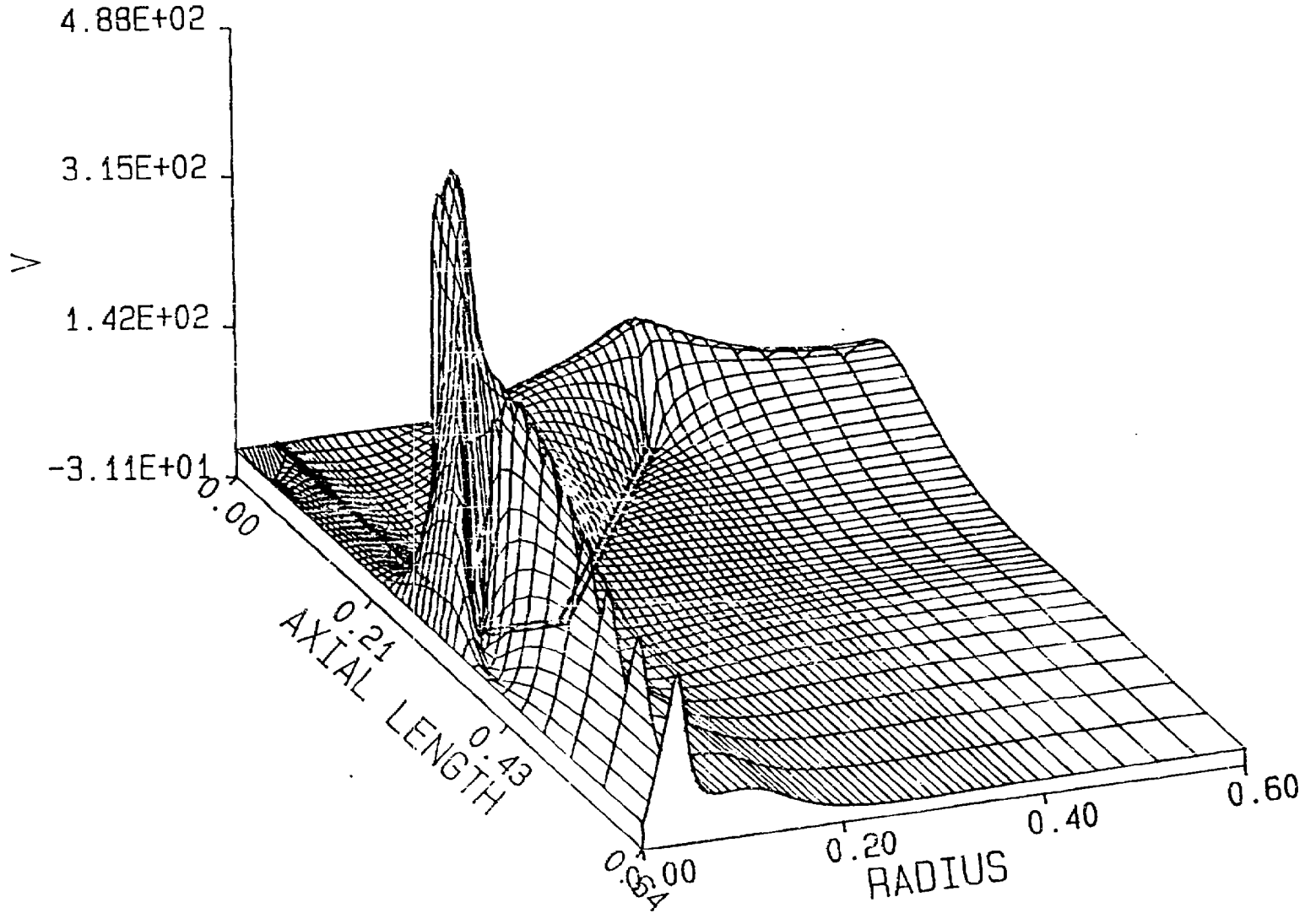

Figure 13e. Mach Number Field with the Silencer at T = 4.0 ms.

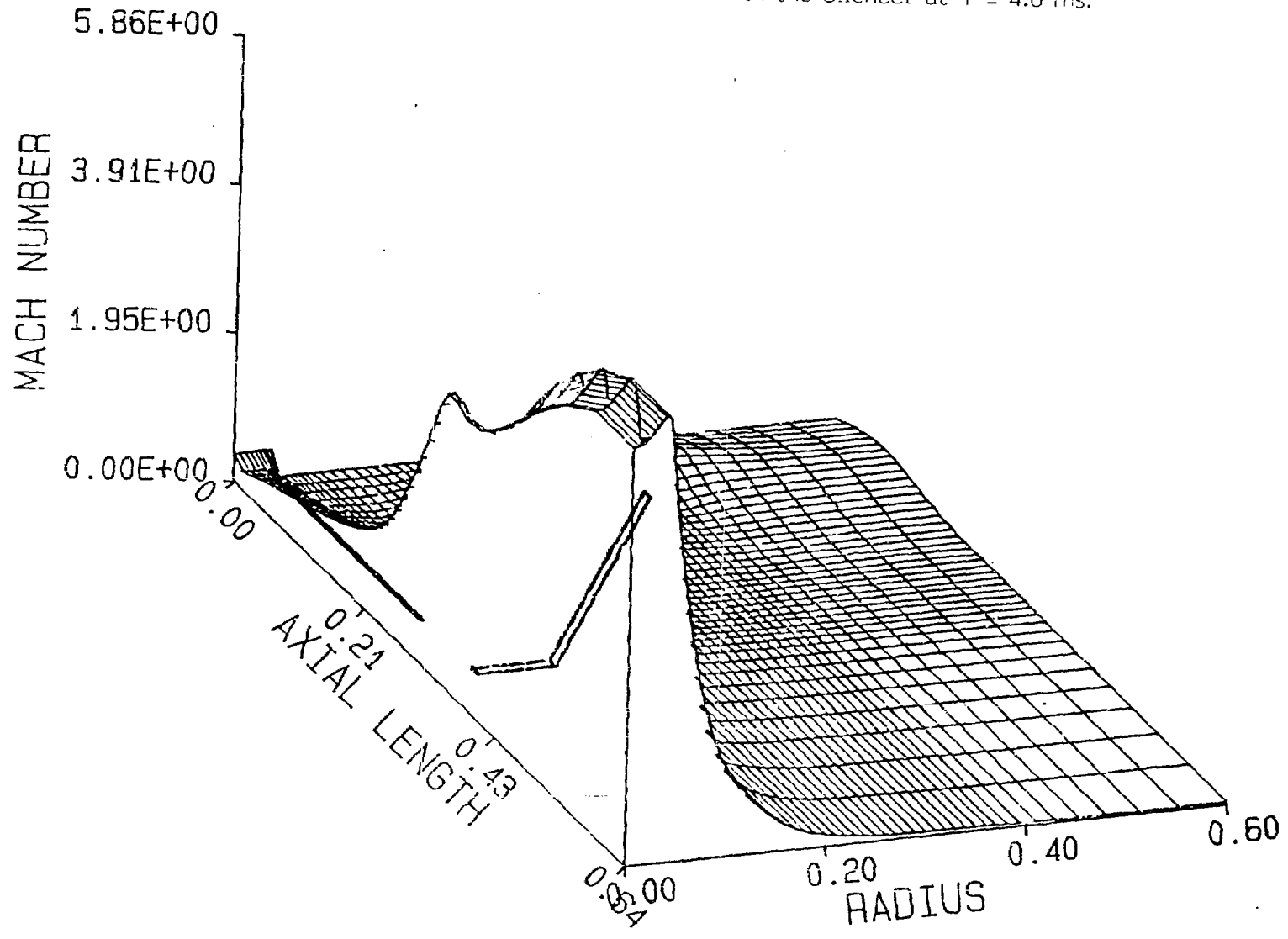

Figure 14a. Velocity Vector Field without the Silencer at T = .2 ms.

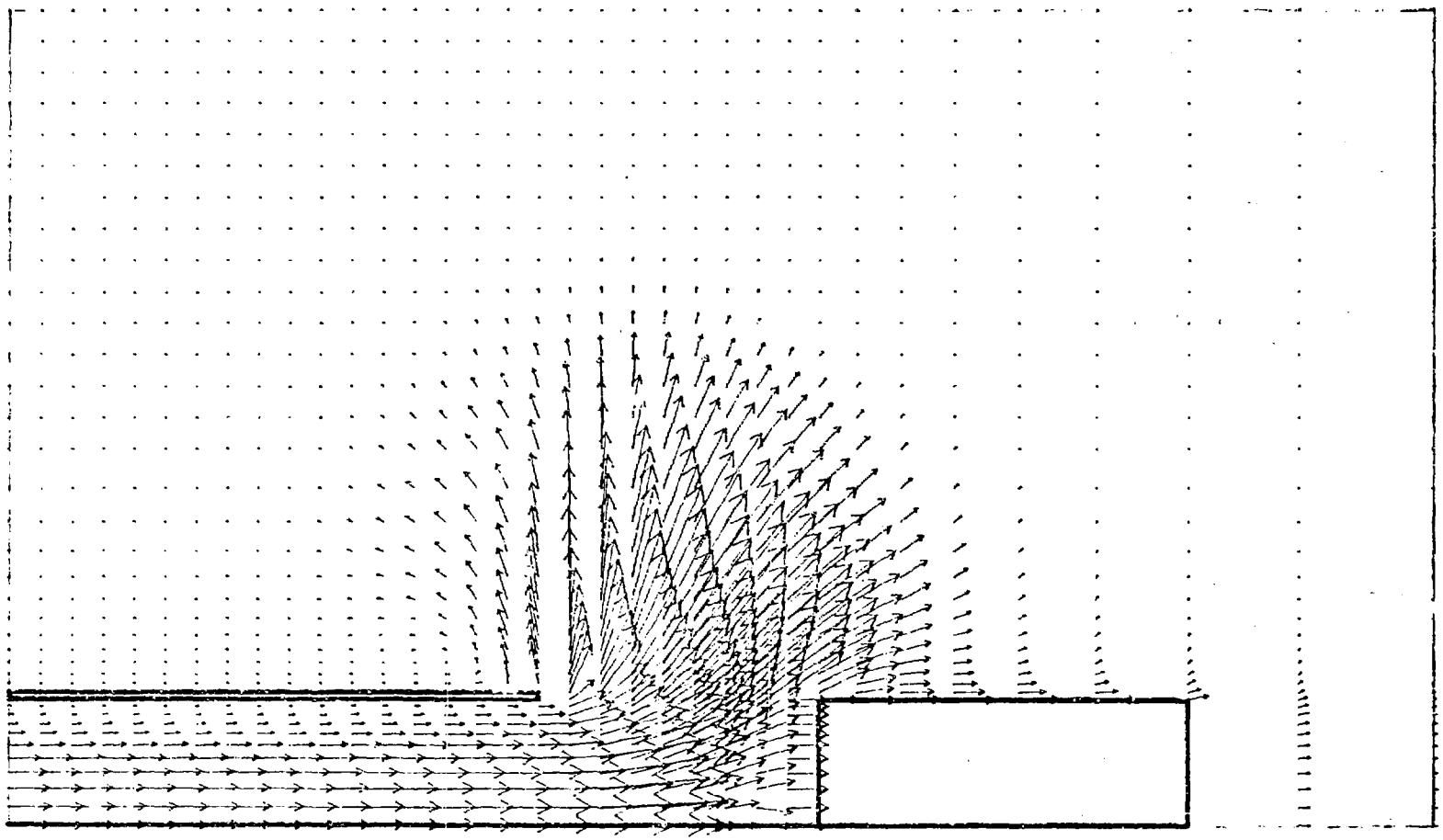

Figure 14b. Pressure Field without the Silencer at T = .2 ms.

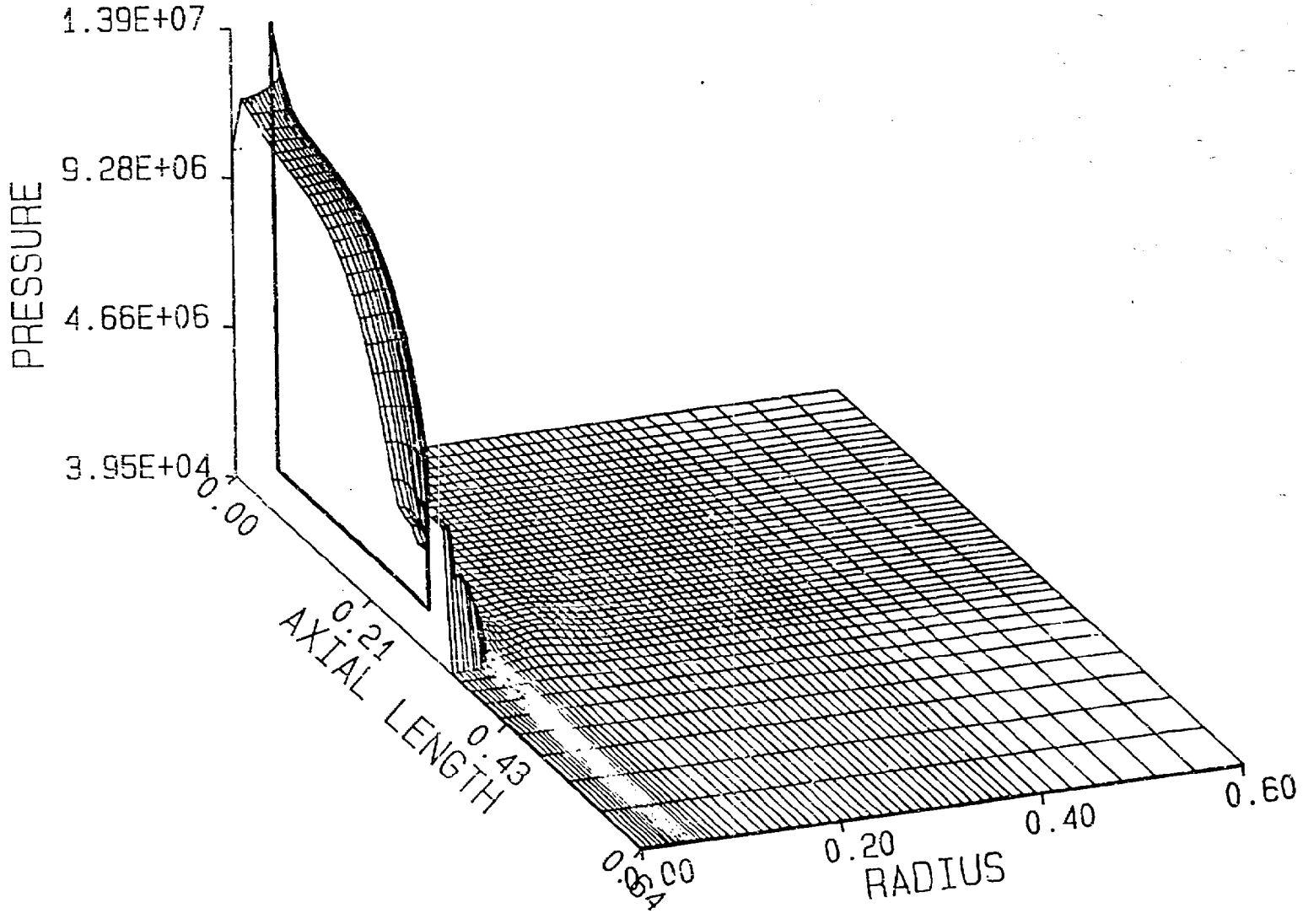

Figure 14c. Axial Velocity Field without the Silencer at T = .2 ms.

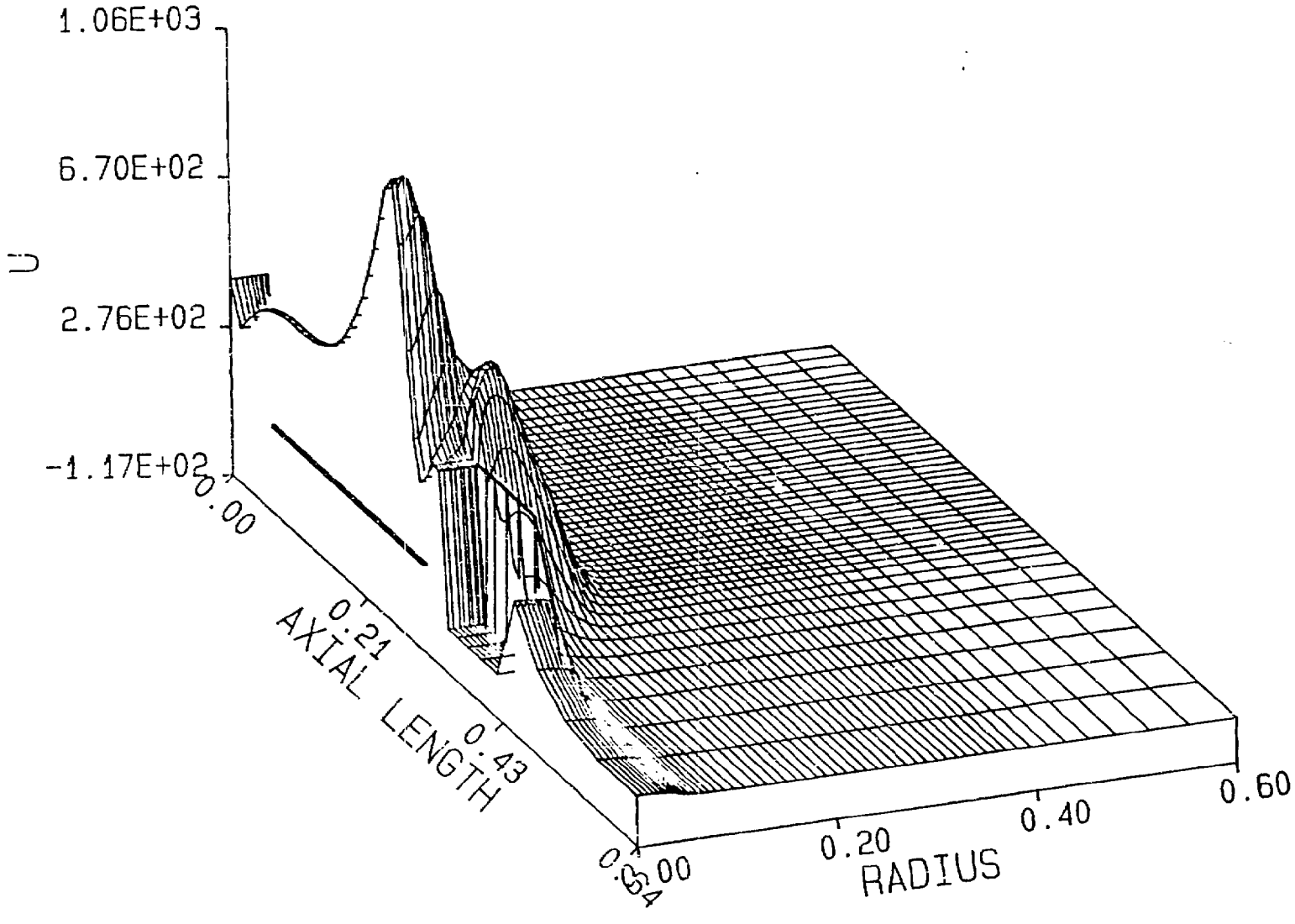

Figure 14d. Radial Velocity Field without the Silencer at T = .2 ms.

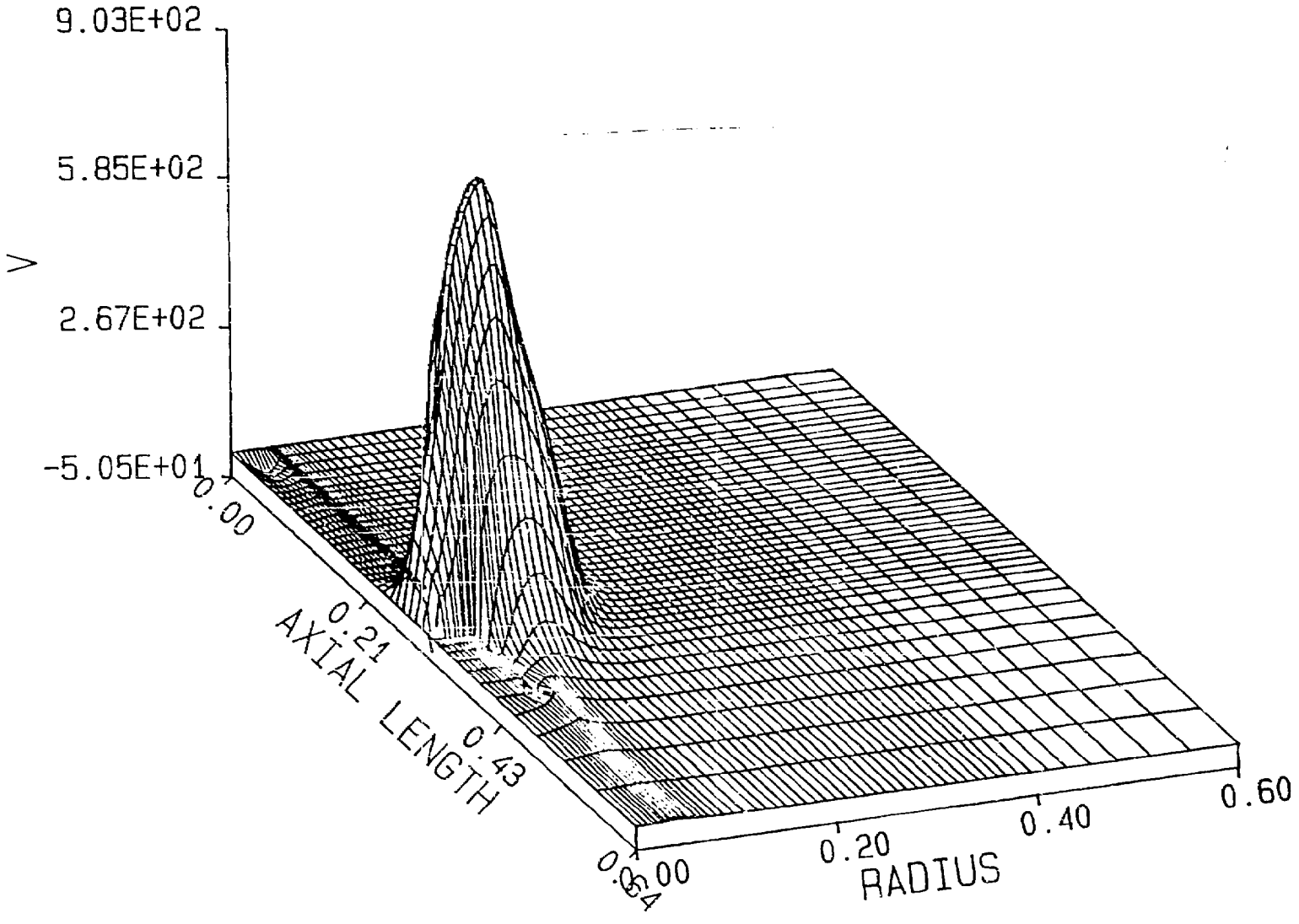

Figure 14e. Mach Number Field without the Silencer at T = .2 ms.

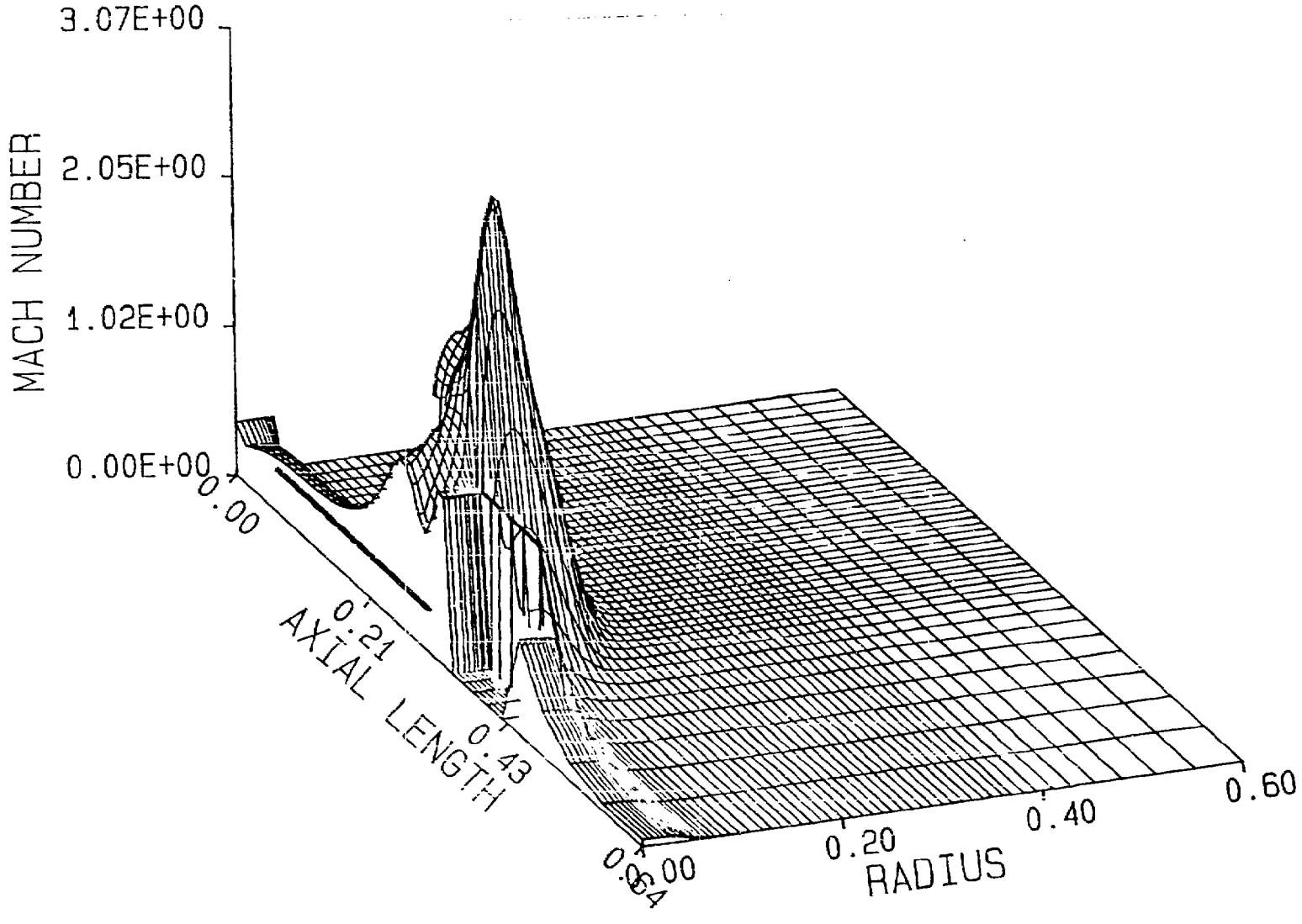

Figure 15a. Velocity Vector Field without the Silencer at T = .4 ms.

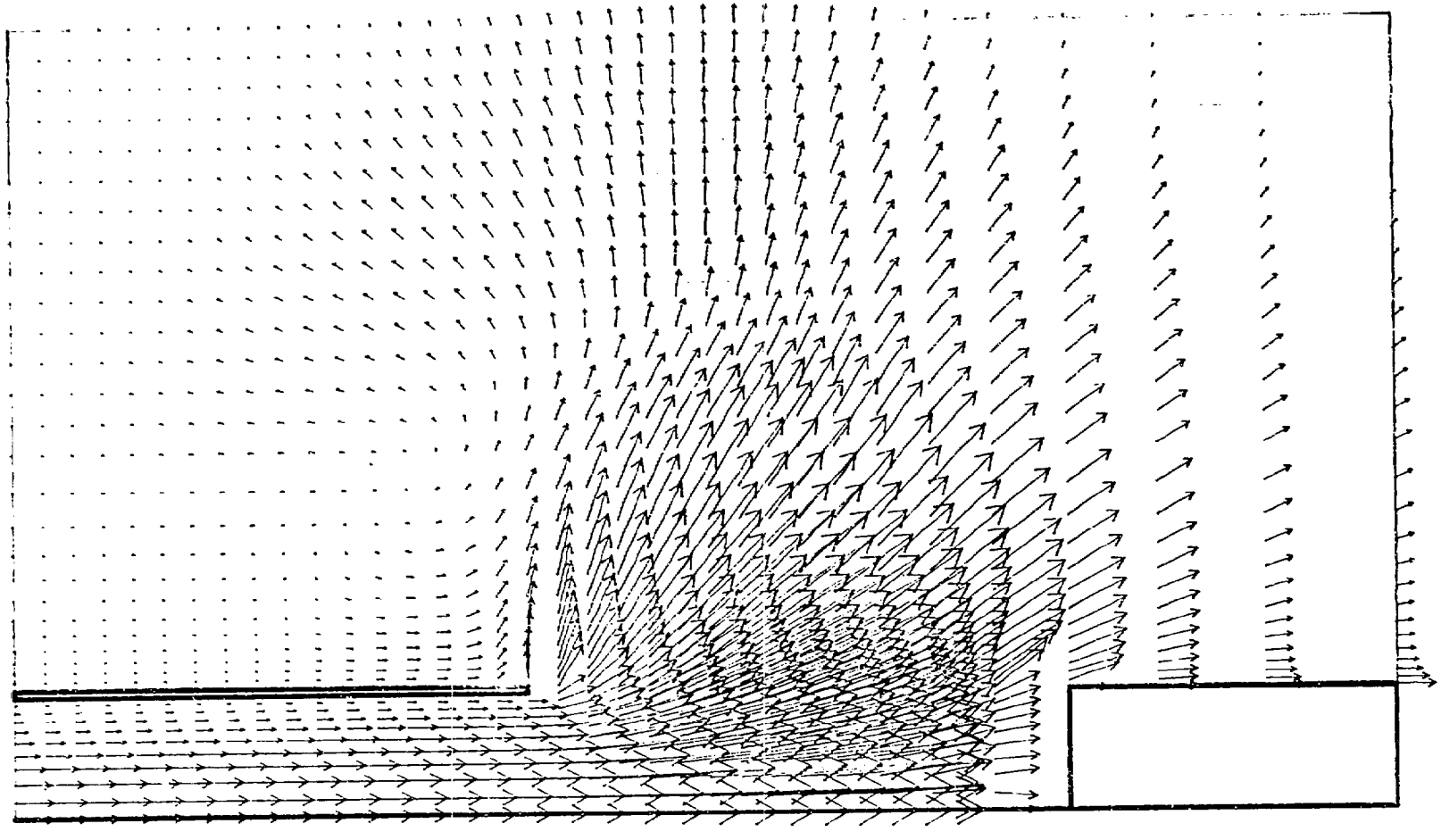

Figure 15b. Pressure Field without the Silencer at T = .4 ms.

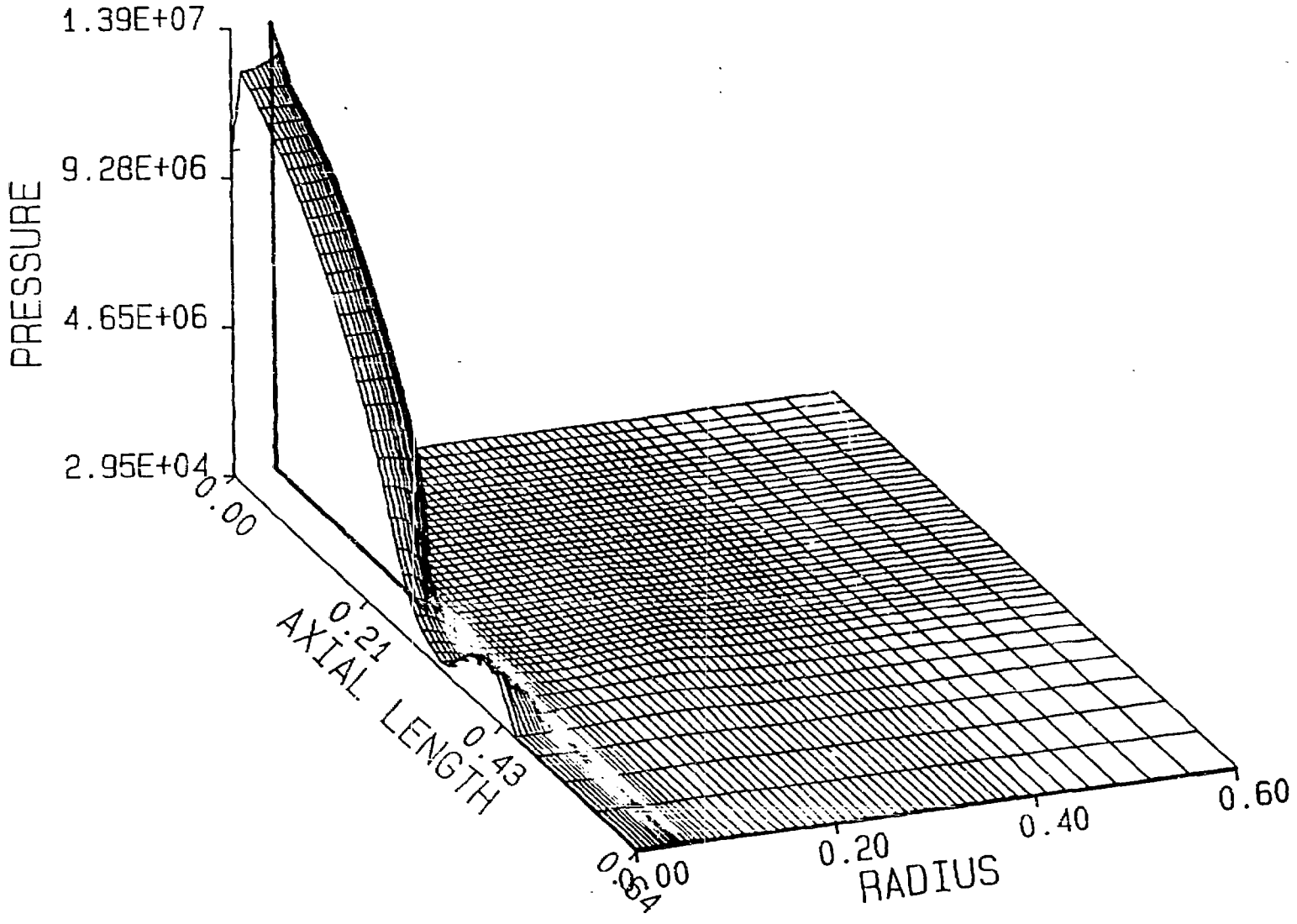

Figure 15c. Axial Velocity Field without the Silencer at T = .4 ms.

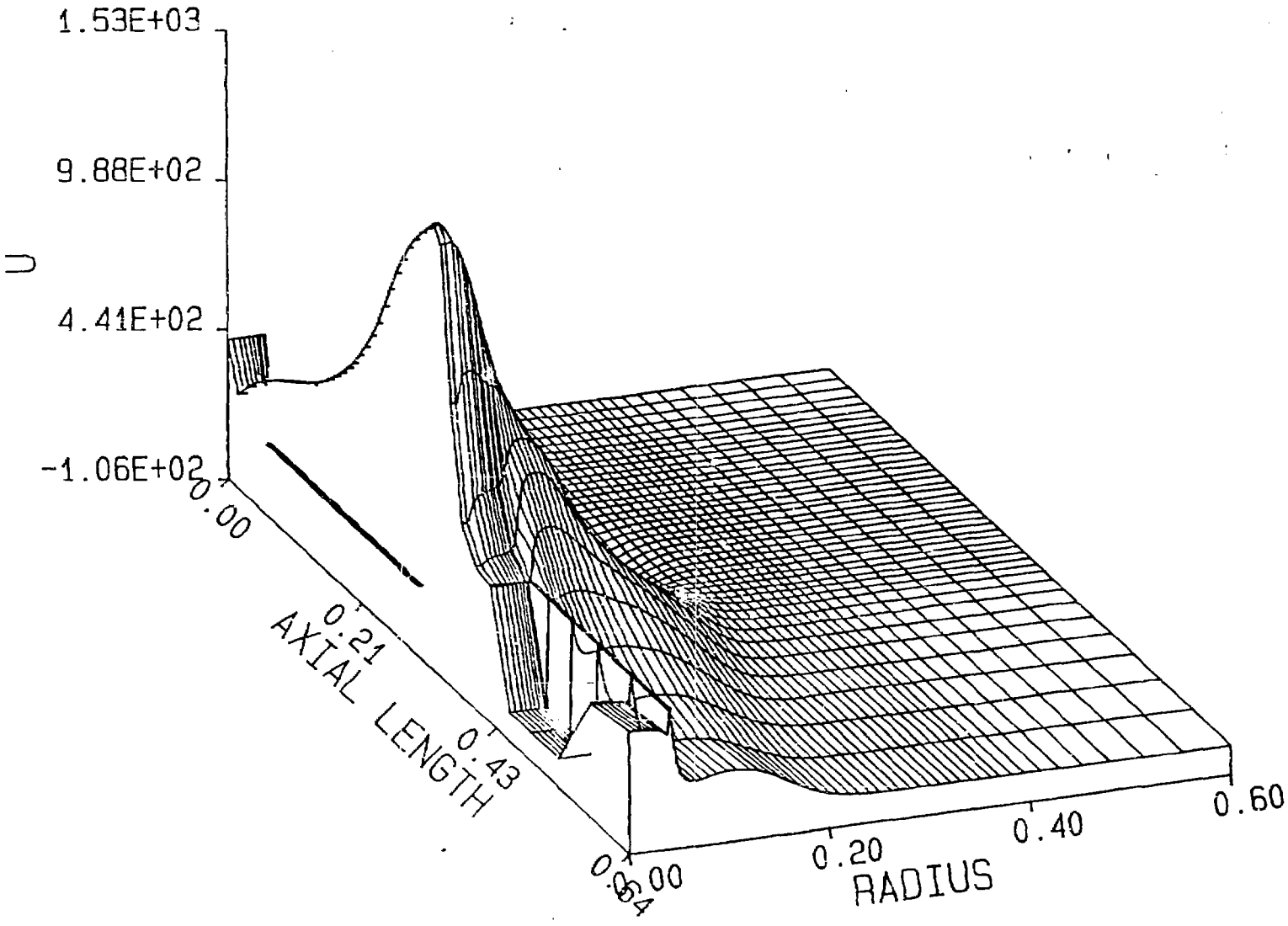

Figure 15d. Radial Velocity Field without the Silencer at T = .4 ms.

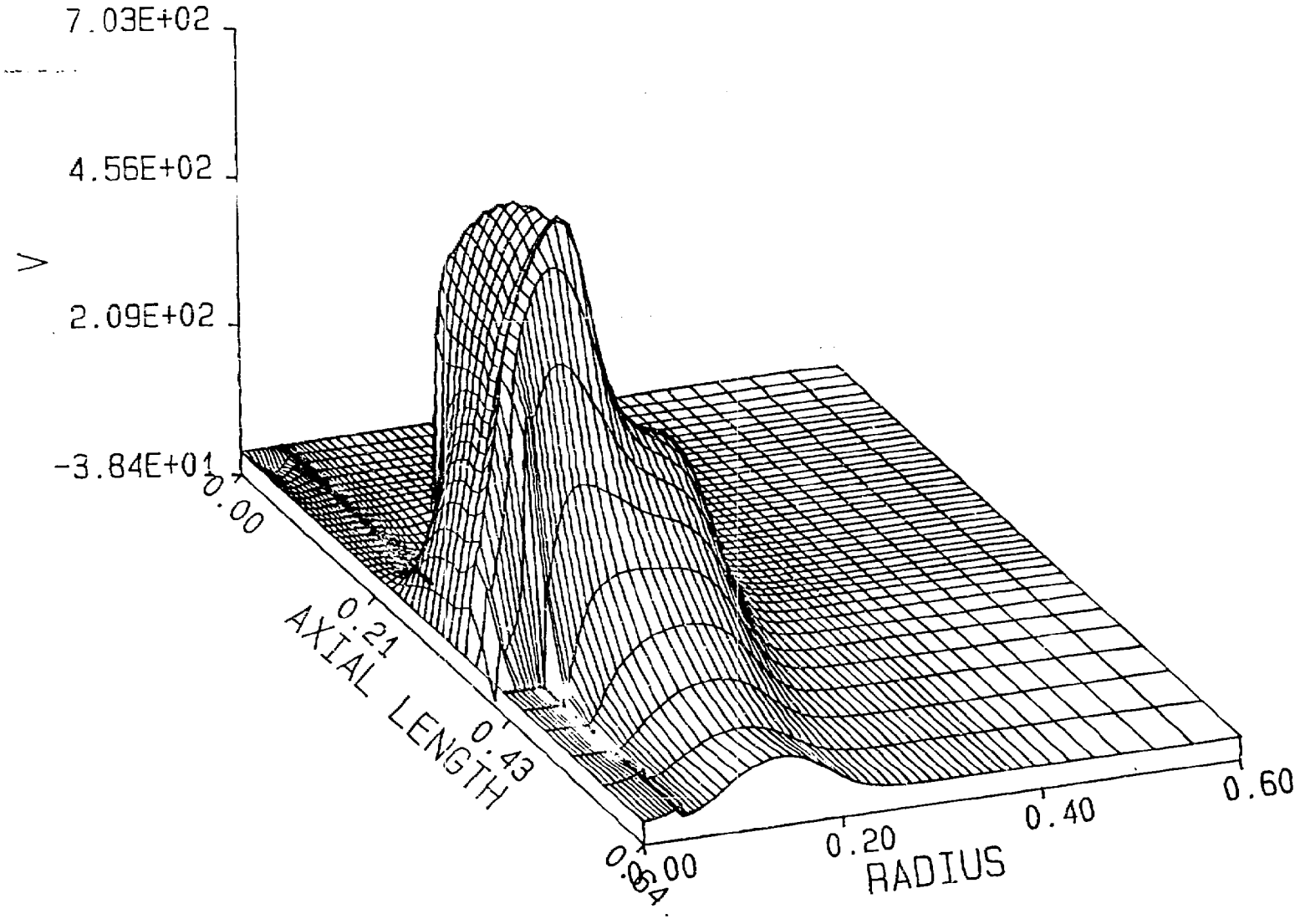

Figure 15e. Mach Number Field without the Silencer at T = .4 ms.

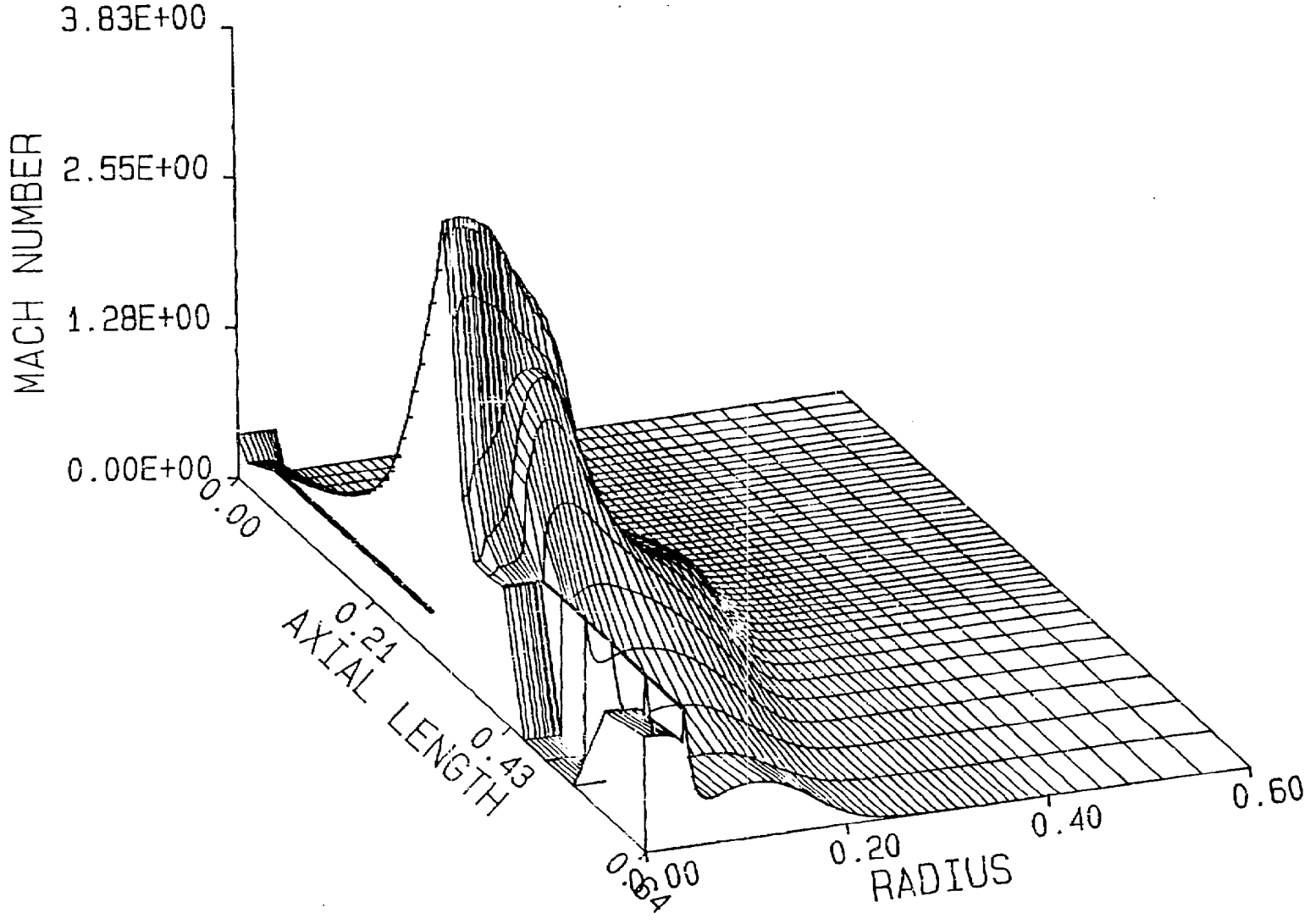

Figure 16a. Velocity Vector Field without the Silencer at T = .6 ms.

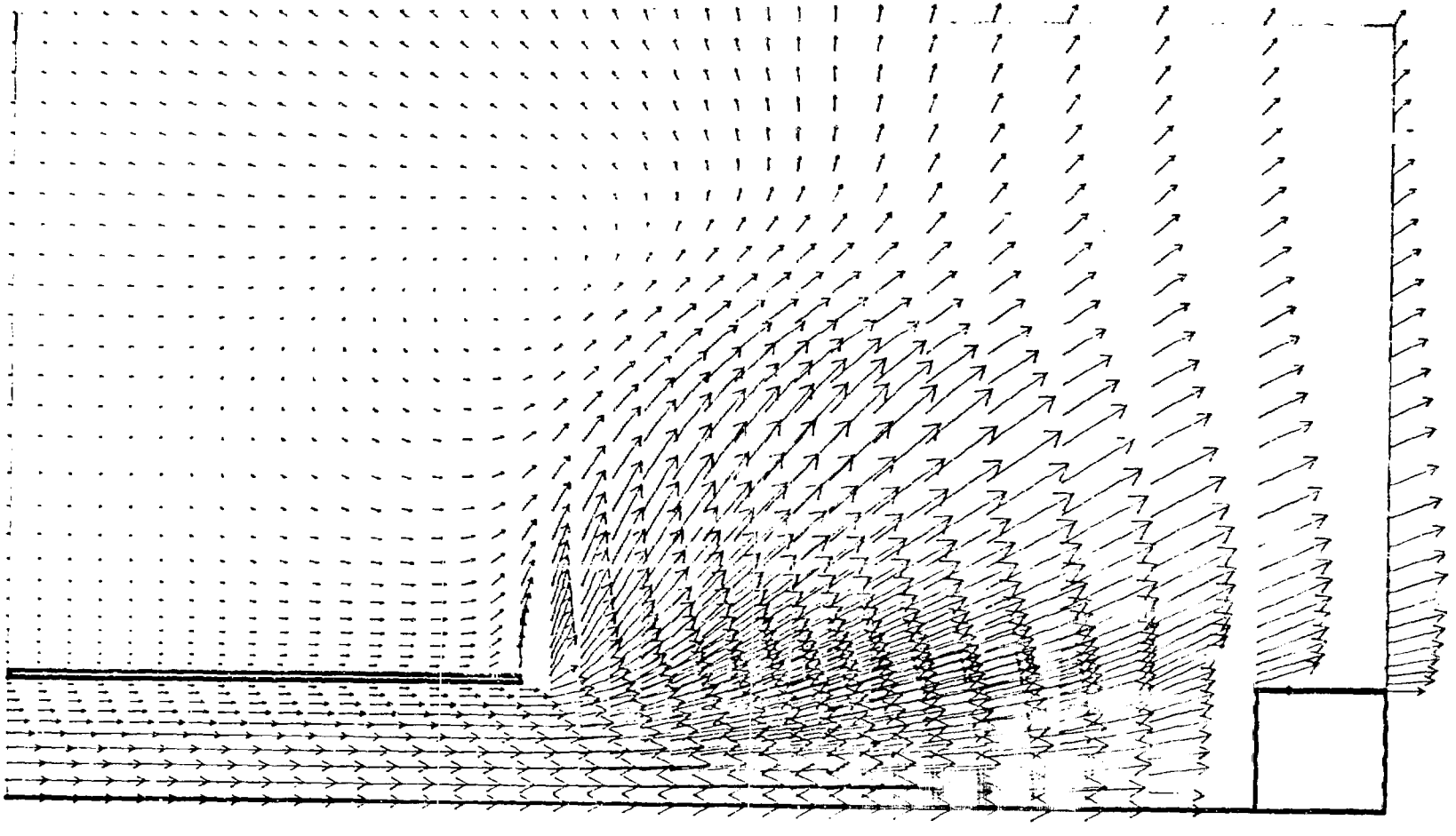

Figure 16b. Pressure Field without the Silencer at T = .6 ms.

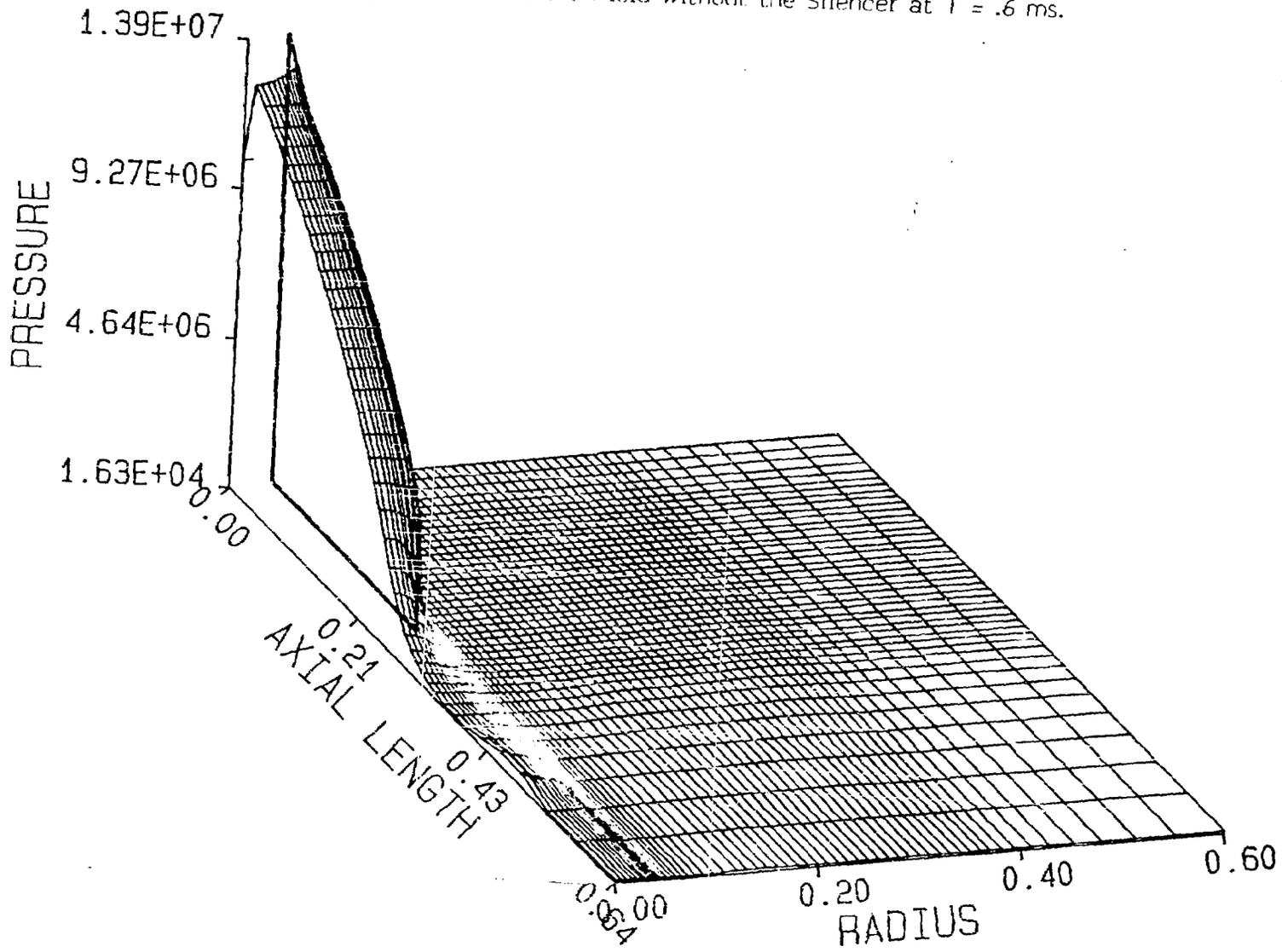

Figure 16c. Axial Velocity Field without the Silencer at T = .6 ms.

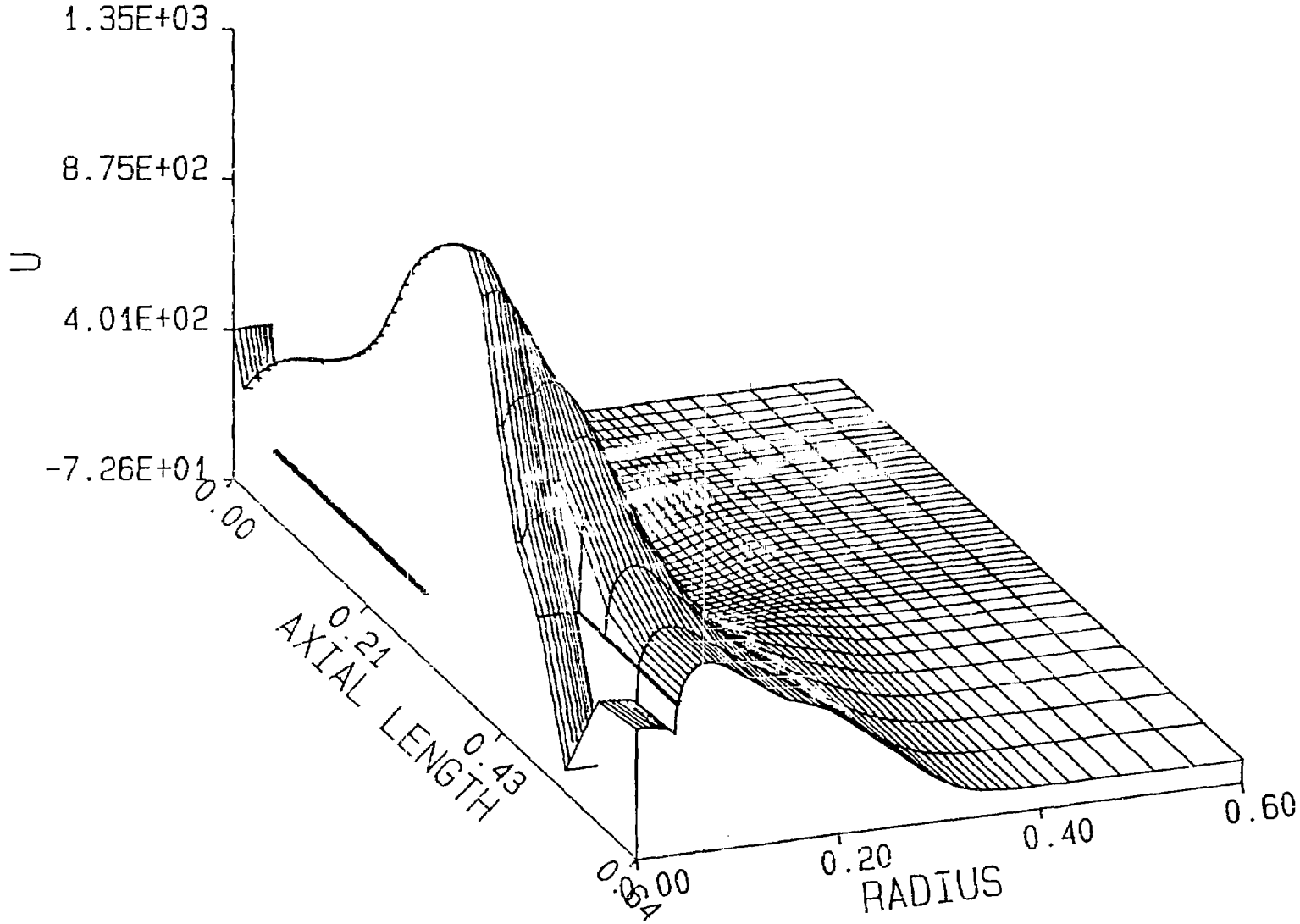

Figure 16d. Radial Velocity Field without the Silencer at T = .6 ms.

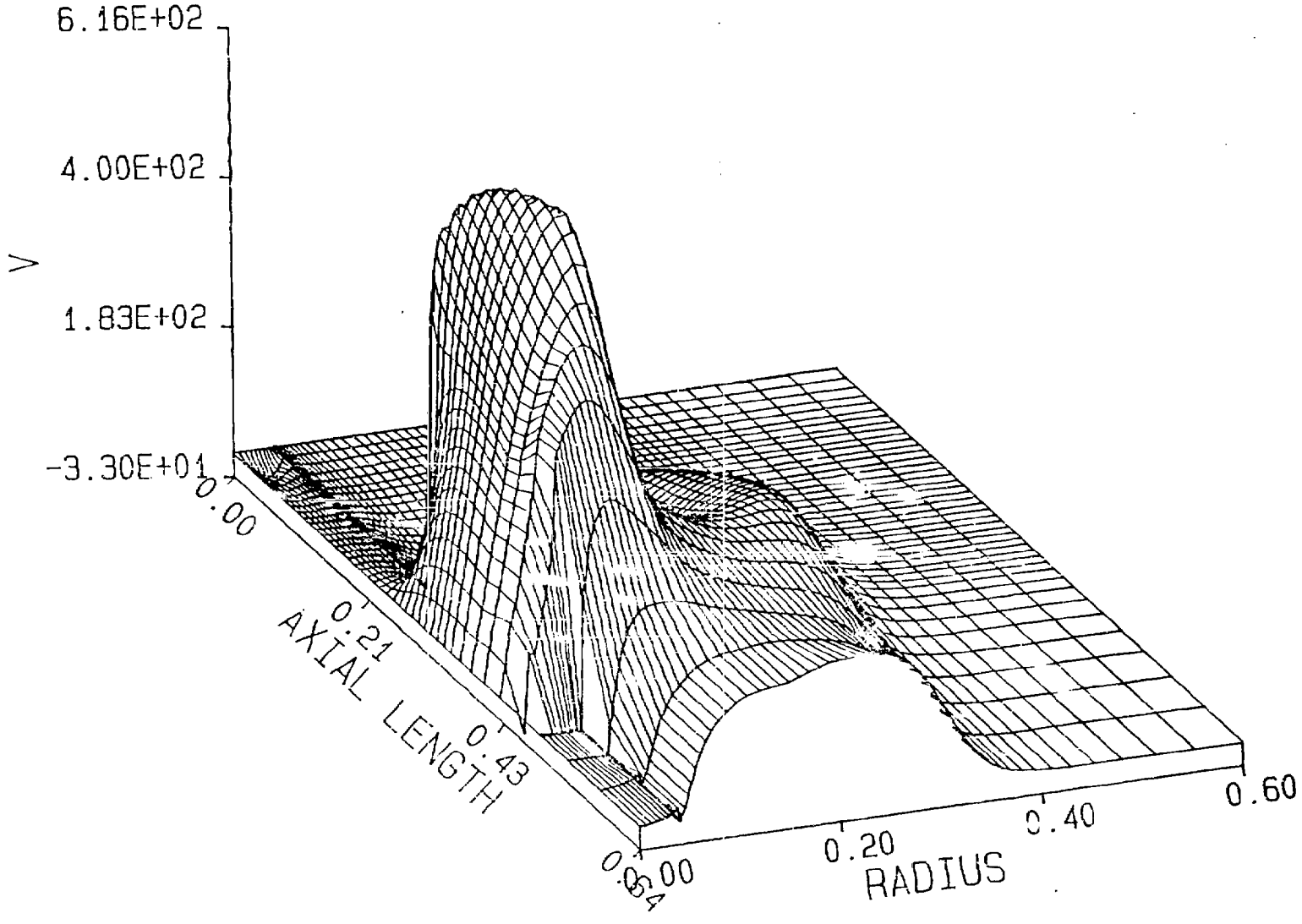

Figure 16e. Mach Number Field without the Silencer at T = .6 ms.

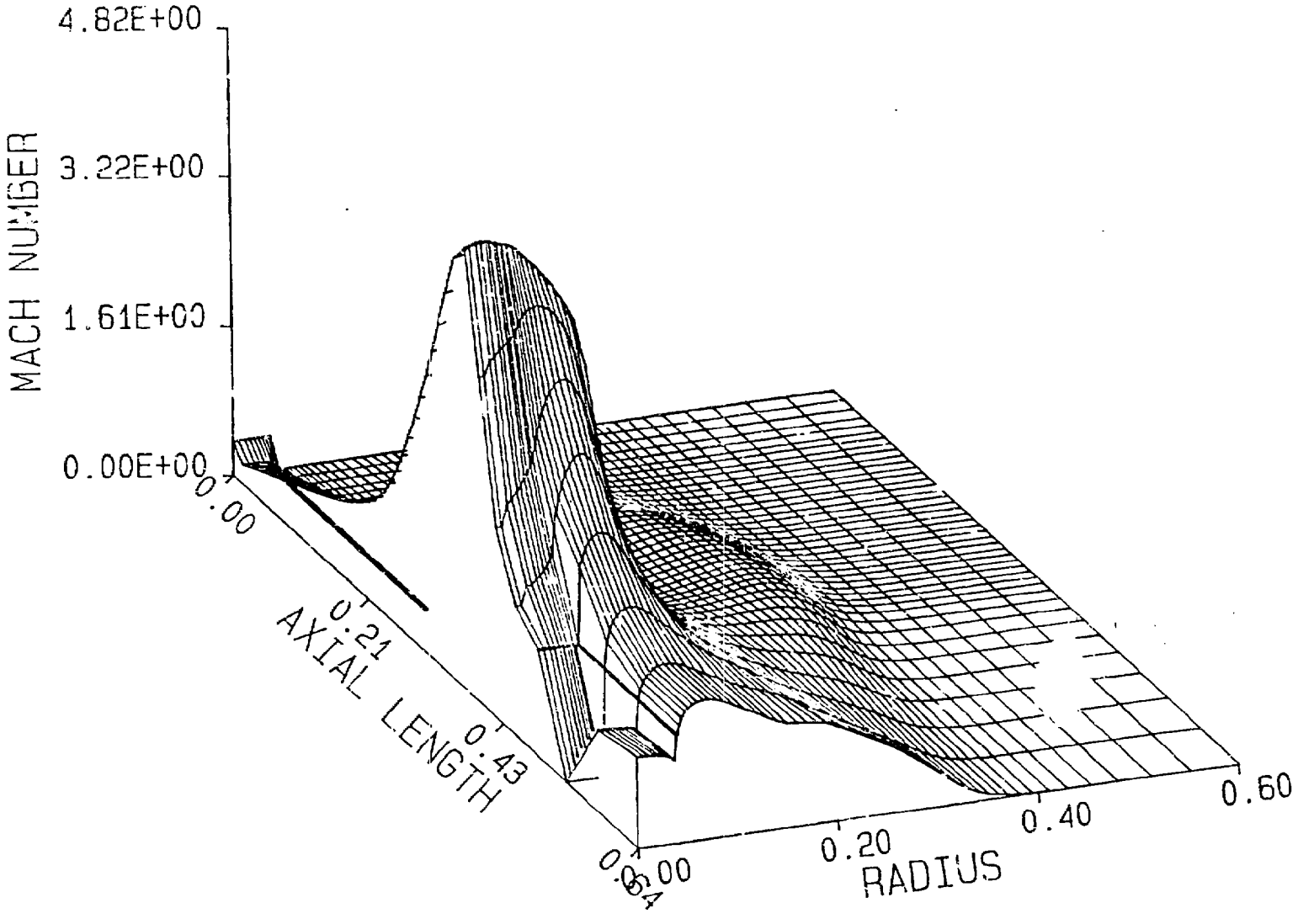

Figure 17a. Velocity Vector Field without the Silencer at T = .8 ms.

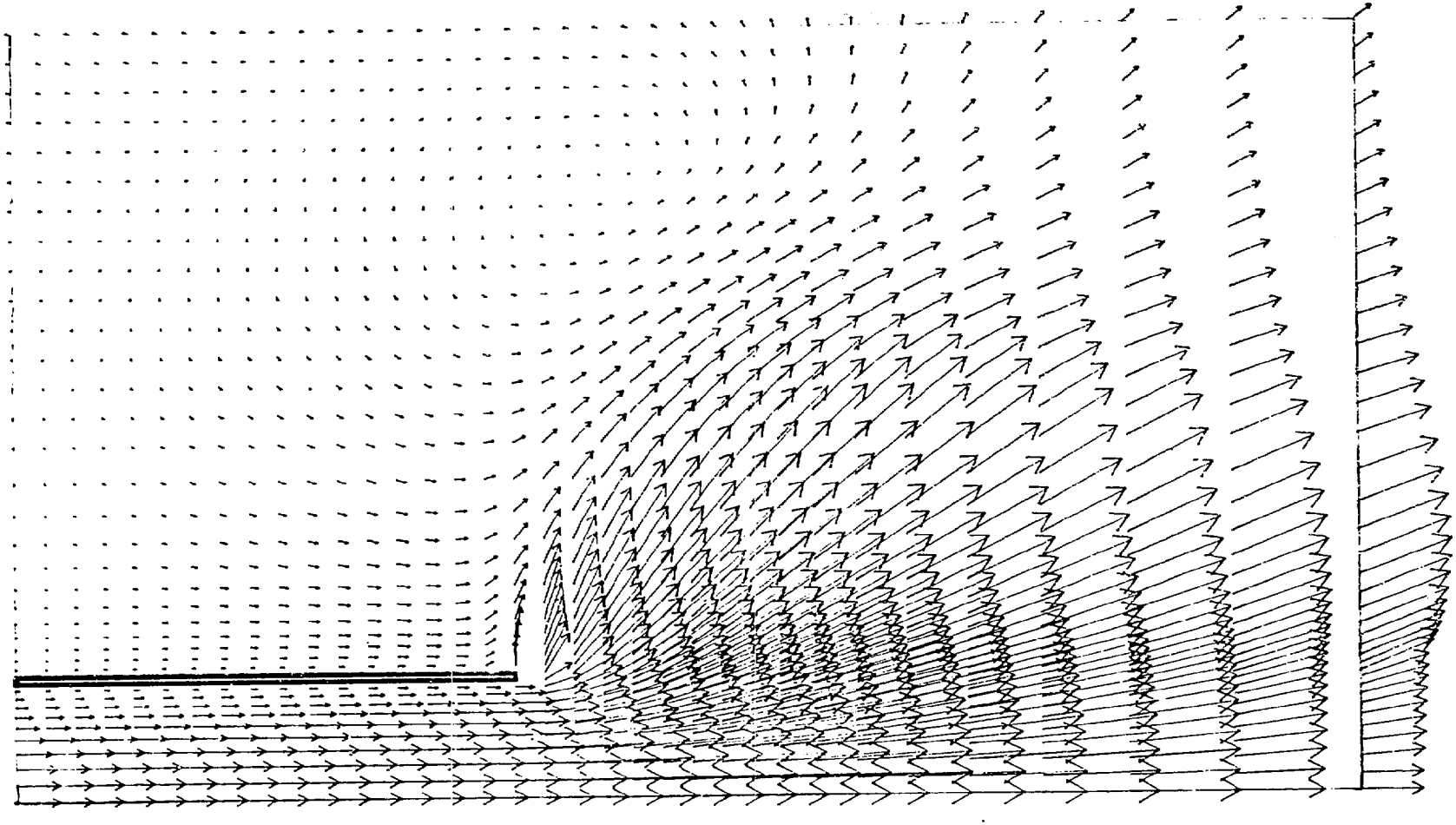

Figure 17b. Pressure Field without the Silencer at T = .8 ms.

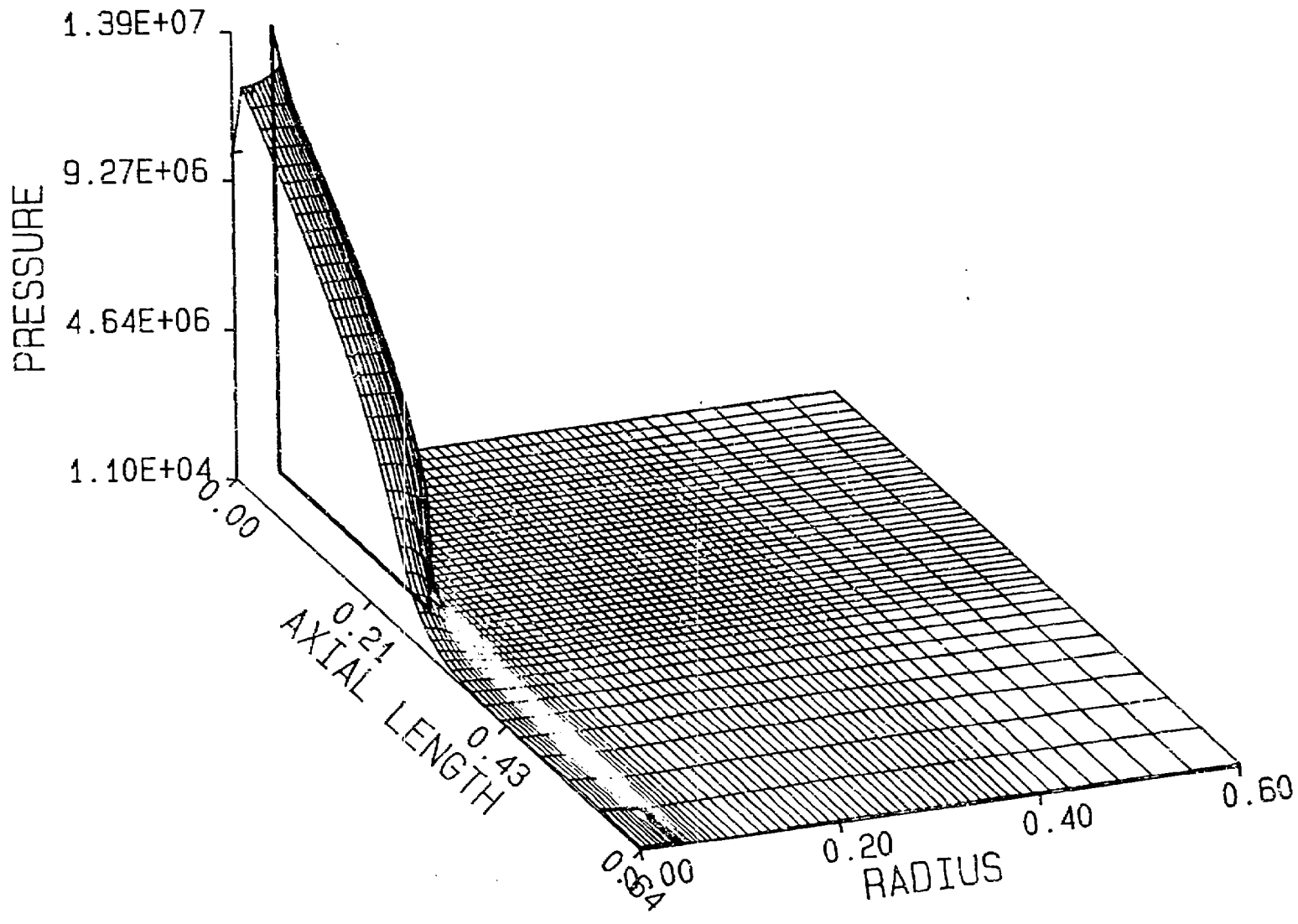

Figure 17c. Axial Velocity Field without the Silencer at T = .8 ms.

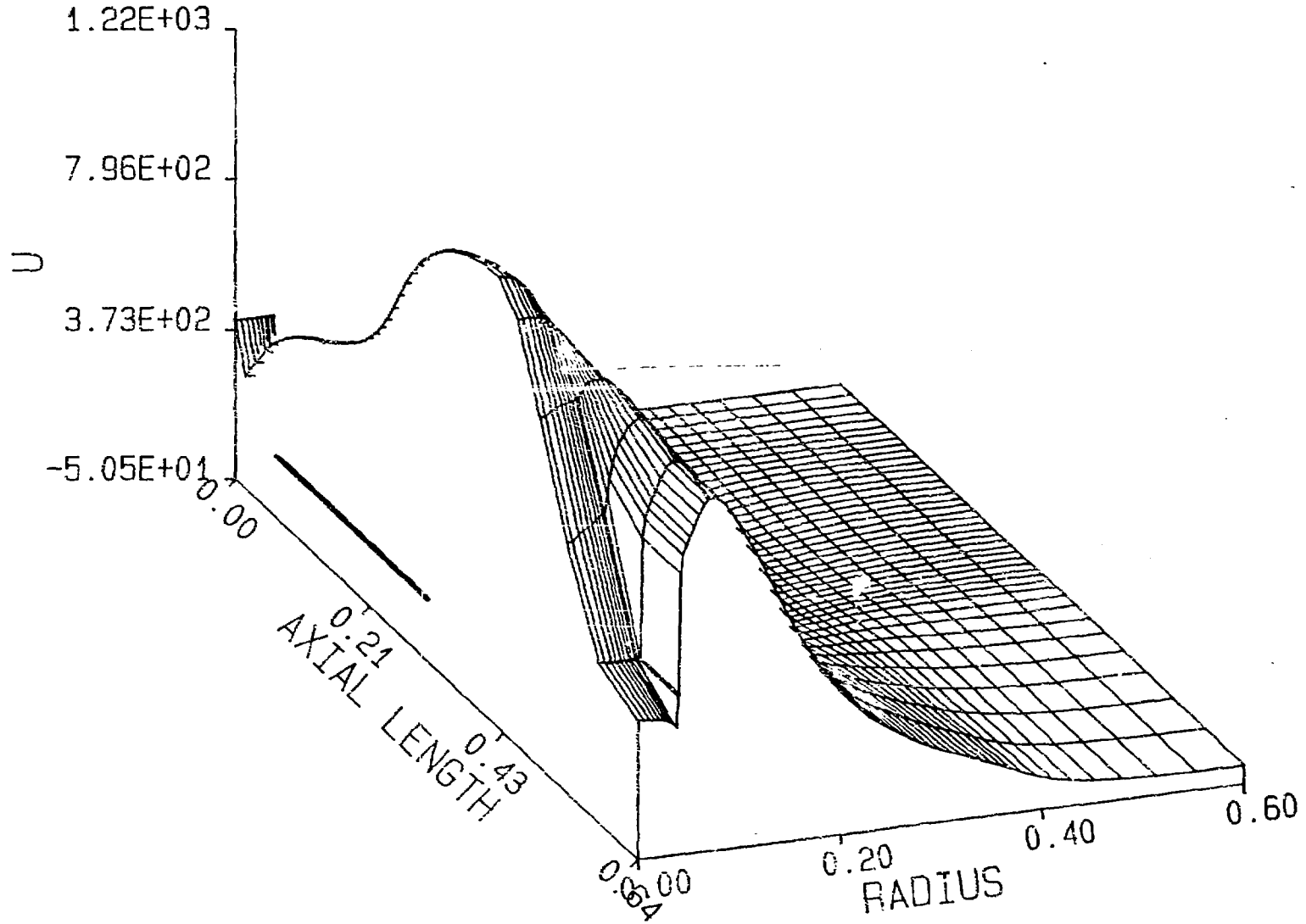

Figure 17d. Radial Velocity Field without the Silencer at T = .8 ms.

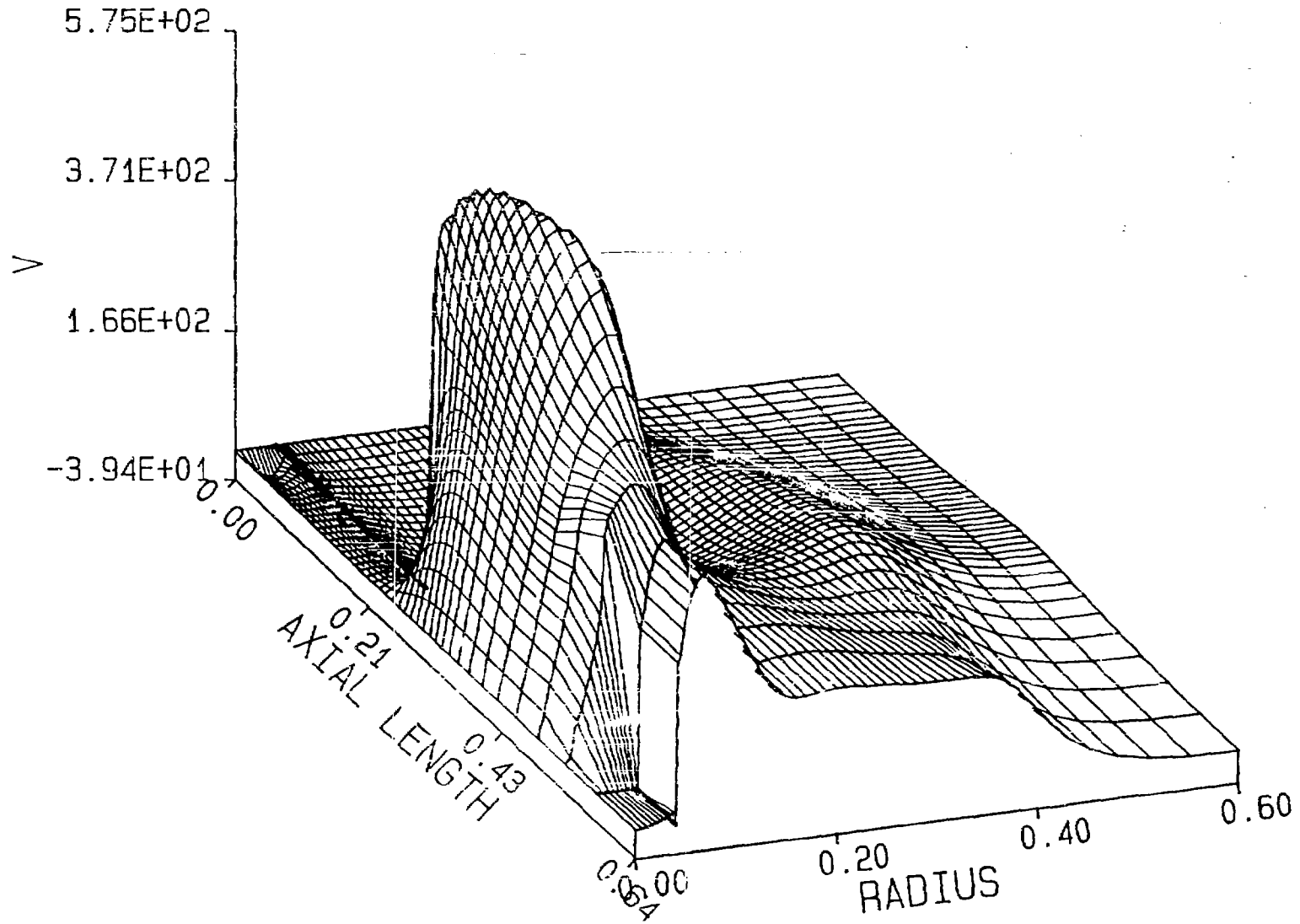

Figure 17e. Mach Number Field without the Silencer at T = .8 ms.

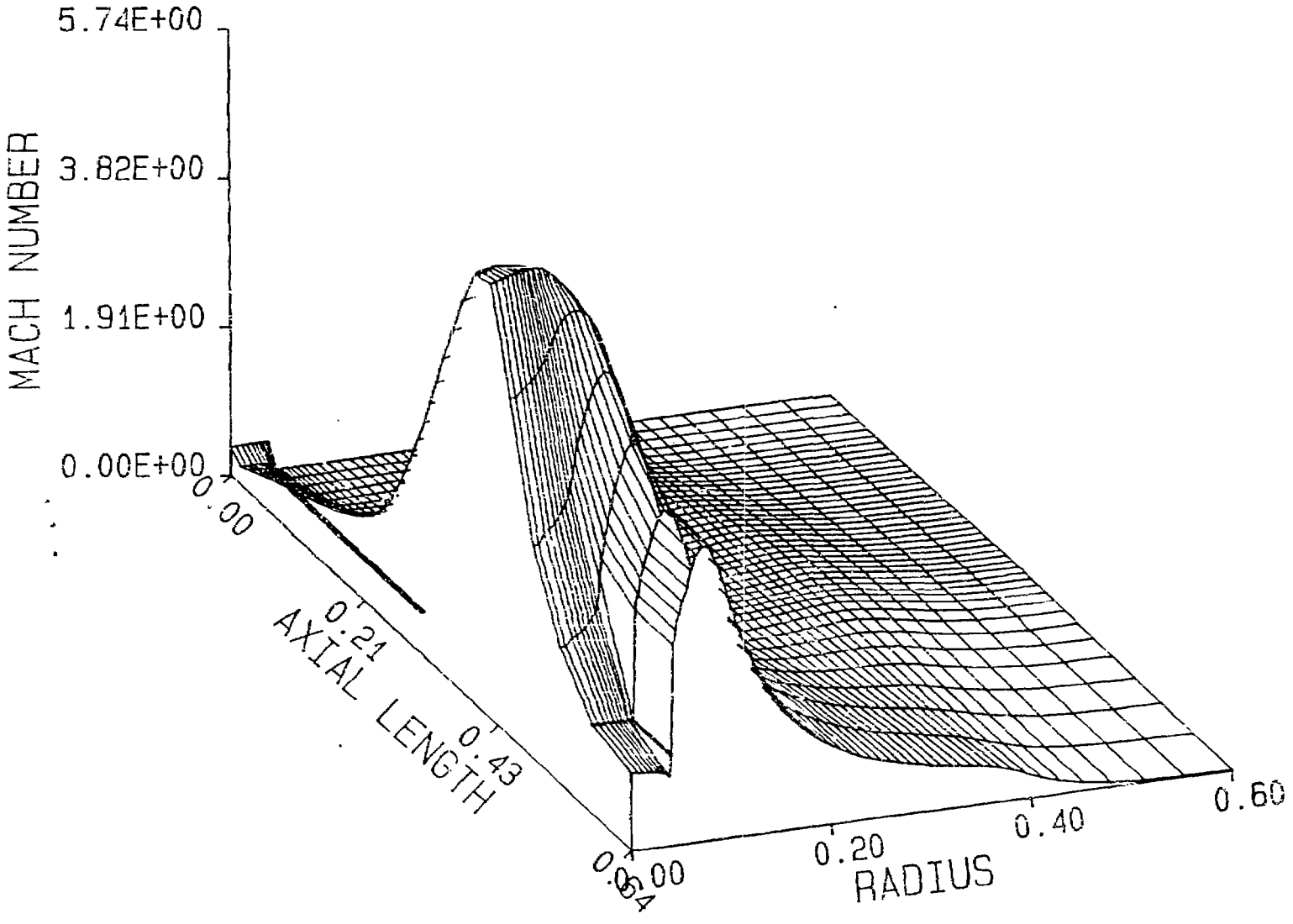

Figure 18a. Velocity Vector Field without the Silencer at T = 1.0 ms.

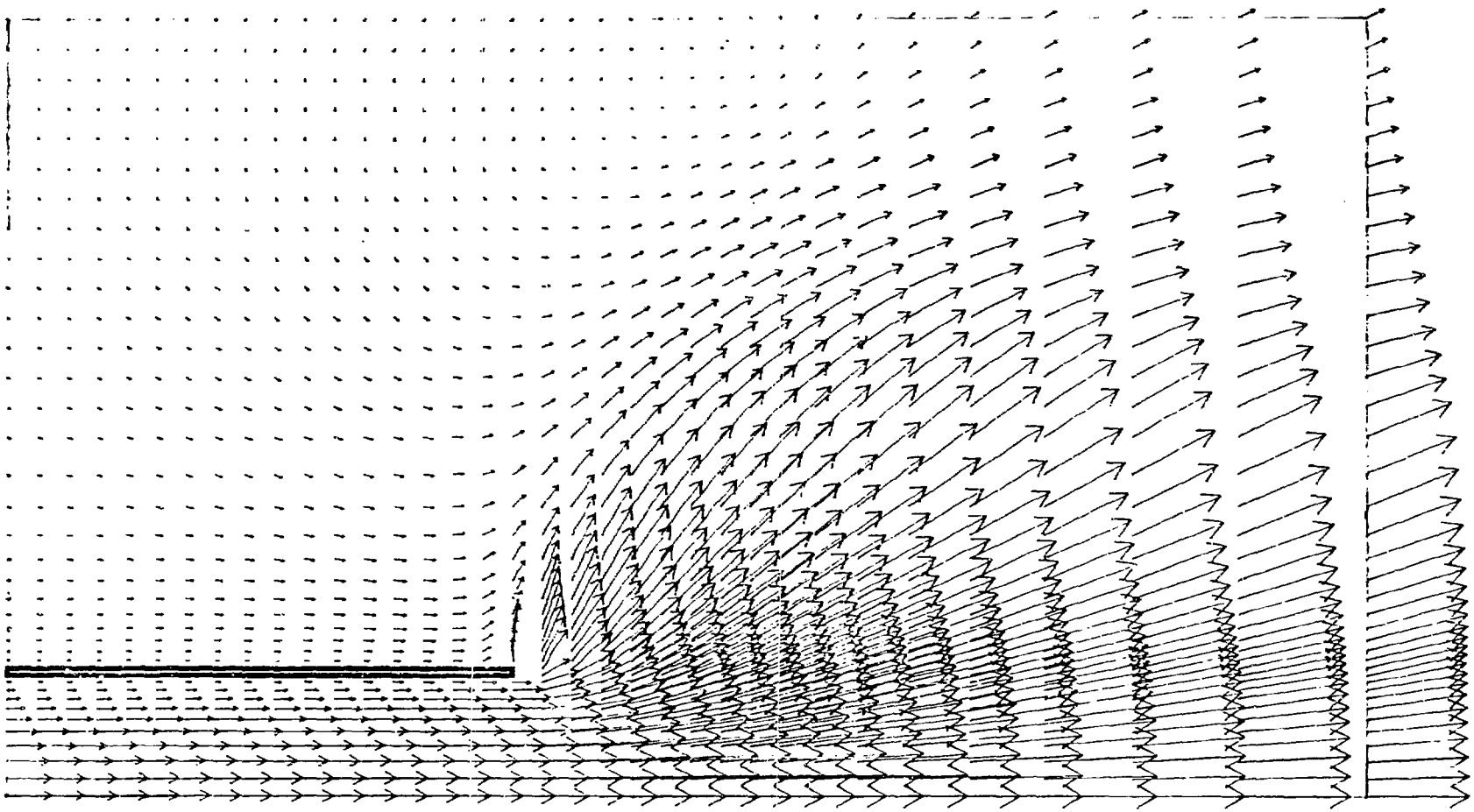

Figure 18b. Pressure Field without the Silencer at T = 1.0 ms.

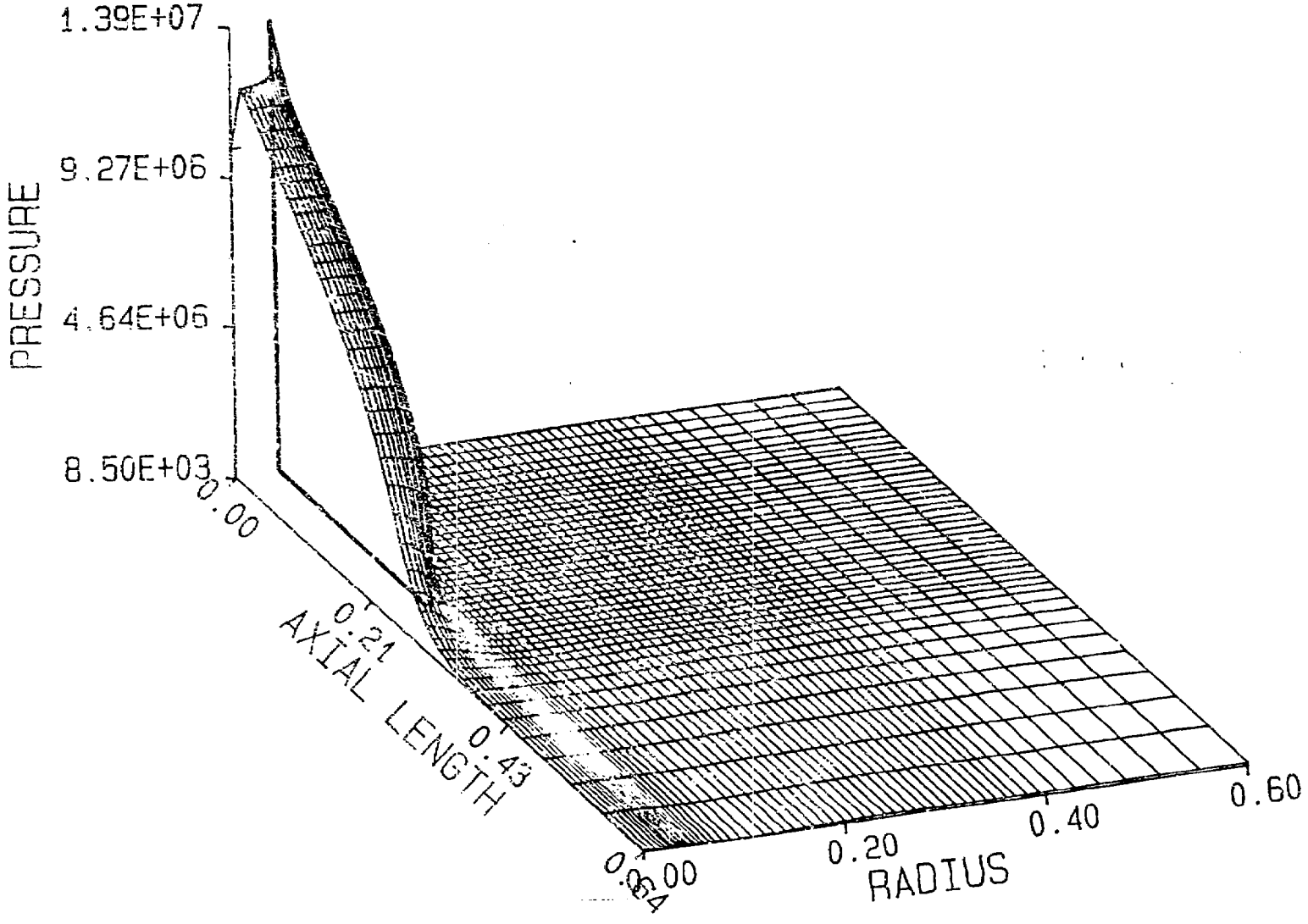

Figure 18c. Axial Velocity Field without the Silencer at T = 1.0 ms.

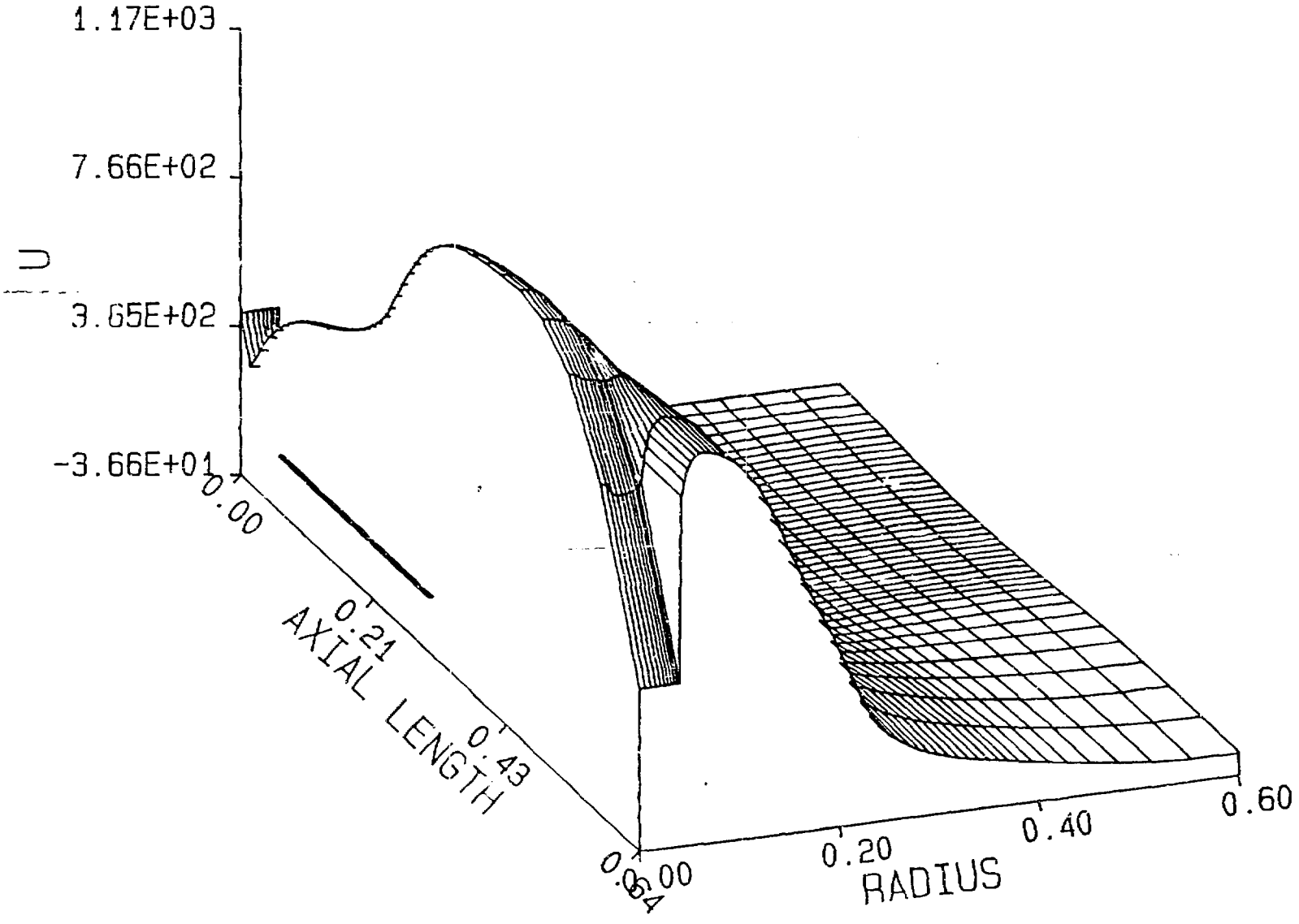

Figure 18d. Radial Velocity Field without the Silencer at T = 1.0 ms.

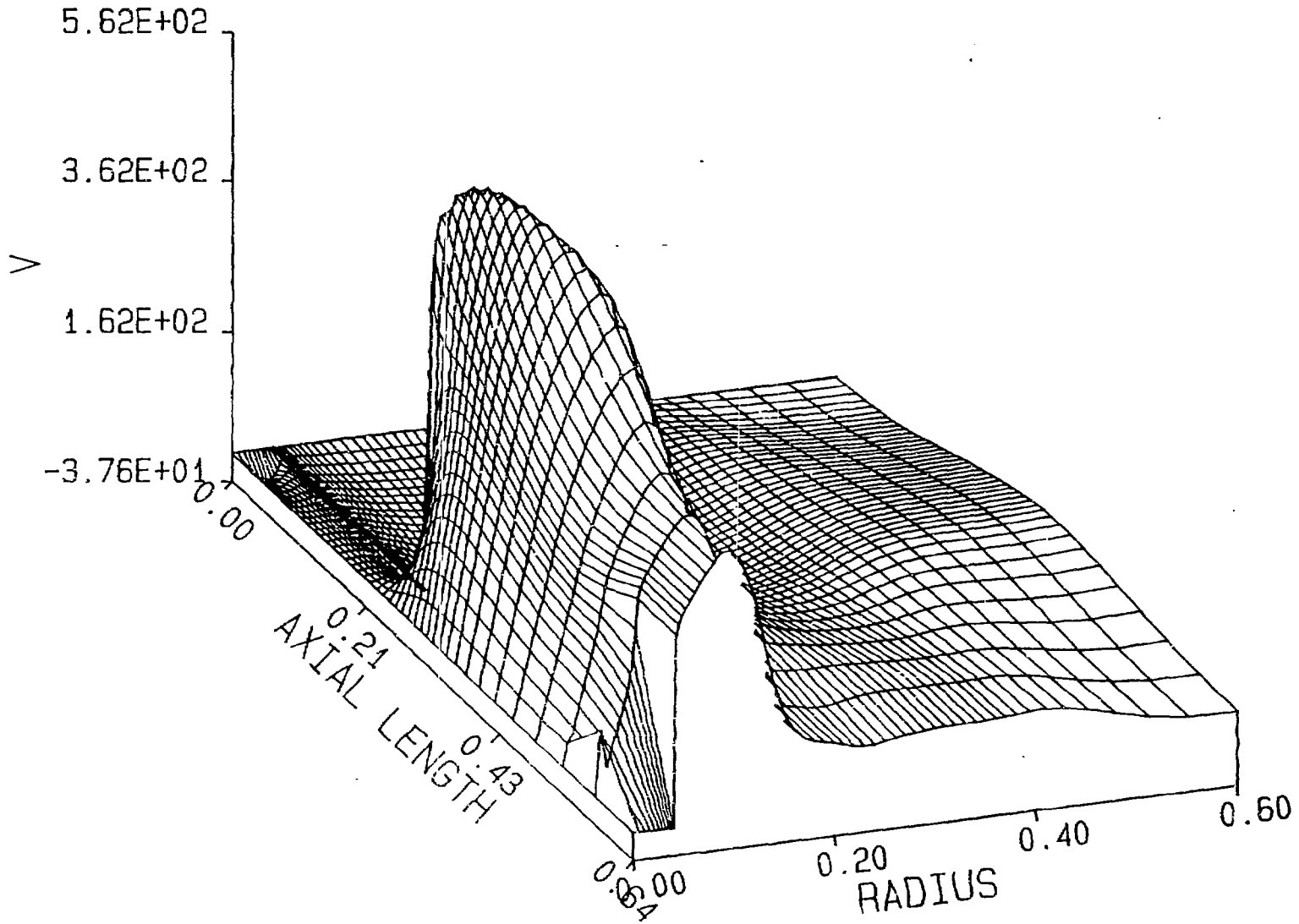

Figure 18e. Mach Number Field without the Silencer at T = 1.0 ms.

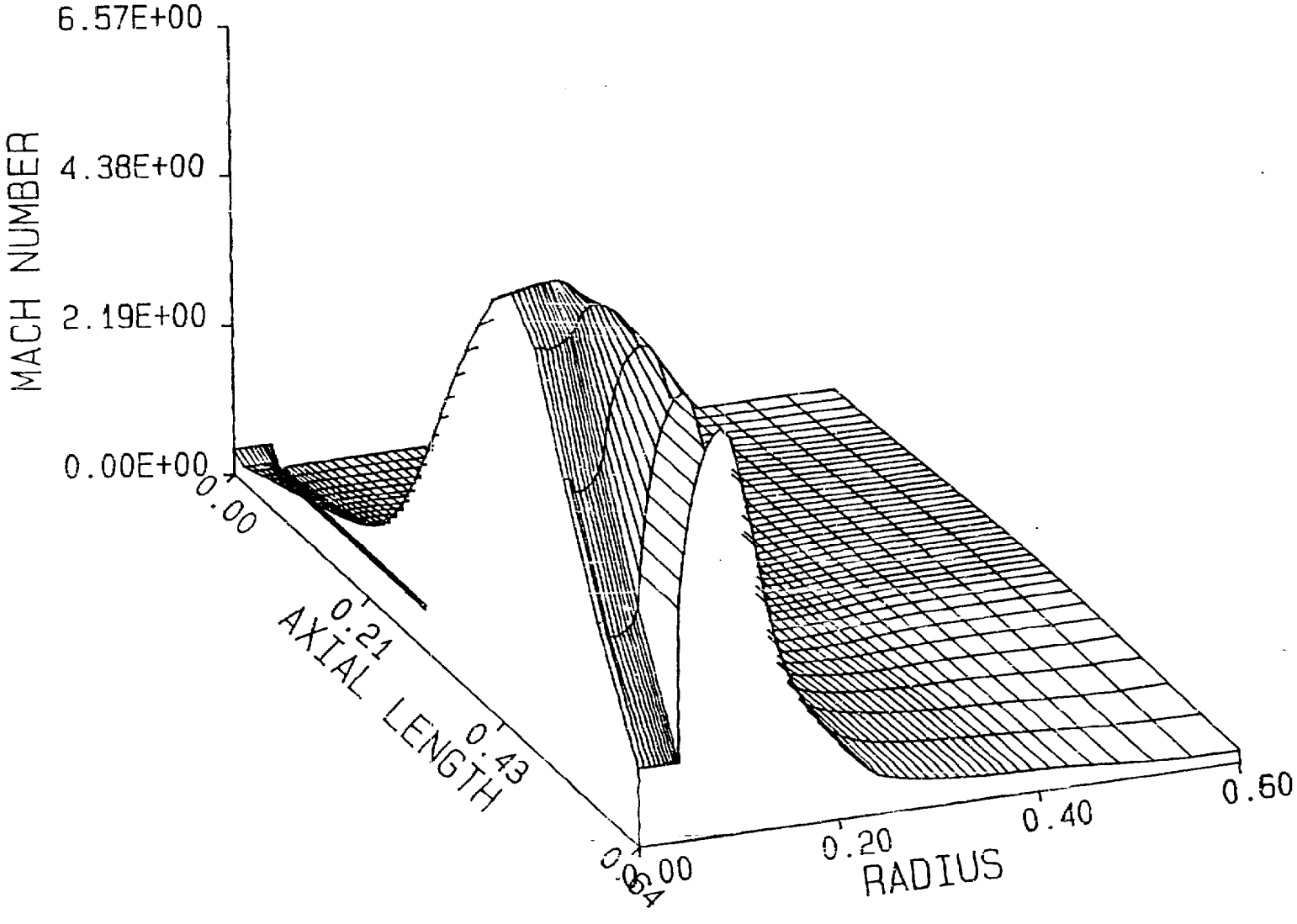

Figure 19a. Velocity Vector Field without the Silencer at T = 1.5 ms.

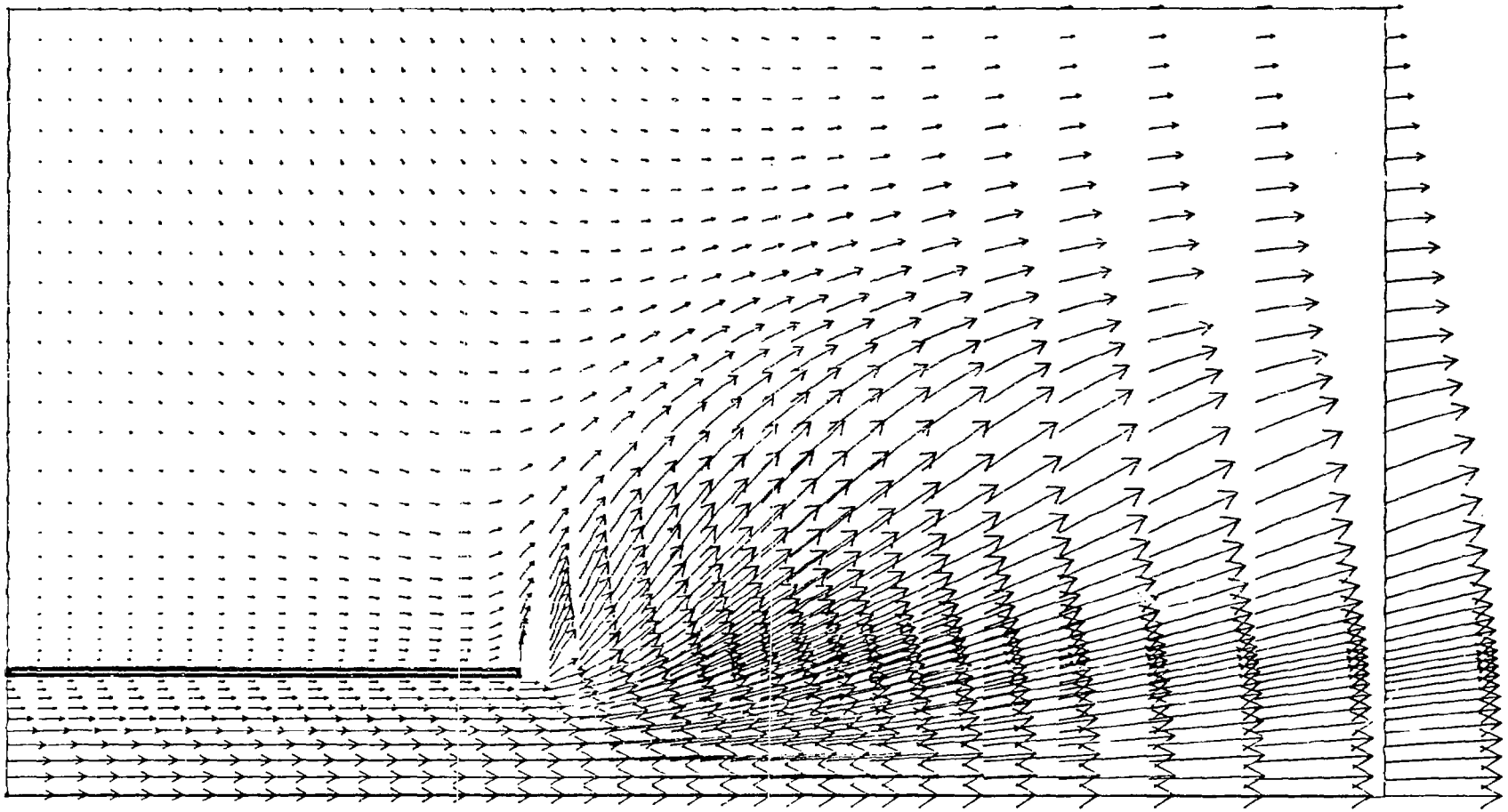

Figure 19b. Pressure Field without the Silencer at T = 1.5 ms.

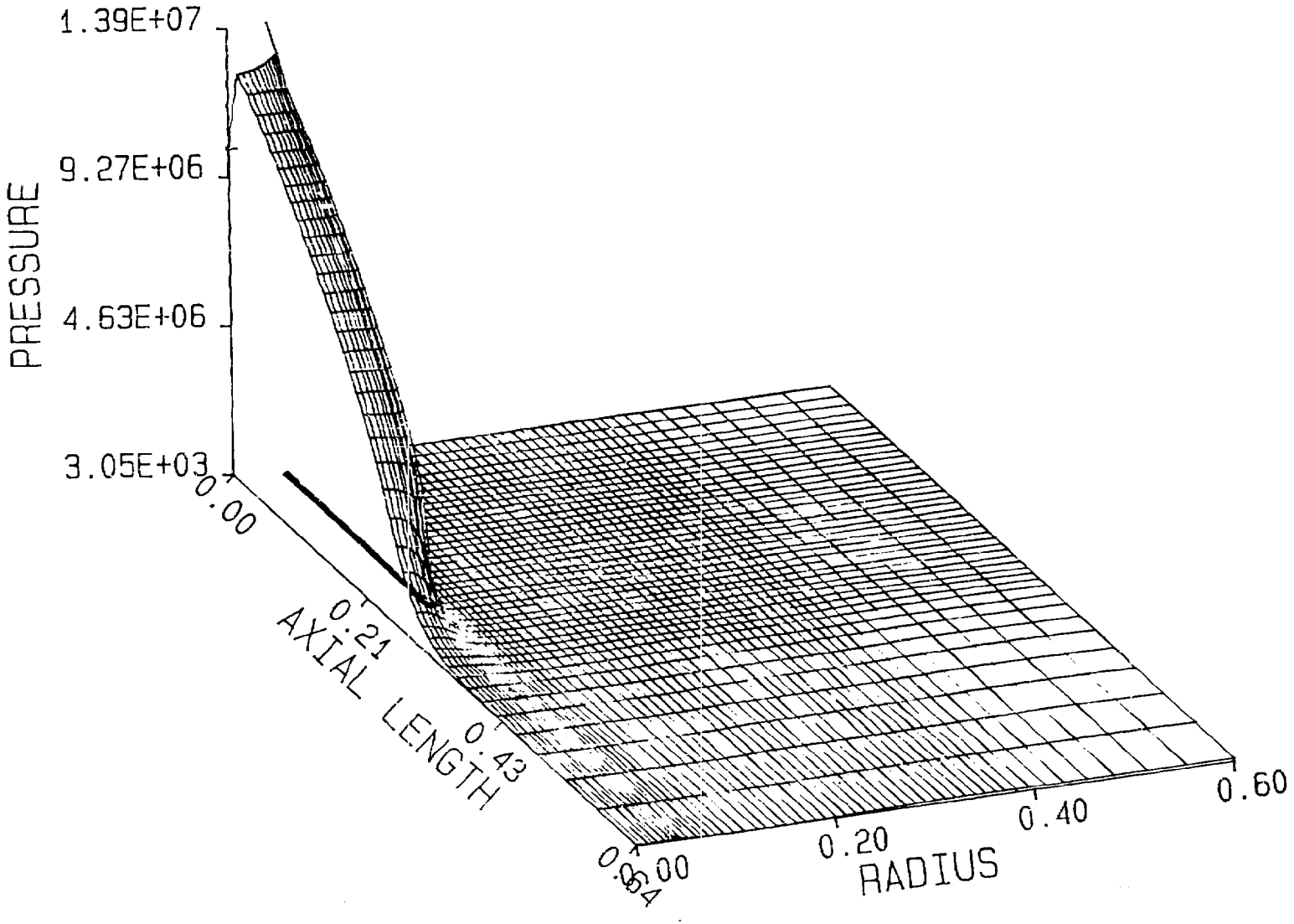

Figure 19c. Axial Velocity Field without the Silencer at T = 1.5 ms.

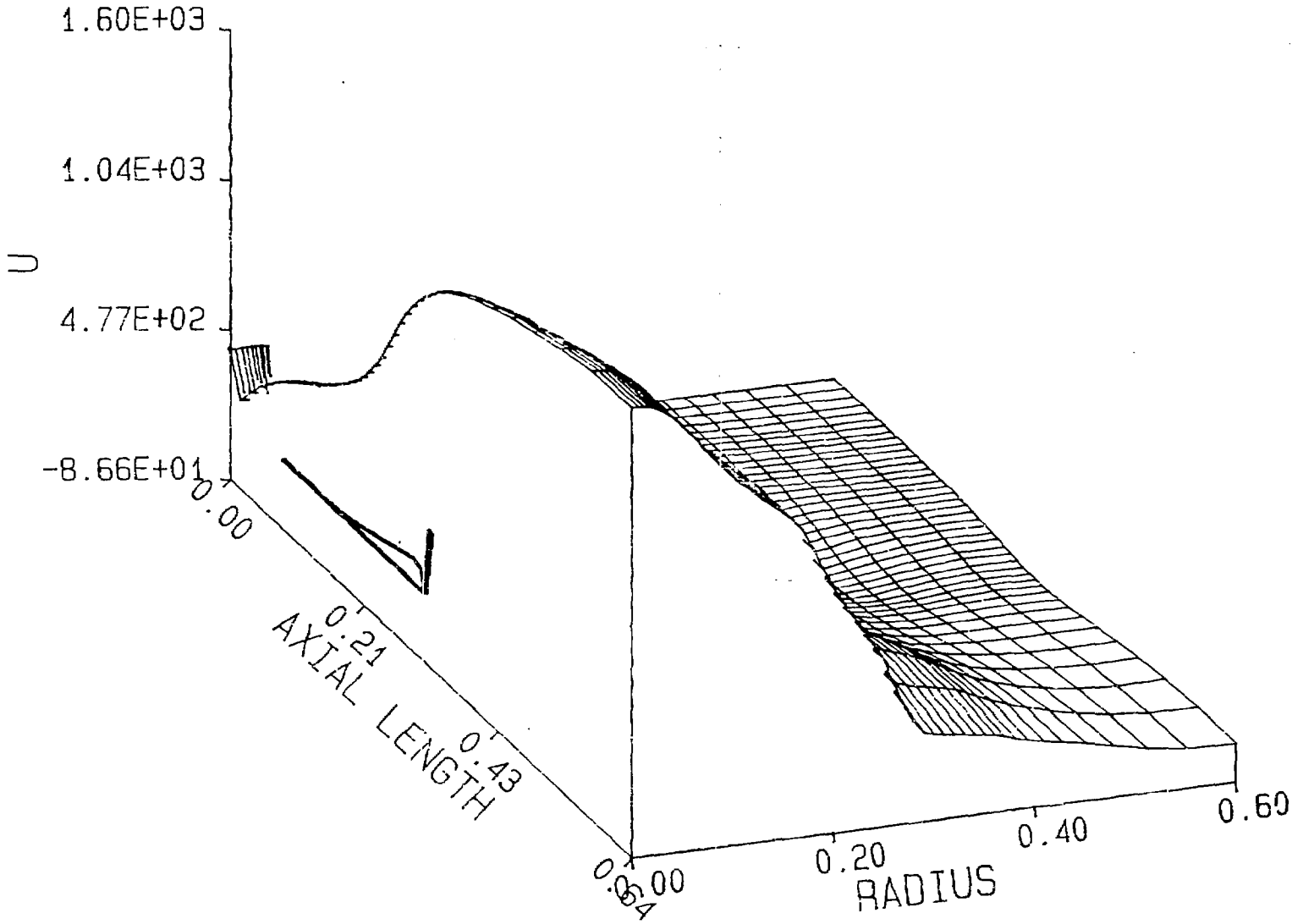

Figure 19d. Radial Velocity Field without the Silencer at T = 1.5 ms.

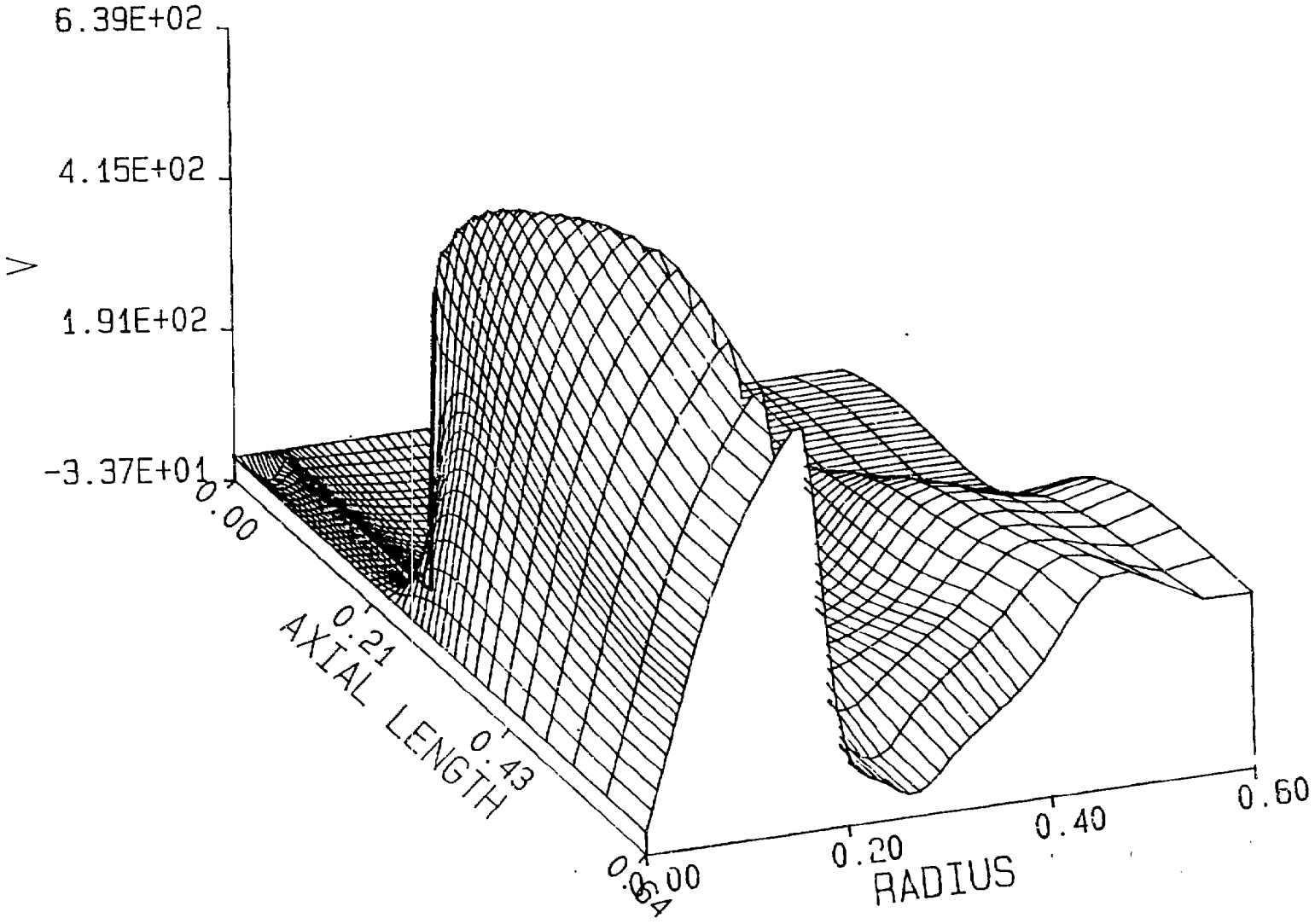

Figure 19c. Mach Number Field without the Silencer at T = 1.5 ms.

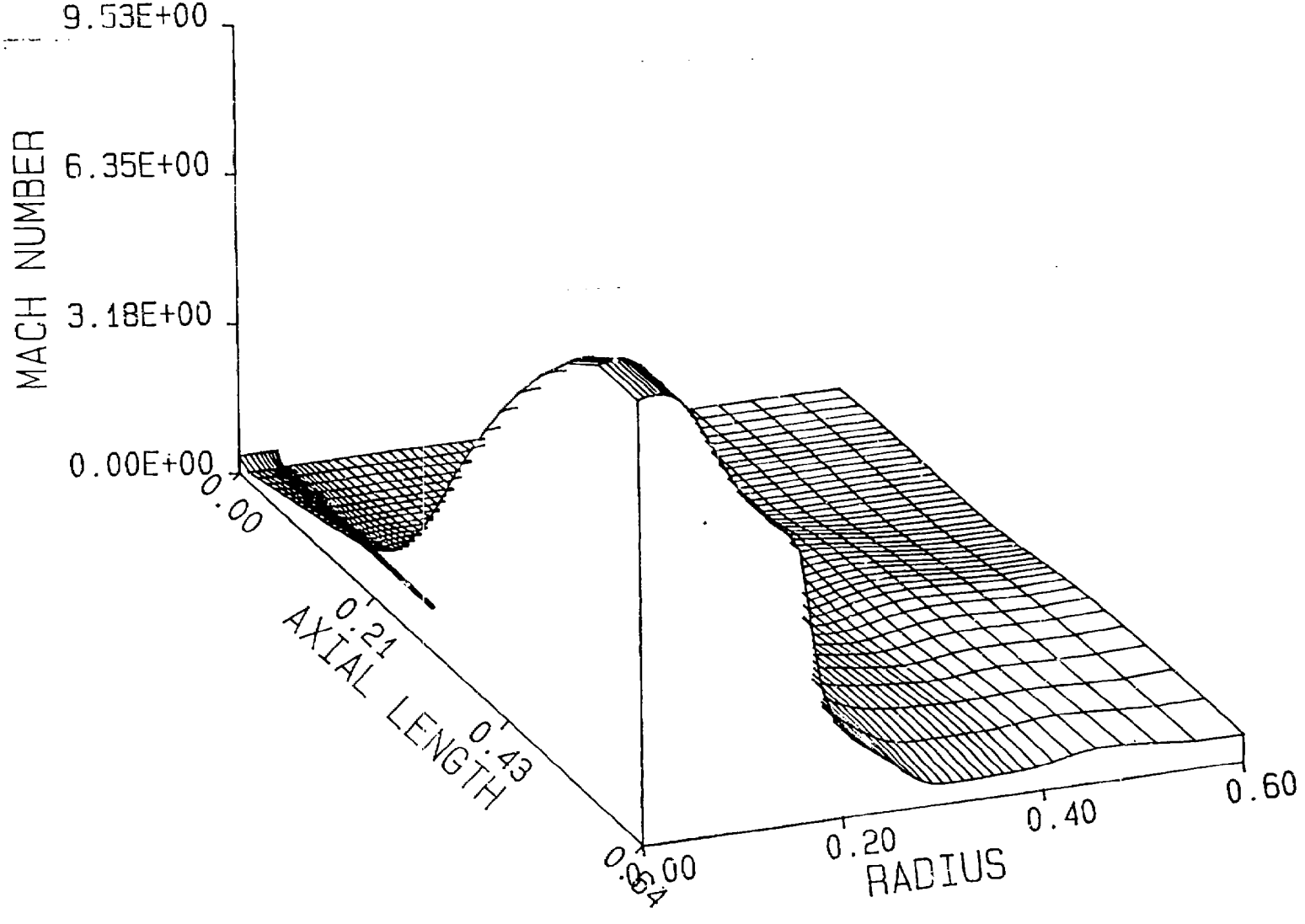

Figure 20a. Velocity Vector Field without the Silencer at T = 2.0 ms.

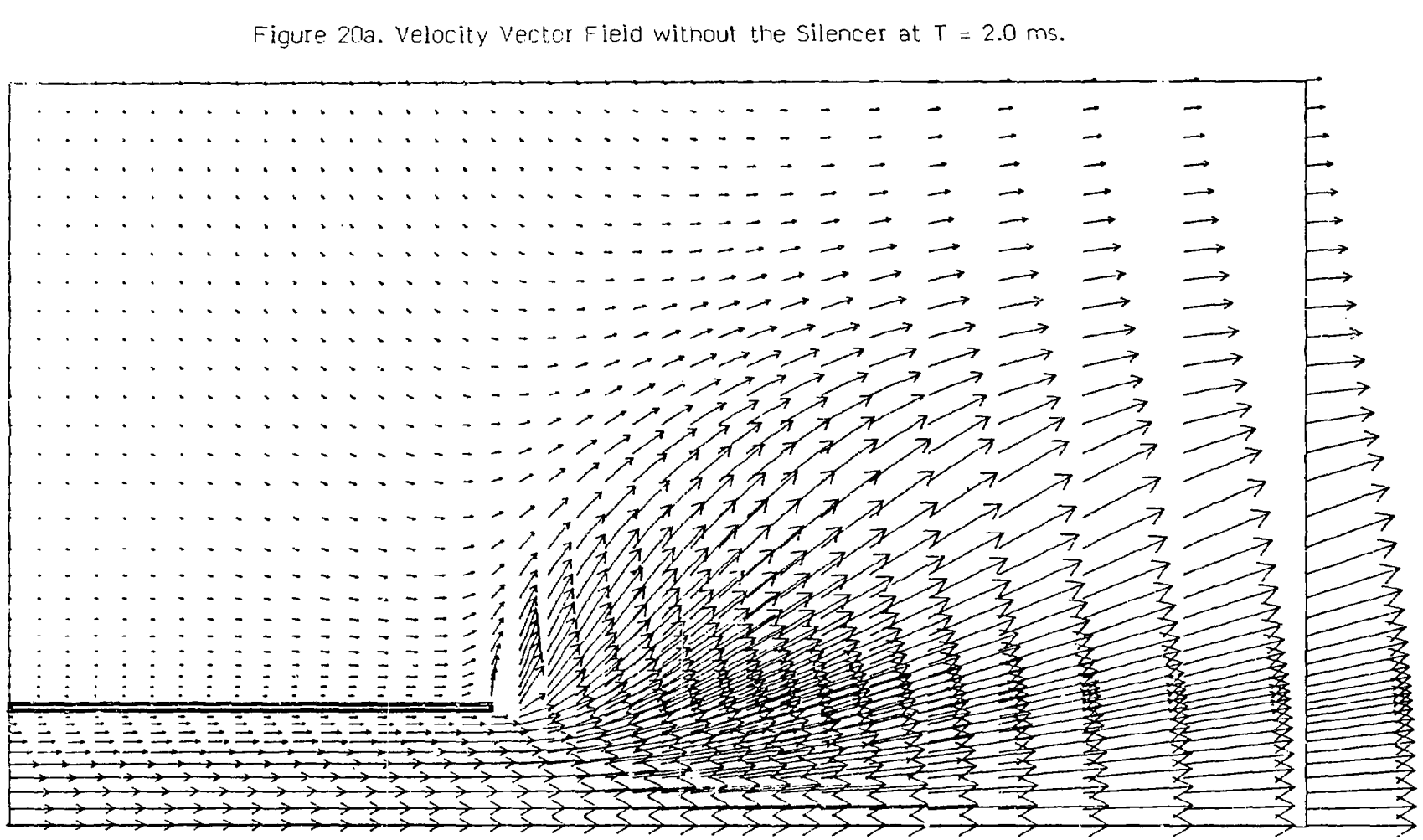

Figure 20b. Pressure Field without the Silencer at T = 2.0 ms.

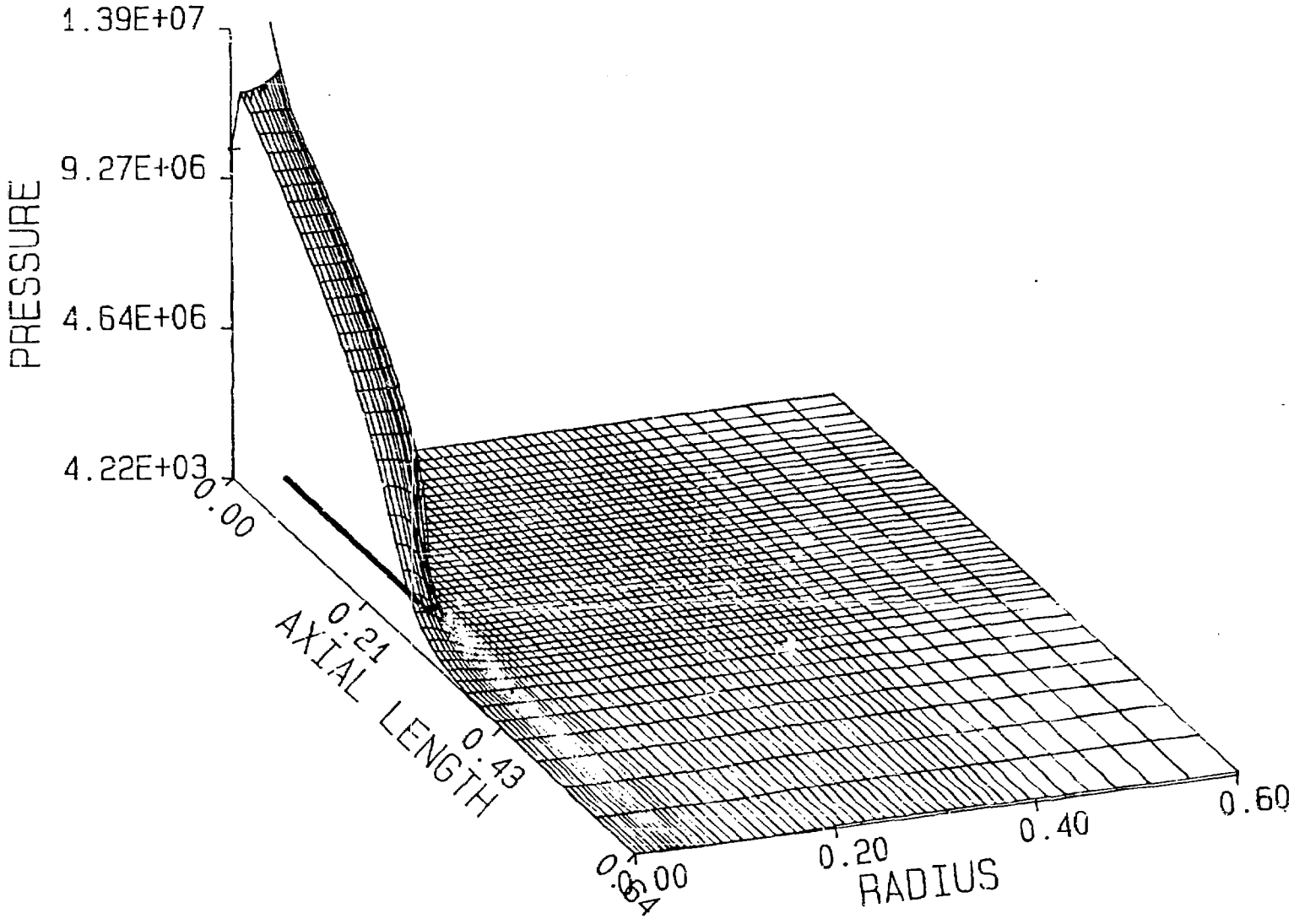

Figure 20c. Axial Velocity Field without the Silencer at T = 2.0 ms.

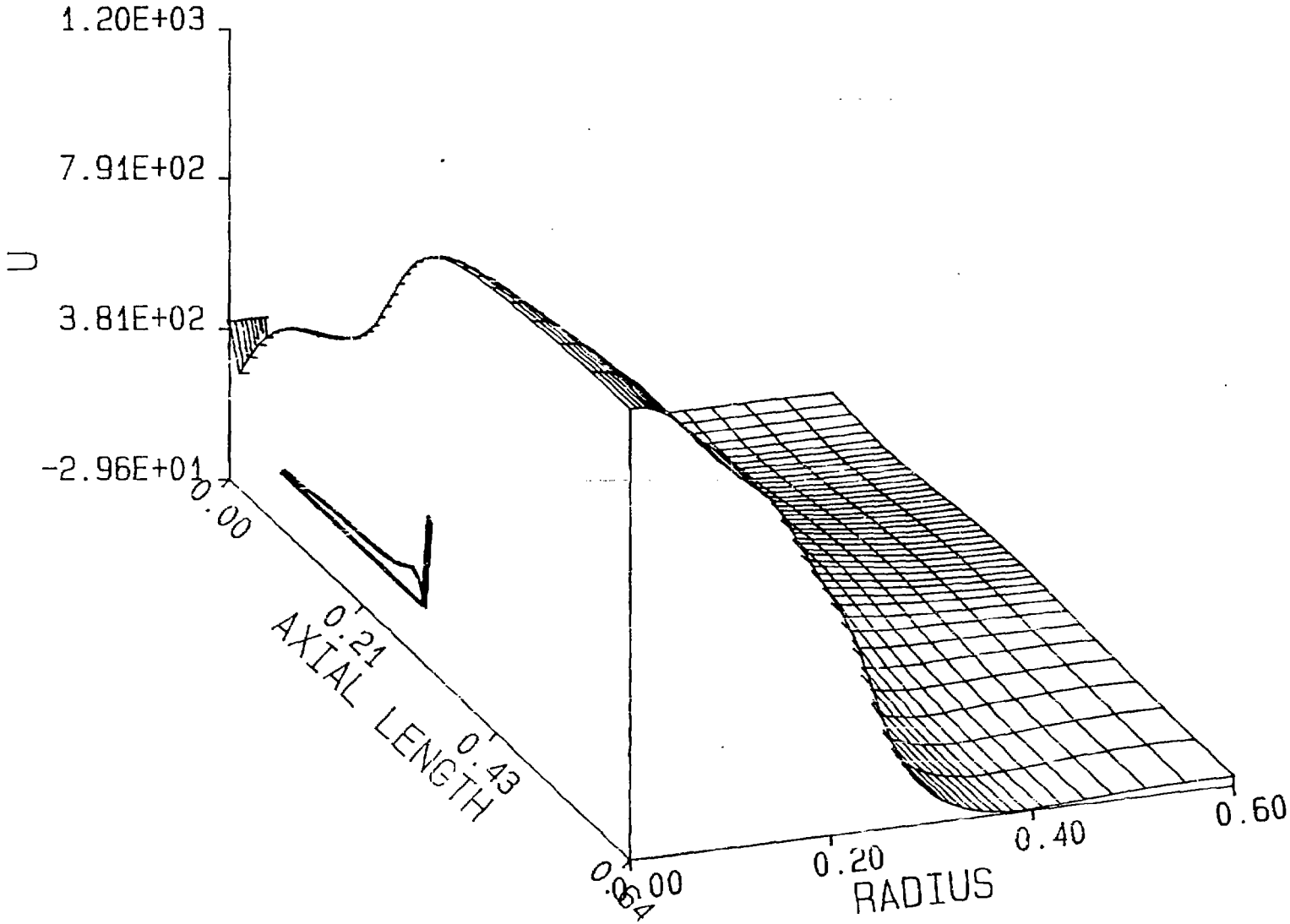

Figure 20d. Radial Velocity Field without the Silencer at T = 2.0 ms.

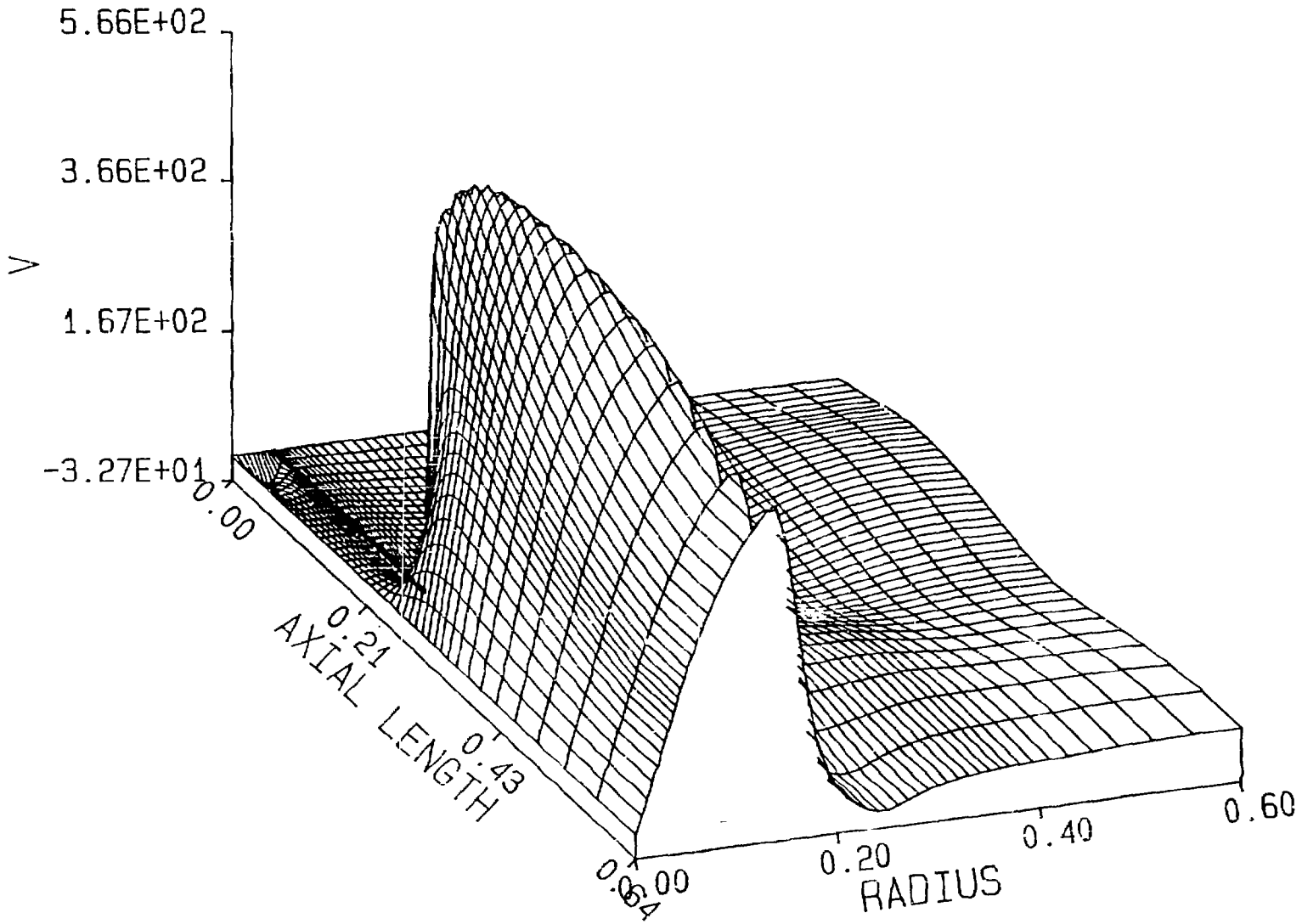

Figure 20e. Mach Number Field without the Silencer at T = 2.0 ms.

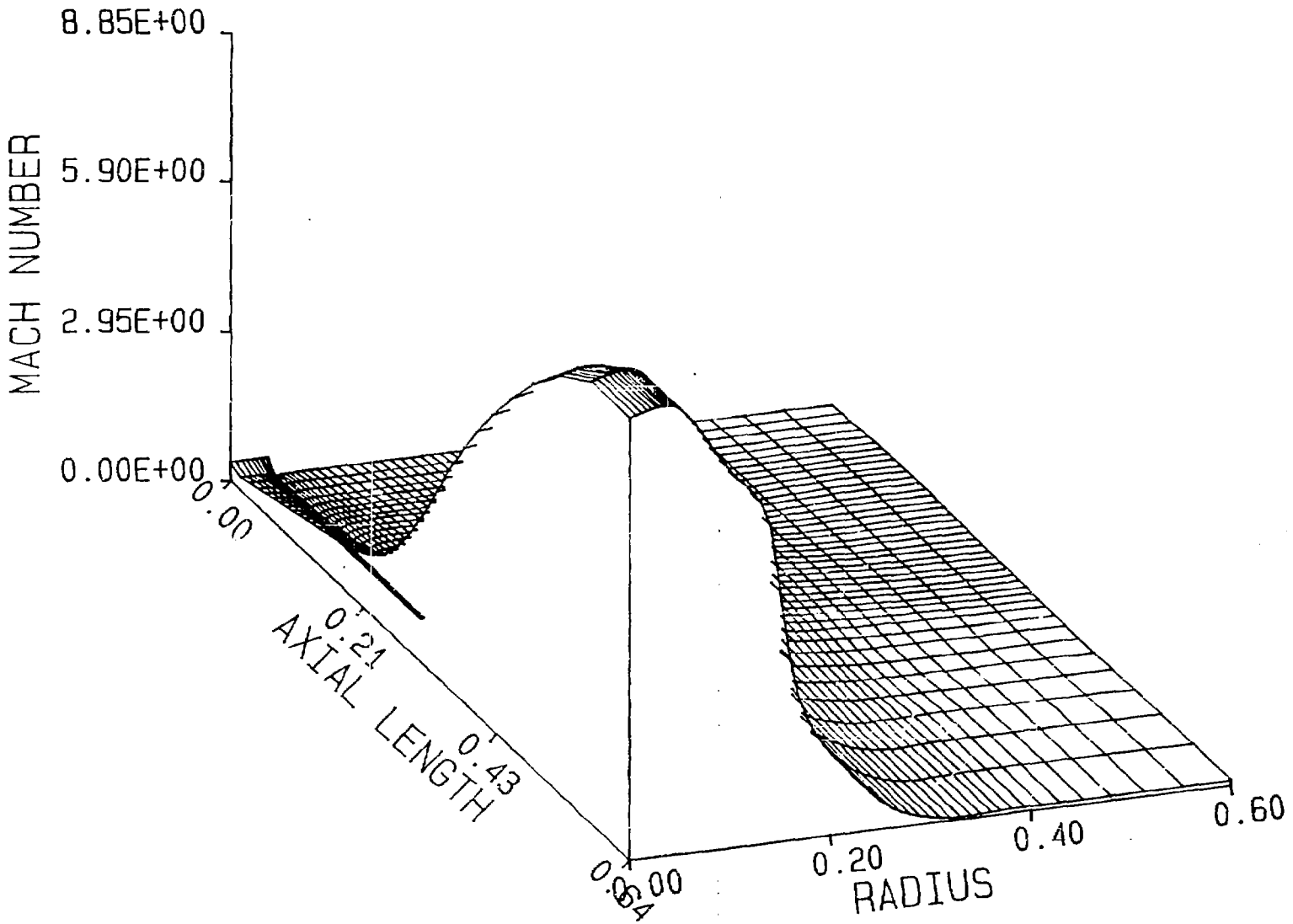

Figure 21a. Velocity Vector Field without the Silencer at T = 3.0 ms.

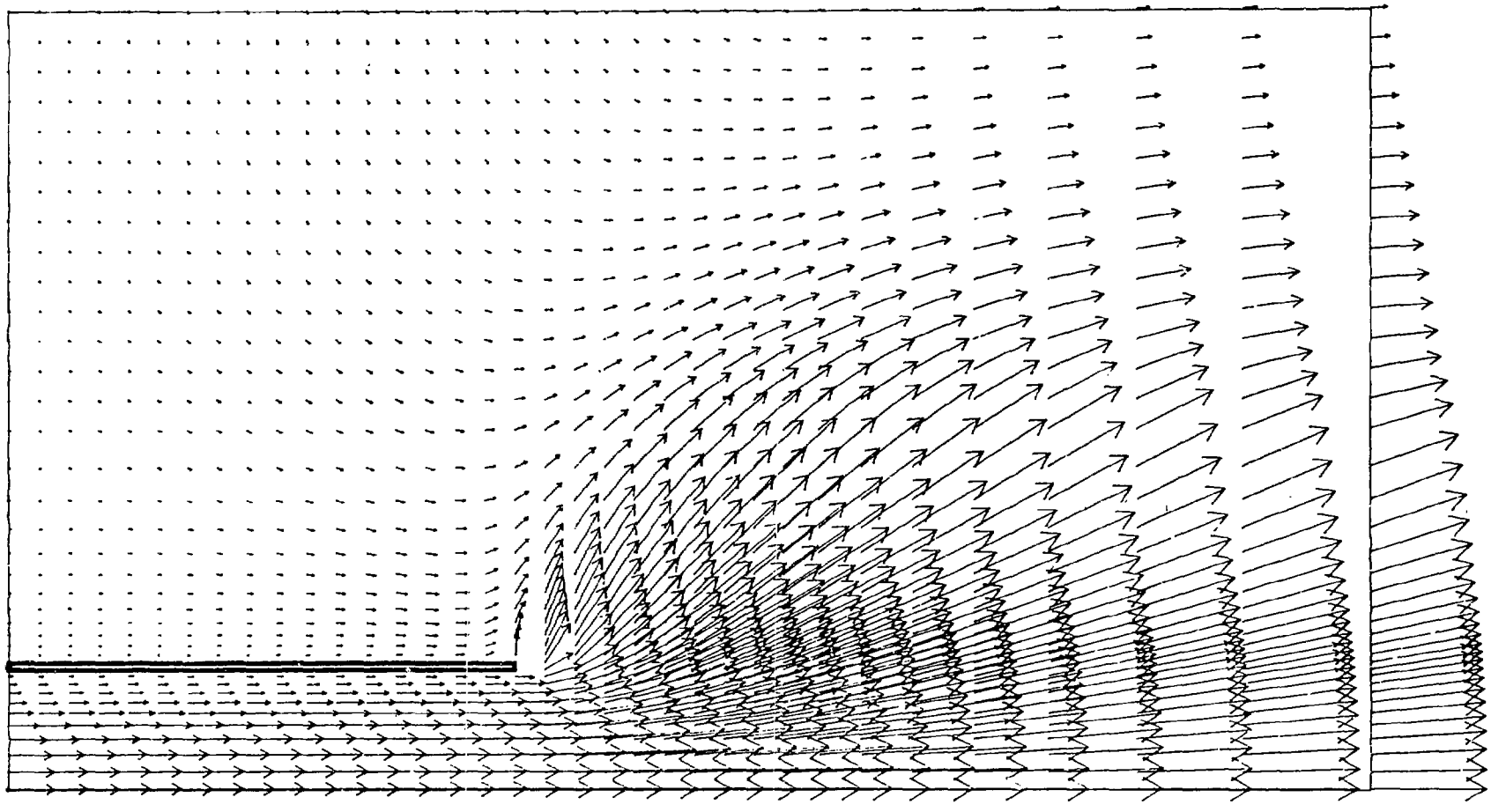

Figure 21b. Pressure Field without the Silencer at T = 3.0 ms.

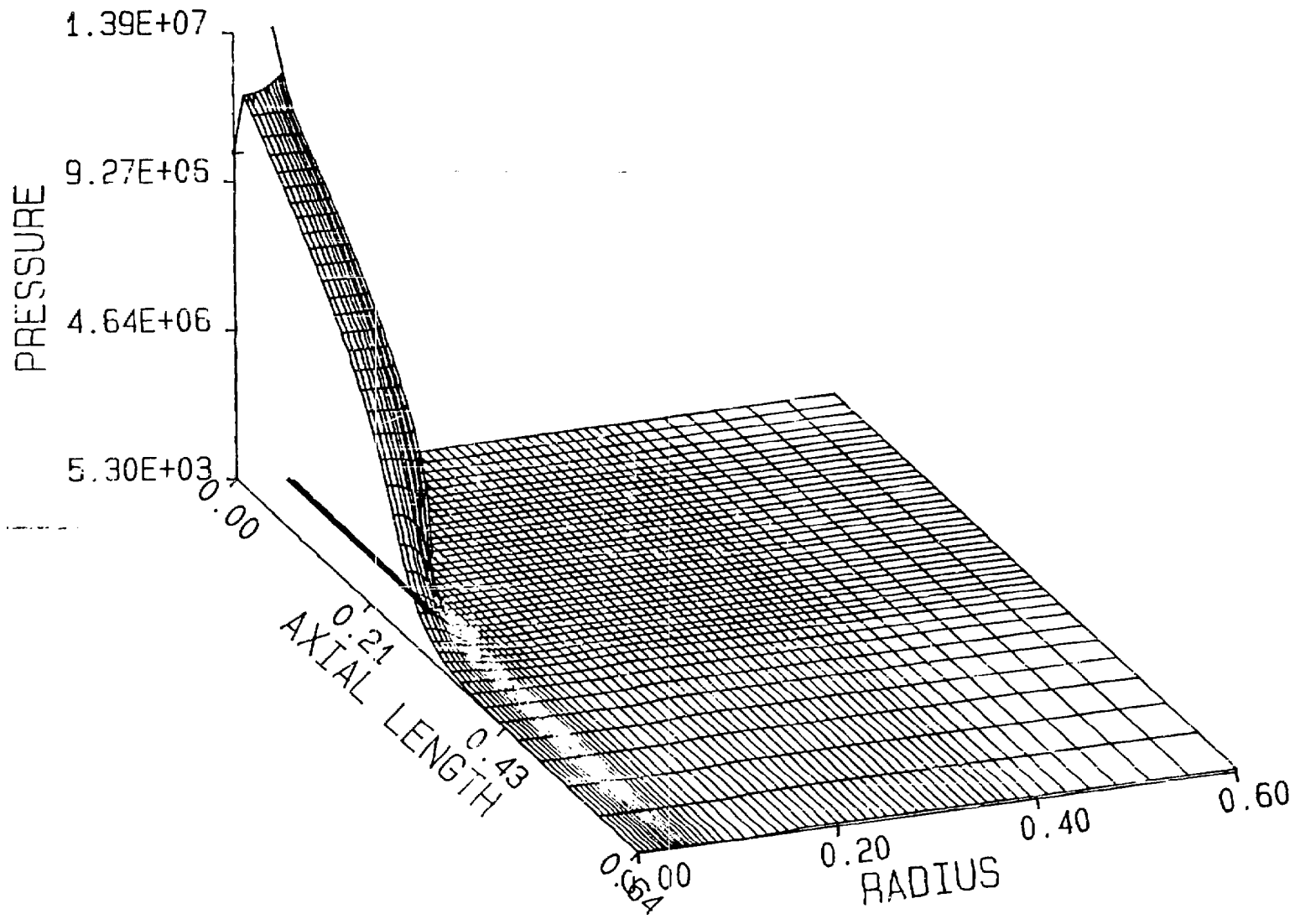

Figure 21c. Axial Velocity Field without the Silencer at T = 3.0 ms.

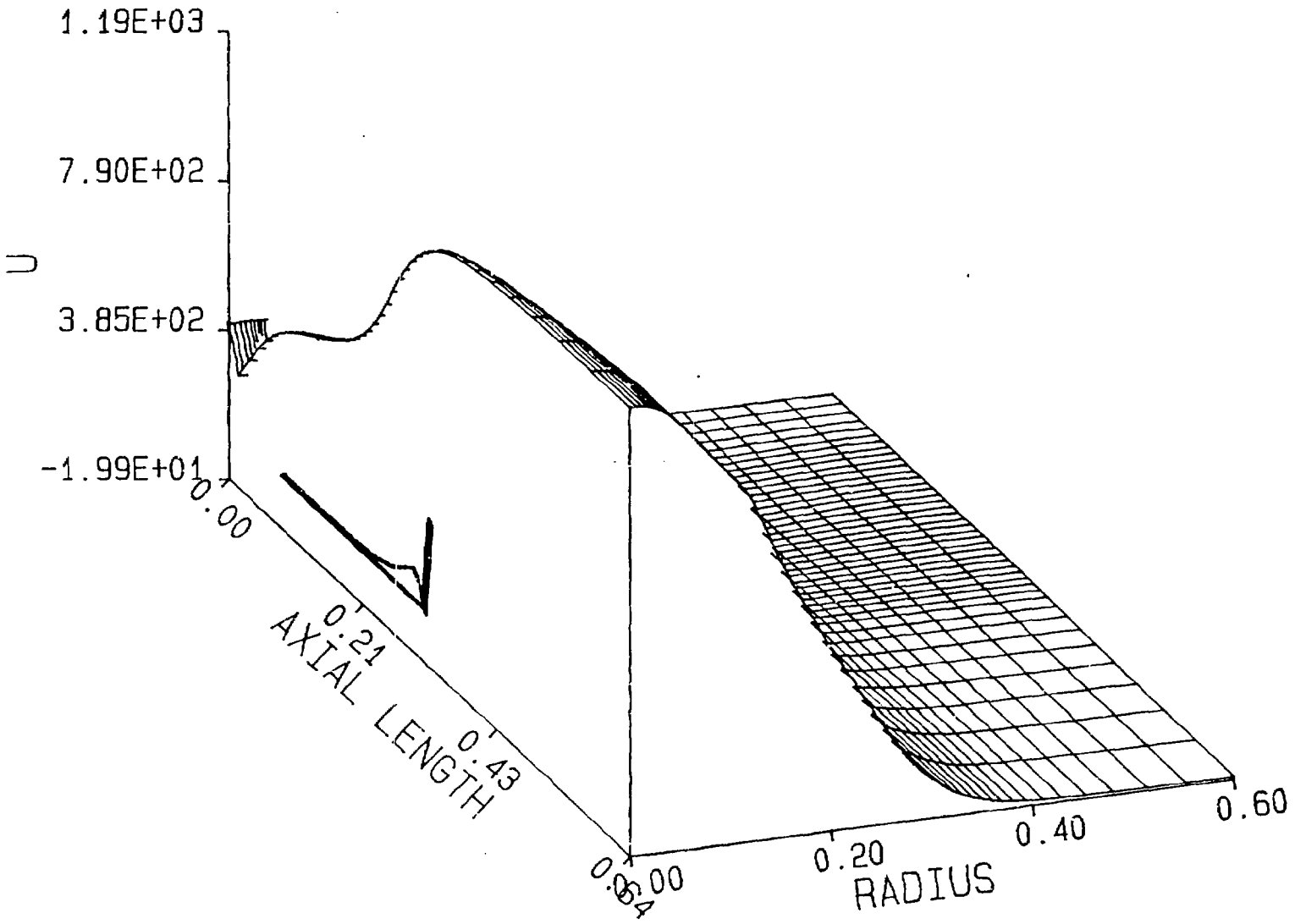

Figure 21c. Radial Velocity Field without the Silencer at T = 3.0 ms.

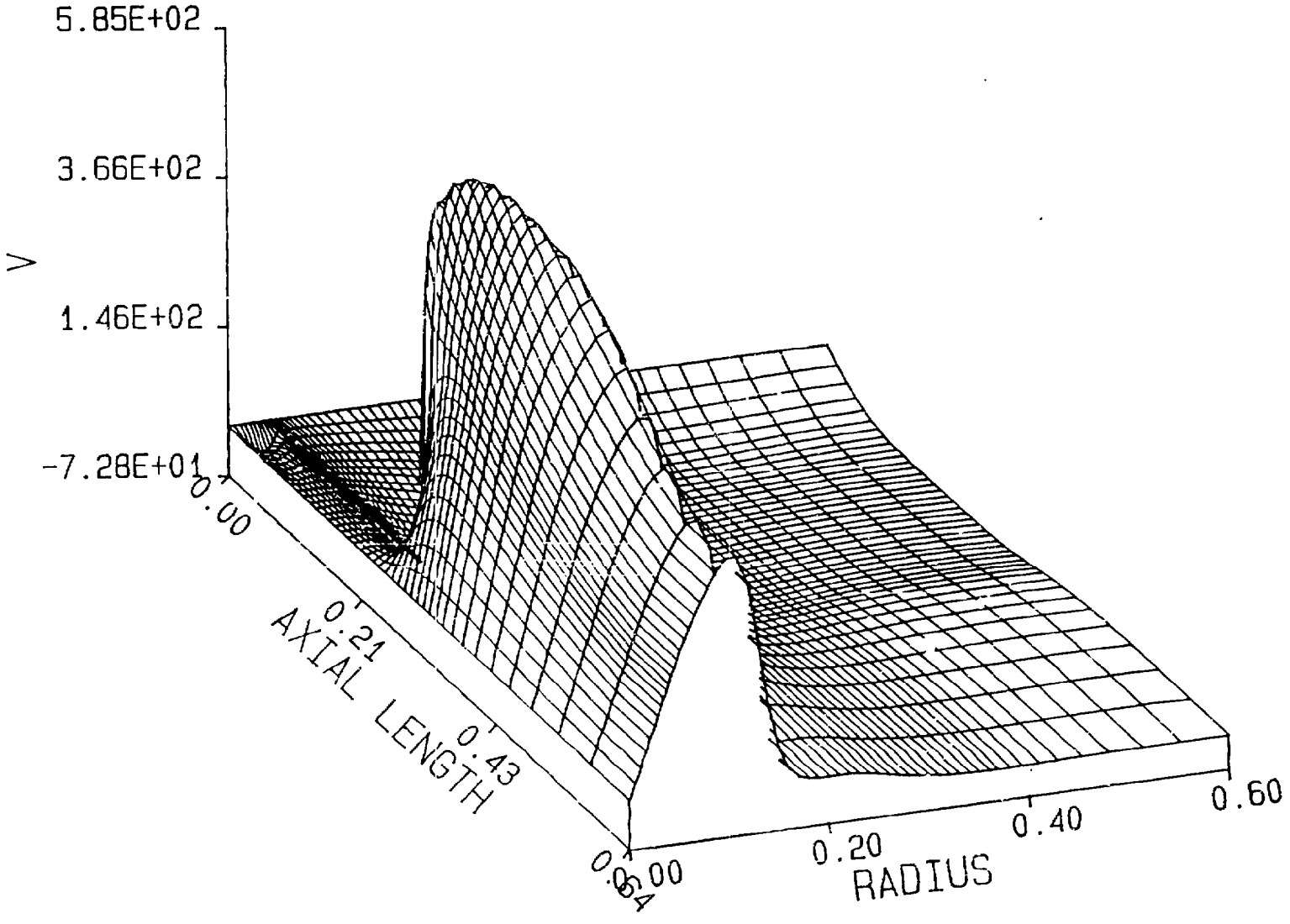

Figure 21e. Mach Number Field without the Silencer at T = 3.0 ms.

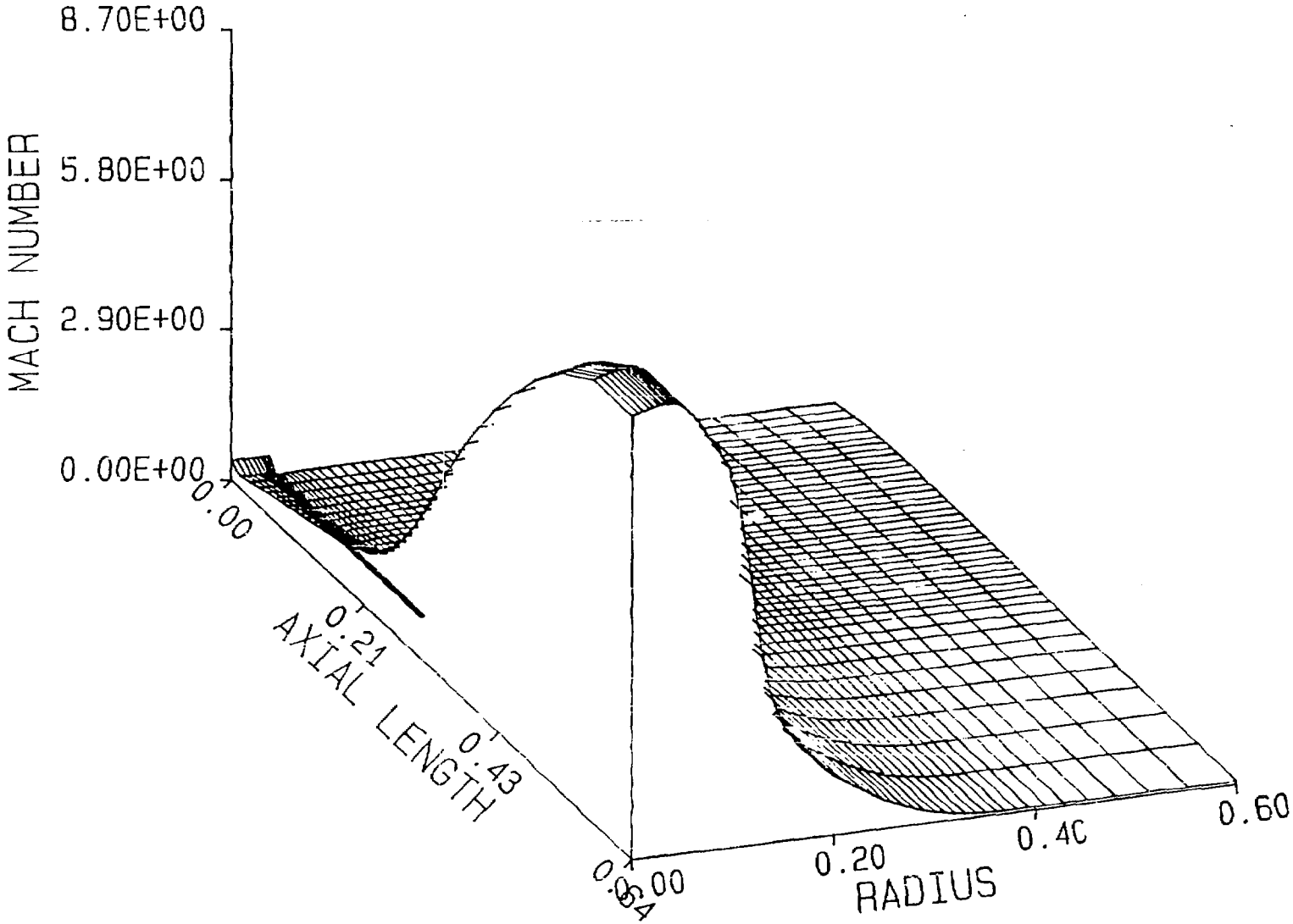

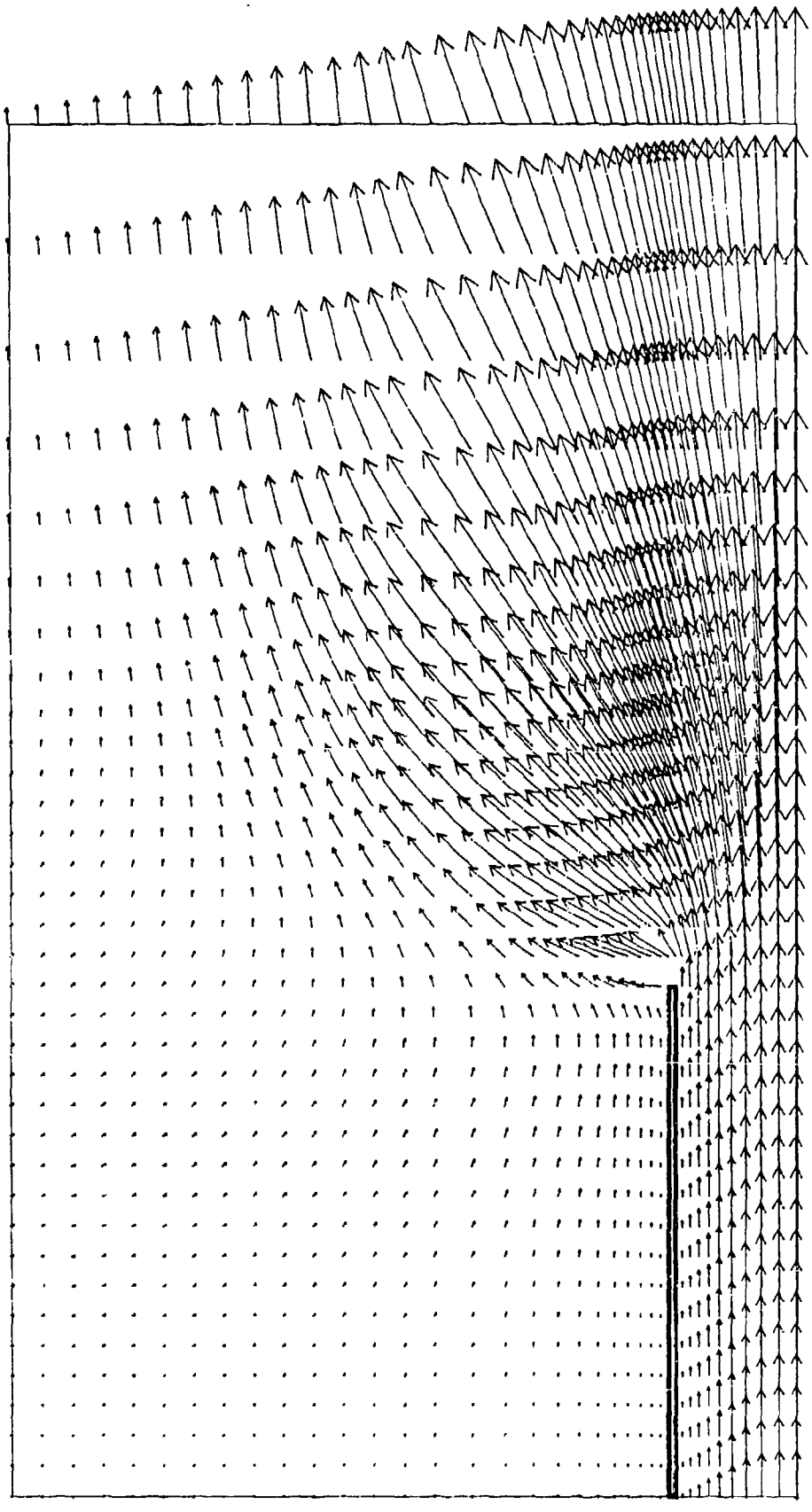

Figure 22a. Velocity Vector Field without the Silencer at T = 4.0 ms.

Figure 22b. Pressure Field without the Silencer at T = 4.0 ms.

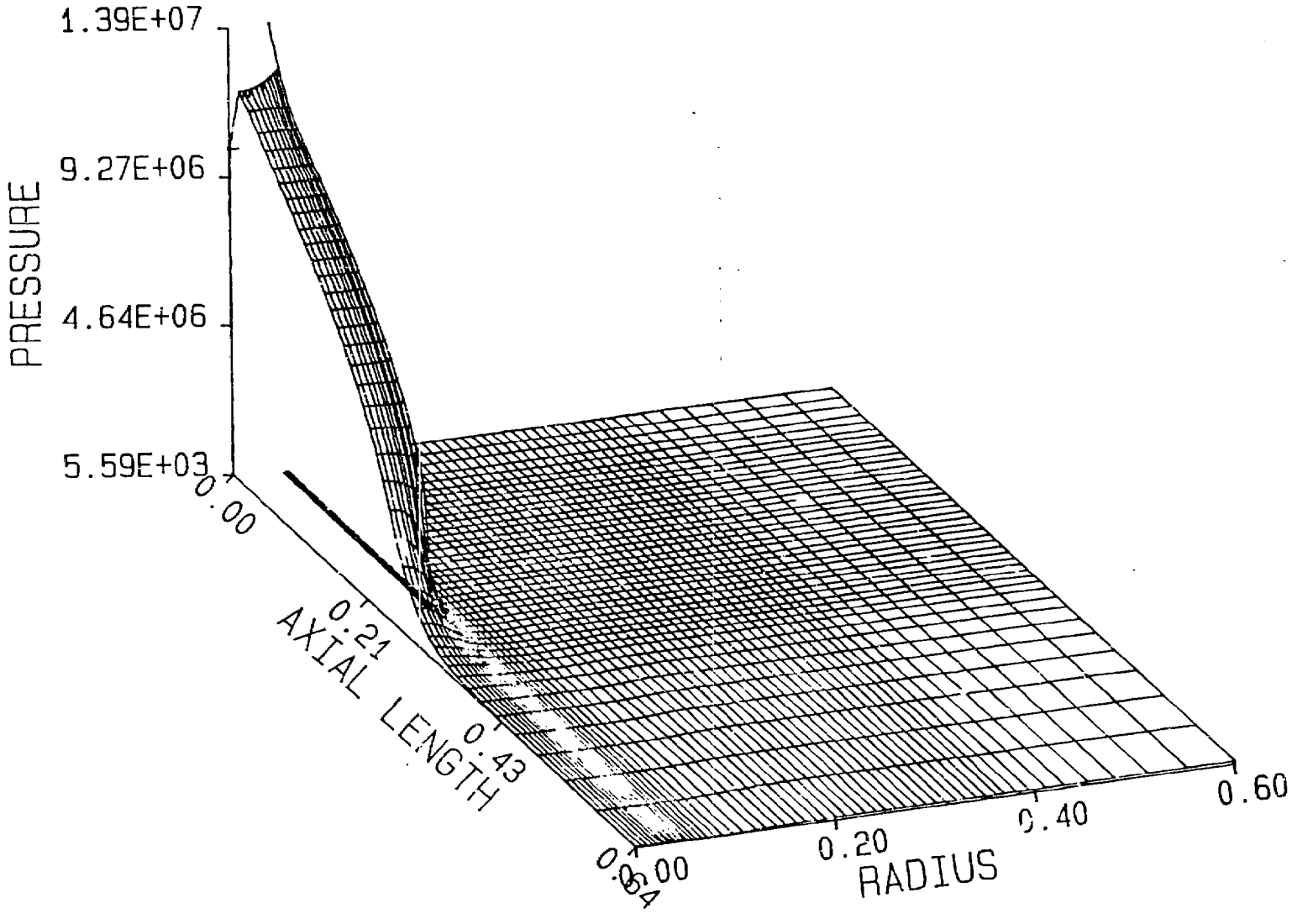

Figure 22c. Axial Velocity Field without the Silencer at T = 4.0 ms.

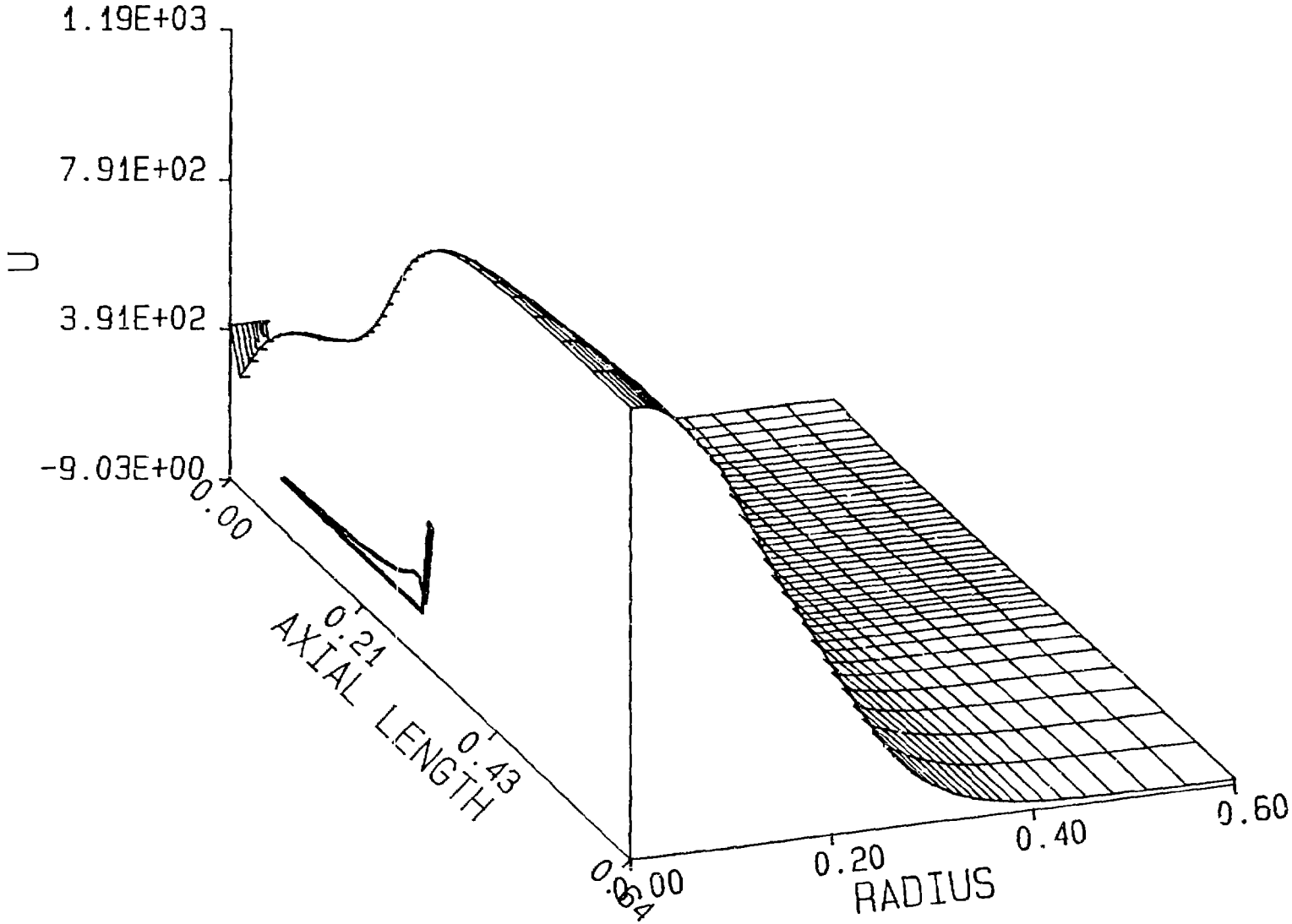

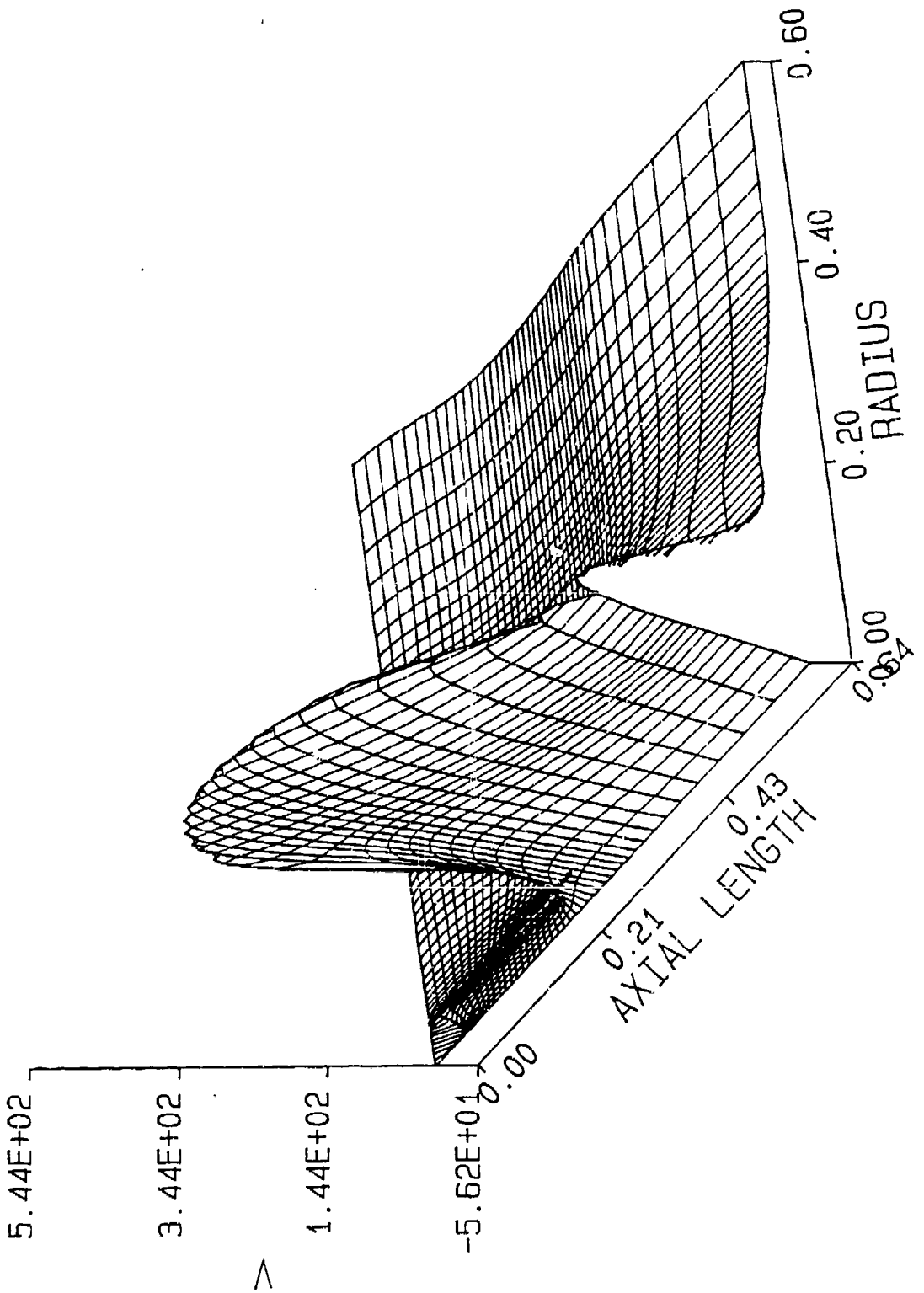

Figure 22d. Radial Velocity Field without the Silencer at T = 4.0 ms.